

AD-A088 187

AMPEX CORP REDWOOD CITY CA ADVANCED TECHNOLOGY DIV  
RECORDING MEDIA ARCHIVAL ATTRIBUTES (MAGNETIC). (U)  
APR 80 N BERTRAM, A ESHEL

F/G 14/3

F30602-78-C-0181

UNCLASSIFIED

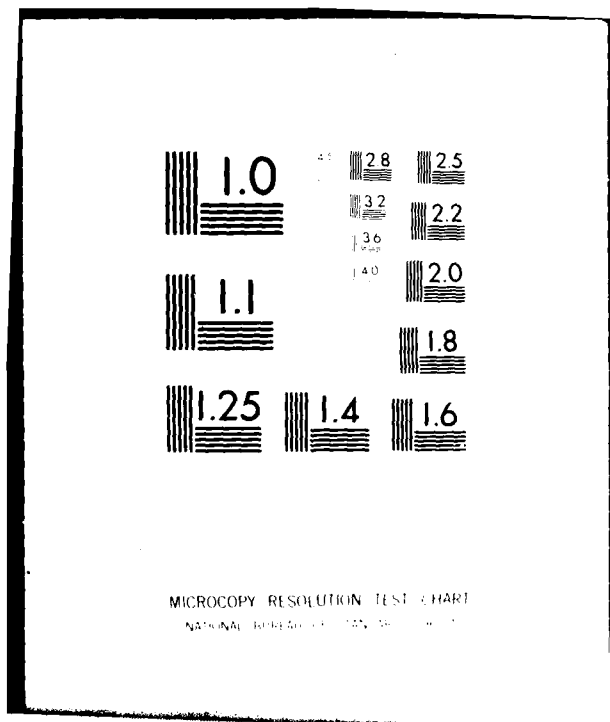
RR-80-01

RADC-TR-80-123

NL

1 OF 2  
AM  
RADC-TR-80-123

RR  
R  
RRR



AD A500178

8 LEVEL II  
12

RADC-TR-80-123  
Final Technical Report  
April 1980

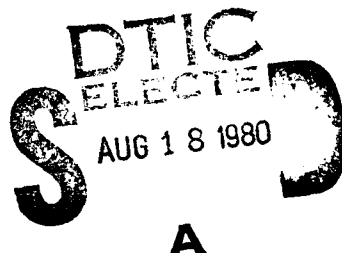


## RECORDING MEDIA ARCHIVAL ATTRIBUTES (MAGNETIC)

Ampex Corporation

Dr. Neal Bertram  
Mr. A. Eshel

APPROVED FOR PUBLIC RELEASE; DISTRIBUTION UNLIMITED



ROME AIR DEVELOPMENT CENTER  
Air Force Systems Command  
Griffiss Air Force Base, New York 13441

DC FILE COPY

80 8 15 080

This report has been reviewed by the RADC Public Affairs Office (PA) and is releasable to the National Technical Information Service (NTIS). At NTIS it will be releasable to the general public, including foreign nations.

RADC-TR-80-123 has been reviewed and is approved for publication.

APPROVED:



ROLFE E. FERRARA  
Project Engineer

APPROVED:



OWEN R. LAWTER, Colonel, USAF  
Chief, Intelligence & Reconnaissance Division

FOR THE COMMANDER:



JOHN P. HUSS  
Acting Chief, Plans Office

If your address has changed or if you wish to be removed from the RADC mailing list, or if the addressee is no longer employed by your organization, please notify RADC (IRAP) Griffiss AFB NY 13441. This will assist us in maintaining a current mailing list.

Do not return this copy. Retain or destroy.

## UNCLASSIFIED

SECURITY CLASSIFICATION OF THIS PAGE (When Data Entered)

REPORT DOCUMENTATION PAGE		READ INSTRUCTIONS BEFORE COMPLETING FORM
1. REPORT NUMBER RADC-TR-80-123	2. GOVT ACCESSION NO. <b>AD-A088/87</b>	3. RECIPIENT'S CATALOG NUMBER <b>9</b>
4. TITLE (and Subtitle) <b>RECORDING MEDIA ARCHIVAL ATTRIBUTES (MAGNETIC)</b>		5. TYPE OF REPORT & PERIOD COVERED <b>Final Technical Report, 30 May 78 - 30 Nov 79.</b>
6. AUTHOR(s) <b>Dr. Neal/Bertram Mr. A. Eshel</b>		7. PERFORMING ORG. REPORT NUMBER <b>RR-80-01</b>
8. CONTRACTOR GRANT NUMBER(s) <b>F30602-78-C-0181</b>		9. PERFORMING ORGANIZATION NAME AND ADDRESS <b>Ampex Corporation Advanced Technology Division Redwood City CA 94603</b>
10. PROGRAM ELEMENT, PROJECT, TASK AREA & WORK UNIT NUMBERS <b>63701B 32050306</b>		11. CONTROLLING OFFICE NAME AND ADDRESS <b>Rome Air Development Center (IRAP) Griffiss AFB NY 13441</b>
12. REPORT DATE <b>Apr 1980</b>		13. NUMBER OF PAGES <b>121</b>
14. MONITORING AGENCY NAME & ADDRESS (if different from Controlling Office) <b>Same</b>		15. SECURITY CLASS. (of this report) <b>UNCLASSIFIED</b>
		15a. DECLASSIFICATION/DOWNGRADING SCHEDULE <b>N/A</b>
16. DISTRIBUTION STATEMENT (of this Report) <b>Approved for public release: distribution unlimited.</b>		
17. DISTRIBUTION STATEMENT (of the abstract entered in Block 20, if different from Report) <b>Same</b>		
18. SUPPLEMENTARY NOTES <b>RADC Project Engineer: Rolfe E. Ferrara (IRAP)</b>		
19. KEY WORDS (Continue on reverse side if necessary and identify by block number) <b>Wideband Recording Digital Data Storage Storage and Retrieval Magnetic Recording</b>		
20. ABSTRACT (Continue on reverse side if necessary and identify by block number) <b>This study focuses on the long term (10-15 year) storage effects on magnetic recording media with emphasis on digital magnetic tape. Both the theoretical and experimental aspects are presented covering the primary magnetic, chemical, and mechanical considerations. Definite storage and handling procedures along with an optimum long term magnetic recording system are discussed. Conclusions are that long term storage is possible with magnetic tapes provided tight environmental controls are maintained</b>		

DD FORM 1 JAN 73 1473 EDITION OF 1 NOV 88 IS OBSOLETE

(Cont'd)

UNCLASSIFIED

SECURITY CLASSIFICATION OF THIS PAGE (When Data Entered)

**402819****M**

UNCLASSIFIED

SECURITY CLASSIFICATION OF THIS PAGE(When Data Entered)

Item 20 (Cont'd)

and low acceleration rewinds are performed at a minimum interval of  
3 1/2 years.

Acceleration Factor	
ITEM	Value
Revolves	
Acceleration	
Deceleration	
Time	
Speed	
Distance	
Dist	Special

UNCLASSIFIED

SECURITY CLASSIFICATION OF THIS PAGE(When Data Entered)

## ACKNOWLEDGEMENT

The authors would like to express their appreciation to the many people who contributed to the completion of this contract. Special thanks are due John Mallinson who contributed the section on an optimum archival system, Bob Perry who contributed the section on tape formulations, Ed Cuddihy (of JPL, Pasadena, CA) for many invaluable discussions, not only on the hydrolysis of tape binders, but on recommendations for reasonable archival storage practices and to Tracy Wood, Martin Booye and Bill Helander (Ford Aerospace, Palo Alto, CA), for stimulating discussions.

### Magnetics

The magnetic measurements were performed with the assistance of a variety of people. Dennis Lindholm programmed and measured the computer tapes; Spiros Moulats and Arlen Comfort recorded and analyzed the TBM tapes and Louis Borne and Paul Guantonio were responsible for the High Density Instrumentation recording and measurements. Rex Niedermeyer recorded, stored and analyzed the tapes for the tape signal loss measurements.

### Mechanics

The mechanics work performed under the contract was the result of team effort. Major contributors responsible for equipment development, testing and analysis were Steve Baker and Albert Hartman. Significant assistance was rendered by Bob Lawson and Henry Van Boekholtz in the design, construction and adaptation of parts for the equipment. Many discussions with Fred Orcutt provided important inputs to the project and in particular the pendulum concept for the creep apparatus is due to him. The initial prototype of this apparatus was designed and built by Bruce Haughey and Moritz Branger. Pete Bondy was generous in supplying Ampex instrumentation tape for testing.

The authors would like to express their indebtedness to all the above as well as to Rolf Ferrara, the contract monitor, for his cooperation and support of this effort.

## TABLE OF CONTENTS

1.0	INTRODUCTION	1
2.0	ARCHIVAL STORAGE STUDY	3
2.1	Identification of Recording Materials and Formulations Suitable for Digital Recording	3
2.1.1	Magnetic Tape Recording Media	3
2.1.2	Magnetic Disc Recording Media	7
2.1.3	Magnetic Recording Media Formulations	7
2.2	Recording Signal Studies	9
2.2.1	Loss of Magnetic Signal With Storage	10
2.2.2	Print-Through	13
2.3	Mechanical Studies of Tape Packs	15
2.3.1	Introduction	15
2.3.2	Survey of Mechanical Effects Significant to Tape Archivability	15
2.3.2.1	Basic Model	15
2.3.2.2	Tension and Pressure Distribution in a Wound Reel	16
2.3.2.3	The Relaxation Mechanism	20
2.3.2.4	Effect of Environmental Cycles	20
2.3.2.5	Effect of Temperature	22
2.3.2.6	Effect of Winding Tension	22
2.3.2.7	Effect of Winding Speed	22
2.3.2.8	Locked-in Air Layers	22
2.3.2.9	Tape Shrinkage	24
2.3.2.10	Effect of Anisotropy	24
2.3.3	Experiments on Creep Rate at Room Temperature	26
2.3.3.1	Motivation for the Experimental Work	26
2.3.3.2	Experimental Apparatus	27
2.3.3.3	Results and Discussion	27
2.3.4	Experiments on Creep Rate and Shrinkage at Moderate Temperatures	32
2.3.4.1	Motivation	32
2.3.4.2	Experimental Apparatus	32
2.3.4.3	Results and Discussion	36

## Table of Contents (Continued)

2.3.5	Experiments on Reel Structural Integrity	36
2.3.5.1	Motivation	36
2.3.5.2	Equipment	40
2.3.5.3	Tests and Results	40
2.3.6	Experiments on Air Locked in Wound Reels	42
2.3.6.1	Motivation	42
2.3.6.2	Equipment	48
2.3.6.3	Tests and Results	48
2.3.7	Analytical Studies	48
2.3.7.1	Introduction	48
2.3.7.2	Winding Speed and Tension During Fast Winding	52
2.3.7.3	Stresses in a Heated and/or Rotating Reel Modeled by a Disk	54
2.3.7.4	A Model for Reel Slippage During Deceleration	62
2.3.7.5	Estimates of Periods Between Rewinds	64
2.3.7.6	Air Entrapment During Packing Roller Assisted Winding	68
2.3.7.7	Dynamics of a Packing Roller Follower	70
2.4	Chemical Kinetics of Tape Binder Degradation	75
2.5	System Storage Investigation	82
2.5.1	System Description	82
2.5.1.1	Computer	83
2.5.1.2	TBM	83
2.5.1.3	Instrumentation	83
2.5.2	Storage Conditions	84
2.5.3	Storage Periods	84
2.5.4	Storage Results	85
2.5.4.1	Low Density Computer	85
2.5.4.2	TBM	86
2.5.4.2A	Addendum - Seven Year Old TBM Tape	89
2.5.4.3	High Density Instrumentation System	92
2.6	Summary and Recommendations for Further Work	93
2.6.1	Summary	93
2.6.2	Recommendations for Further Study	94

**Table of Contents (Continued)**

<b>3.0</b>	<b>ARCHIVAL STORAGE RECOMMENDATIONS</b>	<b>97</b>
<b>3.1</b>	<b>Qualification, Handling and Storage Procedure</b>	<b>97</b>
<b>3.1.1</b>	<b>Tape Qualifications</b>	<b>97</b>
<b>3.1.2</b>	<b>Tape Handling and Storage Procedure</b>	<b>99</b>
<b>3.1.2.1</b>	<b>General Storage Requirements</b>	<b>99</b>
<b>3.1.2.2</b>	<b>Temperature-Humidity Requirement</b>	<b>100</b>
<b>3.1.2.3</b>	<b>Rewind Frequency</b>	<b>100</b>
<b>3.1.2.4</b>	<b>Temperature and Humidity Storage Fluctuation Bounds</b>	<b>102</b>
<b>3.1.2.5</b>	<b>Recommendations for Environmental Variations</b>	<b>102</b>
<b>3.1.2.6</b>	<b>Recommendation for System Variations</b>	<b>104</b>
<b>3.1.2.7</b>	<b>Recommendations Regarding Tape Transports</b>	<b>104</b>
<b>3.1.2.7</b>	<b>Acquisition Storage and Handling Sequence</b>	<b>104</b>
<b>3.2</b>	<b>Optimum System Configuration</b>	<b>105</b>
<b>3.2.1</b>	<b>Introduction</b>	<b>105</b>
<b>3.2.2</b>	<b>Summary of Limiting Parameters</b>	<b>107</b>
<b>3.2.3</b>	<b>Recommended Optimum System Design</b>	<b>108</b>
<b>REFERENCES</b>		<b>111</b>

## LIST OF FIGURES

1	Plated Disc Scheme	9
2	Thermal Demagnetization of CrO <sub>2</sub> Tape	11
3	Characteristics of a 4-Parameter Viscoelastic Material	17
4	Schematic Description of the Effect of Various Parameters on the Stress Distribution in a Reel	19
5	Basic Trends of Normalized Interface Pressure at Hub vs. Relaxation Time	21
6	Essential Features of Creep Data of Polyester Film	21
7	Temperature-Time Interchange Factor $\alpha_T$	23
8	Schematic Description of Interlayer Air Entrapment During Reel Winding	23
9	Predicted Air Film Thickness Trapped During Reel Winding in the Absence of Side Flow	25
10	Shrinkage of a Typical Mylar Sample	25
11	Schematic View of Creep Measurement Apparatus	28
12	Photograph of Creep Measurement Apparatus	29
13	Extension of 24" Samples Nominally at 65°F, 55%RH as a Function of Time	31
14	Creep Strain of Polyester Base Film for Specified Test Periods	33
15a	Photographic View of Creep/Shrinkage Measurement Apparatus for Controlled Environments	35
15b	Detail of Pendulums for Tape Length Measurement	35
16	Time Dependent Strain vs. Time for Different Tensile Stress at 50°C, 50%RH	37
17	Time Dependent Strain vs. Stress for Different Times at 50°C, 50%RH	39
18 a,b	Armature Back EMF of Reel Motor Owing to a "Sudden" Reel Deceleration	41
19	Radial Distribution of Tab Pull Force Showing Various Effects	43
20	Slippage of Ampex 799 Instrumentation Tape in Response to a 400 Ra/Sec <sup>2</sup> Deceleration	44
21	Correlation of Tab Pull Force with Angular Slip During a Sudden Deceleration	45

List of Figures (Continued)

22	Effect of Winding Speed on Tab Pull Force	46
23	Correlation of Tab Pull Force With Time in Oven at 50°C, 50%RH	47
24	Effect of Environmental Conditions on Tab Pull Force	49
25	Tab Pull Force vs. Average Packing Roller Load	50
26	Angular Speed of Take Up Reel as a Function of Radius for Two Values of Roller Load	51
27	Typical Reel Angular Velocities and Tape Winding Tension vs. Take Up Reel Radius	56
28	Qualitative Effect of Various Parameters on Angular Speed and Tension During Constant Torque Wind With No Capstan Control	57
29	Comparison of Theoretically Predicted Pressure Distribution in a Reel With Experimental Results Obtained by Friction Tabs	63
30	Free Body Diagram of a Decelerating Reel (Tightening Direction)	65
31	Schematic Comparison of Terms in the Slip Condition	65
32	Estimated Period Between Rewinds as a Function of Storage Temperature	67
33	Schematic View of Packing Roller Assisted Winding	71
34	Sample Curves Showing Effect of Various Parameters on Lead Required per Unit Width to Reduce Air Film to 100 $\mu$ in	71,72,73
35	Model of Packing Roller Following a Reel with Runout	74
36	Frequency Response of a Typical Packing Roller Follower with Respect to Reel Runout of Form $x_{\max} \sin \omega t$	74
37	Hydrolysis Equilibrium Curves vs. Humidity and Temperature	79
38	Error Rates vs. Storage Time for TBM Tape for Three Different Storage Conditions	90
39	Error Rate vs. Storage Time for Instrumentation Tape for Three Different Storage Conditions	95
40	Tape Storage Environment Recommendation on the Basis of the Hydrolysis of the Tape Binder	101

## **LIST OF TABLES**

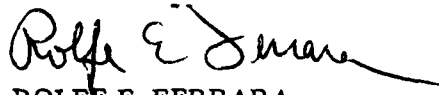
1	Magnetic Tape Particles and Their Properties	4
2	Accelerated Storage	12
3	Accelerated Storage	12
4	Typical Properties of Polyester Base Film	18
5	Order of Magnitude of Length Changes Initially Considered in Construction of Creep/Shrinkage Measurement Apparatus	34
6	System Summary	82
7	Bit Error Rate - TBM	87
8	Bit Error Rate - High Density Instrumentation	91
9	Acquisition Storage and Handling Sequence for Archival Magnetic Tape	106

## PREFACE

This report supersedes Ampex Report RR 79-21 of June 30, 1979. It consists of an amalgamation of the earlier work with new results obtained under Revised Amendment No. 1 to the Statement of Work Contract F30602-78-C-0181.

## EVALUATION

This effort addresses the unknowns of long term Digital Data Base Storage utilizing the most widely used record media, magnetic tape. It has resulted in a comprehensive "profile" of measured and projected characteristics of this storage media over the commercial long term storage range of 10 to 15 years. The study was conducted under TPO R2D, at the request of, and in response to problems surfaced by the Defense Mapping Agency in their digital records operations. The balance between long term data base integrity and operating costs, both in physical resources and manpower, will now be able to be judged with a high degree of confidence. The comprehensive base line magnetic tape storage characteristics detailed in this report are applicable to both present and future AF/DOD magnetic tape digital data bases.

  
ROLFE E. FERRARA  
Project Engineer

## 1.0 INTRODUCTION

This report represents the conclusion to RADC Contract No. F30602-78-C-0181 entitled "Recording Media Archival Attributes (Magnetic)" which began May 30, 1978 and concluded Nov. 30, 1979. In the statement of work for this contract a variety of technical requirements were listed, and the organization of this report is in direct response to those tasks. In the second chapter entitled "Archival Storage Study", discussions are given of the various tasks completed during the course of this study. In the first part, a discussion of the tape coating constituents, the magnetic particles and the chemical binder formulations, are given. In the following subsections, the results of experiments and analysis on possible archival degradation modes of these two constituents and on the mechanical aspects of tape pack integrity are given. The first (Section 2.2) gives an analysis of magnetic signal loss due to archival storage as well as a discussion of the print-through phenomenon. Print-through is negligible for digital recording applications, but the explicit reasons should be set forth.

In the next part (Section 2.3), the mechanical aspects of the tape are analyzed. Experimental results of creep measurements are presented. The most important binder degradation mechanism for the polyurethane binder, hydrolysis, is discussed in Section 2.4, and storage conditions to minimize its effect are evaluated. In Section 2.5 the results of a major requirement of the work statement are presented. This is the study of tape archivability as recorded on actual digital recording systems which span the range of linear recording densities from 1600 bpi to 33k bpi. In the final part of this section, the main conclusions of these studies are summarized and suggestions for further work are given.

In the final chapter, the results of the previous sections are utilized to recommend archival storage conditions. The first part consists of two subsections. The first deals with requirements of magnetic tape in order to be acceptable for archival storage application. The second describes in some detail the actual step-by-step handling and storage procedure from receiving the tape to replaying after a long storage period. In the final part of this section, an outline for an actual archival system is given which meets the various storage capacities, data rates and access times requirements cited in the statement of work.

## **2.0 ARCHIVAL STORAGE STUDY**

### **2.1 Identification of Recording Materials and Formulations Suitable for Digital Recording**

In this section magnetic recording media as well as the tape binder system will be discussed. The constituents of magnetic tape are generally suitable for all magnetic recording applications. For digital recording the main requirement is in uniformity and/or surface cleanliness since it is the dropout-induced error rate which limits performance. Surface homogeneity or cleanliness depends primarily on processing conditions and not on the particular tape ingredient. Thus the following listing of media components will not be categorized under suitability for digital recording.

#### **2.1.1 Magnetic Tape Recording Media**

A list of the various magnetic particles used in magnetic recording media are given in Table 1 along with their primary magnetic characteristics. The first two listed, gamma ferric oxide ( $\gamma\text{Fe}_2\text{O}_3$ ) and chromium dioxide ( $\text{CrO}_2$ ), are currently the most widely utilized. The following, iron particles (Fe) and the Co-epitaxy -  $\gamma\text{Fe}_2\text{O}_3$ , three columns further on, are relatively new particles; however, in the near future they will probably enjoy widespread application. Conventional Co- $\gamma\text{Fe}_2\text{O}_3$  and Co- $\gamma\text{Fe}_3\text{O}_4$  refers to cobalt addition by uniform doping whereas Co-epitaxy  $\gamma\text{Fe}_2\text{O}_3$  or  $\text{Fe}_3\text{O}_4$  refers to the process in which the cobalt ions are placed solely on the surface of the particles. The conventional cobalt doped gamma ferric oxide, Co- $\gamma\text{Fe}_2\text{O}_3$ , and doped magnetite Co- $\gamma\text{Fe}_3\text{O}_4$  have been available for 10-15 years; however, their use has remained limited due to unresolved instabilities which will be discussed below.

In the first and second rows the particle specific moments and saturation magnetizations are given. These two quantities are directly related by the particle density since magnetization (gauss) is simply moment (emu) per volume (cc). It is desirable to utilize particles with as high a magnetization as possible since the output of a tape recorder is proportional to the recorded magnetization level on the tape. Except for the iron particle, (Fe), all the particles exhibit similar particle magnetizations. These values are significantly smaller than that given by iron, since iron particles approach the ideal

Table 1 Magnetic Tape Particles and Their Properties

PIGMENT	$\gamma\text{Fe}_2\text{O}_3$	$\text{CrO}_2$	$\text{Fe}$	$\text{Co}\cdot\gamma\text{Fe}_2\text{O}_3$	$\text{Co}\cdot\text{Fe}_3\text{O}_4$	CO-EPIITAXY $\gamma\text{Fe}_2\text{O}_3$	CO-EPIITAXY $\text{Fe}_3\text{O}_4$
MOMENT (EMU/G)	72	75	150	72	80	68	77
SATURATION MAGNETIZATION (GAUSS)	350	375	930	350	400	335	385
CURIE TEMPERATURE (°C)	590	130	770	590	585	DECOMPOSES FIRST BUT SUITABLY HIGH	
SIZE ( $\mu\text{M}$ )	.09x.09x.9	.05x.05x.4	.05x.05x.4	.05x.05x.4	same as $\gamma\text{Fe}_2\text{O}_3$	same as $\gamma\text{Fe}_2\text{O}_3$	same as $\gamma\text{Fe}_2\text{O}_3$
COERCIVITY (Oe)	300-400	480	800-1100	300-1200	300-1200	300-500	300-800
IN TAPE:							
REMANENT FLUX DENSITY ( $B_r$ -GAUSS)	1400	1400		3000	1200	1500	1400
SQUARENESS ( $B_r/B_s$ )	.83	.83		.75	.71	.80	.85

maximum moment where no non-magnetic ions reduce the magnetic density and the magnetic iron moments are all parallel (ferromagnetic). One of the advantages of a tape utilizing iron particles, thus, is the 8 dB (eventually 12 dB) increase in magnetization which, in fact, results in an increase in signal output of at least that much over conventional  $\gamma\text{Fe}_2\text{O}_3$ .

In the third column the Curie temperatures of the particles are given. All particle magnetizations decrease with temperature, and the Curie temperature is the temperature at which the particle becomes non-magnetic. Except for chromium dioxide, all the Curie temperatures are extremely high so that no catastrophic loss in signal can be expected at any realistic temperature elevation. The decomposition comment about the epitaxial cobalt doped  $\gamma\text{Fe}_2\text{O}_3$  and  $\text{Fe}_3\text{O}_4$  refers to the diffusion of the surface cobalt atoms to volume sites before the Curie temperature is reached. However, this is thought to occur at temperatures on the order of 250°C-350°C, which again is well above tape storage temperatures. Chromium dioxide, however, has a sufficiently low Curie temperature that care must be taken with its handling. Usually all magnetic tape is kept below approximately 70°C since at that temperature substrate deformation can occur. However, more important are the effects of temperature in a small range around room or ambient temperature (20°C, 50%RH). Virtually all particles are suitable under these conditions.

The individual particle size is given next. For noise considerations, it is desirable to utilize particles as small as possible. Complete manufacturing control over particle size is impossible; however,  $\text{CrO}_2$  and Fe particles are smaller than the  $\gamma\text{Fe}_2\text{O}_3$  or  $\text{Fe}_3\text{O}_4$  based particles and this factor does contribute to a better signal to noise ratio for tapes composed of these particles.

Following the particle sizes is a row giving the particle coercivities. In fact, these numbers represent measurements on unoriented particle powders and yield values which are close to final tape values but perhaps as much as 30% below that of an isolated particle. The coercivity is the magnetic field required to reduce the magnetization to zero from a state of saturation. The advantage of a large coercivity is that it prohibits tape demagnetization (particularly at short wavelengths or high frequencies). The difficulty is that large coercivities require large recording currents and can, with the use of ferrite record heads, lead to head saturation problems. The increased  $\text{CrO}_2$  coercivity over that of  $\gamma\text{Fe}_2\text{O}_3$  does in fact lead to higher short wavelength output even though the particle magnetizations are very close. The greatly increased performance of Fe tapes is due to the simultaneous increase of coercivity with particle magnetization. The coercivity of iron ( $\sim 1000$  Oe) perhaps represents a practical limit due to ferrite head saturation.

Nevertheless, in the coercivity range of 300-1000 Oe, as evidenced by the table, the trend has been towards higher coercivities which uniformly has led to improved short wavelength outputs.

In the last two rows actual tape properties are given. In the first row, the tape remanent magnetization or flux density ( $B_r$ ) is given. These numbers differ from the particle magnetizations by first a conventional factor of  $4\pi$  and second, a volume loading factor reduction which typically is 35-45%. Again, all the remanence flux densities are similar except for the iron tape which is at least twice that of the others. The remanent flux densities also differ from the particle magnetizations by the squareness which is given in the next row. The squareness or remanence ratio indicates how well the particles are oriented in the tape. Perfect orientation would be unity. Good orientation leads not only to large remanent flux densities but to M-H loops with "straighter sides" (narrow spreads in switching fields). The first contributes to a wide band signal increase whereas the latter results in improved short wavelength outputs. In the past ten years squarenesses have increased from about .65 to almost .85 due to better dispersions, cleaner more needle like particles, etc. Tapes made from Fe particles exhibit squarenesses  $\approx .75$  which may be due in some sense to being under development for fewer years than the more common tapes.

The high squarenesses of the conventional  $\text{Co}-\gamma\text{Fe}_2\text{O}_3$  and  $\text{Co}-\gamma\text{Fe}_3\text{O}_4$  are not due to orientation but due to an overall cubic crystalline anisotropy. All the others exhibit uniaxial anisotropy which yields squareness which vary from .5 (unoriented) to 1.0 (completely oriented).

Finally, it is of interest to point out some possible instability problems which might have a bearing on archivability. First, all tapes are sensitive to temperature and pressure. All but the conventional  $\text{Co}-\gamma\text{Fe}_2\text{O}_3$  have reasonably low magnetization loss with temperature or loss with pressure. The  $\text{Co}-\gamma\text{Fe}_2\text{O}_3$ , because its behavior is dominated by cubic crystalline anisotropy, is susceptible to such losses. This difficulty has led to the Co-epitaxy  $\gamma\text{Fe}_2\text{O}_3$  in which the nature of the anisotropy is altered by the fact that the Co ions are restrained to the particle surface. These epitaxial particles exhibit very small temperature or pressure losses similar to the others in the table. It is possible in the future that this problem with conventional Co-doped  $\gamma\text{Fe}_2\text{O}_3$  will be solved.

As mentioned earlier, it is possible that at high enough temperatures,  $\sim 300^\circ\text{C}$ , the Co-epitaxy  $\gamma\text{Fe}_2\text{O}_3$  converts to the conventional  $\gamma\text{Fe}_2\text{O}_3$  and then would exhibit the latter instability or loss problems. However, since the temperature required is so high with respect to realistic environments, this effect may be discounted.

### **2.1.2 Magnetic Disc Recording Media**

Disc recording media comprise essentially two categories: in one, tape particles are simply coated on the disc substrate and in the other, the recording media consists of a plated layer of a cobalt, nickel, phosphorous granular compound. In the first case, it is possible to use any of the tape particles in Table 1 for a rigid or floppy disc. However, until now, only  $\gamma\text{Fe}_2\text{O}_3$  has been utilized. The binder system is phenolic epoxy and until recently, the particles have been unorientated, with squareness ratios in the circular direction on the order of .55-.65. Recently, however, attempts at orientation have been made in order to increase the signal output and squarenesses .75 or more have been achieved. Orientation in discs is difficult since it is essential that no signal modulation (or orientation variation) occurs around the disc.

Plated discs were developed 10-15 years ago and a cross-sectional view is shown in Fig. 1. In the plating process a 250 mil aluminum substrate is first polished. Then an electroless nickel layer is plated followed by a polishing of its surface. The magnetic layer is then plated with a 85% cobalt 14% nickel, 1% phosphorous solution to a depth of 2 - 10 $\mu\text{in}$ . A final protective coating of rhodium or oxide protects the magnetic layer and is itself 7 - 10 $\mu\text{in}$ . thick. It is believed that the magnetic layer structure is comprised of 500 Å size magnetic grains separated by a small non-magnetic interface. The coercivity can be controlled by the plating composition but typically is approximately 500 Oe. The particle magnetization is 1200 gauss due to the high concentration of very magnetic ions. With virtually unity packing and a .7 - .8 squareness ratio, large remanent flux densities on the order of 10,000 G are achieved.

### **2.1.3 Magnetic Recording Media Formulations**

Magnetic tape and coated discs consists of a magnetic coating on a normally flexible substrate. The substrate serves as an inert carrier, and in the great majority of applications, this material is polyethylene terephthalate film.

Magnetic coatings contain the following kinds of materials: magnetic pigment (already described in Section 2.1.1), binder, dispersant, usually with other minor ingredients including lubricants, conductive pigments and fungicides. A typical composition contains 70 - 80 wt % magnetic material, 15 - 20 wt % binder, and the remaining 5 - 10 wt % "additives". The present discussion will be limited to a description of binders commonly used since it is this component which is primarily responsible for the cohesive and adhesive strength of the coating and ultimately its durability.

(1) Polyurethanes - These stand out among all available polymers because of their unusually good combination of properties, e.g., tensile strength and elongations (toughness), abrasion resistance, adhesion as well as their ability to permit the formation of suitable dispersions of pigments. The base resins are thermoplastic and are of two structurally different types: polyester and polyether. Most all precision magnetic tapes employ thermoset systems, and these are formed by the addition of a reactive component which is not a binder itself but which cross links reactive sites in the polymer chains. Thermoset systems are harder, tougher, and more solvent resistant than thermoplastic systems and are more durable and environmentally inert.

(2) Phenoxy - Phenoxy resins are a copolymer of bis-phenol-A and epichlorohydrin and, while they are not suitable for use as binders alone, they serve to harden polyurethane-containing tapes and provide in them further sites for cross-linking with curing agents. Some precision-tape applications require this co-binder combination for optimum performance.

(3) Polyvinylidene dichloride/acrylonitrile - These resins are also hard and are particularly useful as co-binders with polyurethanes. Many of the older tape formulations employed these resins as the sole binder, but the toughness and durability of these coatings were not comparable to that of present day coatings. Also, the rheological properties of coating mixes employing this binder alone are often poor, a factor which has detracted from its use as a major component in magnetic tape.

(4) Cellulose Nitrate - This resin is not normally used alone but is effective in hardening polyurethane binder systems. In addition, high-gloss coatings are readily obtained, partly a manifestation of smooth surfaces, a very important requirement in recording short wavelengths. The tensile properties of cellulose nitrate are very poor compared with those of polyurethanes.

(5) Acrylonitrile/Butadiene - These co-polymers are thermoplastic or elastomeric materials and possess high tensile strength but poorer abrasive resistance and toughness, generally, relative to the polyurethanes. They have been used for many years in some of the less sophisticated tape products, especially in combination with harder binders such as the chlorinated resins. Formulations containing this binder require stabilizers to inhibit long-term oxidative degradation of the polymer.

(6) Vinyl/Chloride/Vinyl Acetate - Vinyl resins are a discrete step below polyurethanes in tensile properties and resistance to wear. Nonetheless, certain vinyl copolymers containing high vinyl chloride polymer component (90%VC, 10%VA) are useful in

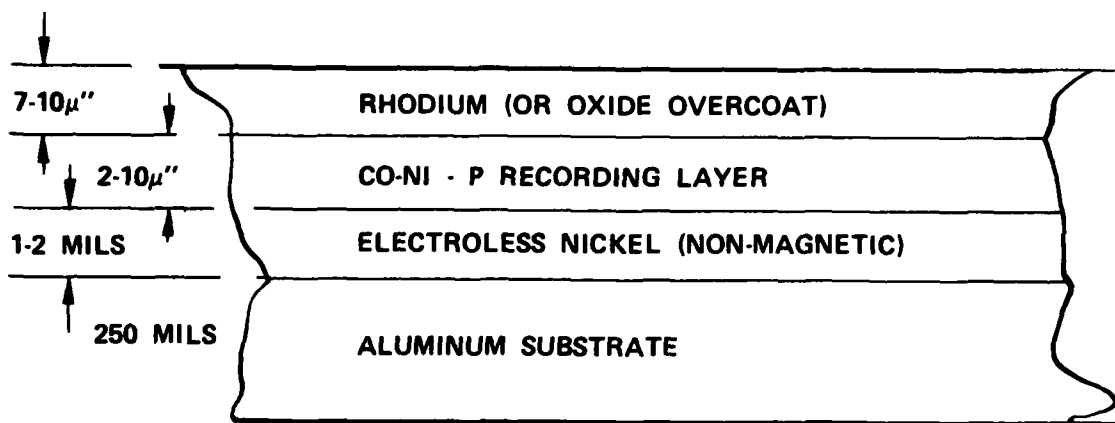


Figure 1 Plated Disc Scheme

tapes in which high abrasion resistance and durability are not a primary concern. These resins are especially useful as co-binders with elastomeric polymers such as acrylonitrile/butadiene or butadiene/styrene copolymers.

(7) Epoxy - These resins are used in place of phenoxy resins (see above) in some applications. In the case of non-flexible discs, the high modulus of "pure" (cross-linked) epoxy systems is not a problem, and the unusual inertness and adhesion of these polymer types is exploited.

(8) Polyesters - Polyesters vary widely in physical properties but none has stress-strain properties comparable to those of polyurethanes, and abrasion resistance is less. They normally are present as co-binders with other resins which have greater elongation and toughness but lack hardness. Polyesters are used to a limited extent in some present-day, precision magnetic tape coatings.

## 2.2 Recording Signal Studies

There are two primary mechanisms by which the magnetic pattern recorded on a tape archivally stored may be altered to produce increased error rates. The first discussed in 2.2.1 is simply the long-term signal degradation due to the presence of finite activation energies. The other is print-through which is discussed in 2.2.2. Print-through is important for longwavelength recording applications and is shown here to be negligible for digital recording applications.

### 2.2.1 Loss of Magnetic Signal With Storage

A possible tape degradation mechanism under archival storage is the loss of recorded signal. This is a magnetic instability phenomenon which involves not the chemistry of the tape but the magnetic particles themselves. When tape is recorded, the magnetic moments align themselves on the average in the direction of the recording field. When tape is stored on a reel, the particles are stable against demagnetization since fields on the order of the coercivity are required to reverse the particle moment directions. The coercive force corresponds to an energy barrier which inhibits reversal. This barrier also acts as a thermal activation energy so that storage at elevated temperature over long time periods could cause some demagnetization. The coercive force of a tape is the average switching field and represents a virtually unsurmountable barrier against thermal agitation. However, two factors might allow for significant thermal demagnetization under archival storage periods. One is that tape coercivities are distributed over a rather broad range so that the low coercivity particles will switch more easily due to thermal excitation (i.e., lower energy barrier). The second is that for short wavelength recording, demagnetization fields exist due to the recording pattern which can significantly lower the effective coercivity or thermal excitation barriers. These two factors lead to questions about the stability during archival storage of the recorded magnetization or signal on the tape. Thus it was felt that an investigation of stability would be appropriate under the scope of this study. The plan was to store recorded tape at elevated temperatures for short periods of time in order to determine activation energies for the thermal demagnetization process and thereby be able to predict archival behavior.

The experiment is to record a tape with a range of wavelengths encompassing the lowest and highest bit densities. The tape is then stored at an elevated temperature for a long period. The replay signal after storage gives the loss due to thermal demagnetization. From such time-temperature data and some theorizing it is possible to obtain activation energies as a function of recorded density. From that information it would then be possible to predict archival storage effects.

In Table 2 a sample of the measurements are presented. The tape utilized was Ampex's '456'  $\gamma\text{Fe}_2\text{O}_3$  audio mastering tape and the measurements were made on an Ampex 'ATR100' professional audio recorder. The recording speed was reduced to 4 cm/sec so that short wavelengths (high densities) could be recorded. In this example, the storage condition was room temperature ( $20^\circ\text{C}$ ), nominal humidity ( $\sim 50\%$ ) for a period of 10 months. The shortest wavelength recorded was  $1.6 \mu\text{m}$  corresponding to a density of  $1.25 \times 10^6 \text{ bpm}$  or 31.25k bpi. Square wave current signals were utilized

and the current at all wavelengths was that which optimized the  $1.6 \mu\text{m}$  output. The obvious conclusion from the data in Table 2 is that there was virtually no signal change at any wavelength from initial recording to the final reading. This is perhaps not too surprising since the temperature is low. In Table 3 results are presented for storage at an elevated temperature ( $55^\circ\text{C}$ ) for a shorter period (37 days). One section of data is shown although three separate regions of tape were utilized for a consistency check. The results are virtually identical with the room temperature measurements. That is, there is no discernable demagnetization loss due to a thermal activation process.

The conclusion from these experiments is that no reasonable acceleration test yields thermal demagnetization. Thus, it appears that the archivability of  $\gamma\text{Fe}_2\text{O}_3$  magnetic tape at nominal ( $20^\circ\text{C}$ , 50%RH) (or cooler) temperatures is reasonably guaranteed.

Accelerated magnetic tests ( $55^\circ\text{C}$ ) were also performed on  $\text{CrO}_2$  and  $\text{Co}-\gamma\text{Fe}_2\text{O}_3$  tapes. In those cases, some loss was measured. In Fig. 2 the loss for  $\text{CrO}_2$  is shown.

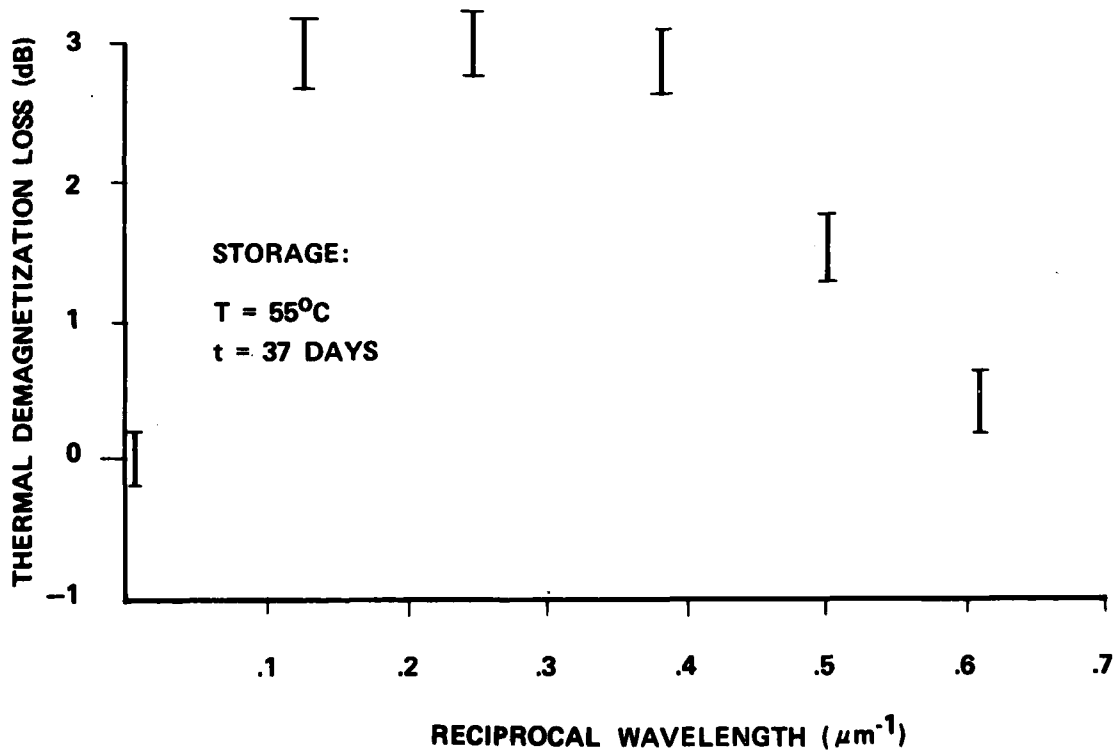


Figure 2 Thermal Demagnetization of  $\text{CrO}_2$  Tape

**Table 2**

**Accelerated Storage**

Tape: Ampex '456'    Oven Condition:    Temp: 20°C    Storage Time: 10 Months  
Humidity: 50%

Wavelength	Equivalent BPI	Level Before	Level After	Difference
1.6 μm	31,250	-48.3 dB	-48.6 dB	-0.3 dB
2.0	25,000	-37.8	-38.0	-0.2
2.7	18,500	-29.8	-29.4	+0.4
4.0	12,500	-22.0	-21.5	+0.5
8.0	6,250	-14.8	-14.6	+0.2
80.0	625	-17.6	-17.5	+0.1

**Table 3**

**Accelerated Storage**

Tape: Ampex '456'    Oven Condition:    Temp: 55°C    Storage Time: 37 Days  
Humidity: 50%

Wavelength	Equivalent BPI	Initial Rec Level	Post Oven Rec Level	Level Change
1.6 μm	31,250	-51.5 dB	-51.6 dB	-0.1 dB
2.0	25,000	41.7	-41.8	-0.1
2.7	18,500	-32.1	-32.5	-0.4
4.0	12,500	-23.6	-24.2	-0.6
8.0	6,250	-16.5	-17.0	-0.5
80.0	650	-23.9	-23.9	+0.0

Surprisingly, no loss occurs at either short (31k bpi) or long (625 bpi) wavelengths; the Co- $\gamma$ Fe<sub>2</sub>O<sub>3</sub> consistently showed loss patterns similar to CrO<sub>2</sub>. The reason for this peculiar pattern is not yet explained. Most likely it results from a combination of the wavelength dependence of the demagnetization fields (which may not be greatest at the shortest wavelengths!) and the large temperature dependence of the coercivity for both CrO<sub>2</sub> and Co- $\gamma$ Fe<sub>2</sub>O<sub>3</sub>. These results indicate that these tape materials may not be suitable for long archival storage. However, further study needs to be done since the temperature dependent coercivity entails a temperature dependent thermal demagnetization energy barrier which complicates the analysis. A coercivity which strongly decreases with temperature such as exhibited by CrO<sub>2</sub> and Co- $\gamma$ Fe<sub>2</sub>O<sub>3</sub> unfairly enhances normal (20°C, 47%RH) temperature, long-term demagnetization loss, predictions from a higher temperature accelerated test.

## 2.2.2 Print-Through

In this section we discuss a slightly peripheral question, however, one that is continually raised in magnetic recording: the subject of print-through. Print-through occurs during tape storage since, with the assistance of time and temperature, the fields from one recorded layer in the reel cause a magnetic signal to be recorded in the adjacent layers. Print-through is solely a long wavelength phenomenon and is negligible for short wavelength applications.

It will be shown in this section that print-through is negligible for all archival (25-50 year) storage periods for even low density computer applications. The essential question is: does print-through ever reach the -30 dB level to cause error rate degradation in digital recording applications? We answer that question by examining a formula (Eq. 1), which relates the print-through at one set of temperature T (°C), storage time t (sec), recorded wavelength  $\lambda$ , media thickness d, and substrate thickness  $d_s$  to that at another set:

$$\begin{aligned}
 P(T_2, t_2, \lambda_2, d_2, d_{s2}) &= P(T_1, t_1, \lambda_1, d_{1m}, d_{s1}) \\
 &+ .14 (T_2 - T_1) + 20 \log_{10} \left\{ \frac{\log_{10} t_2}{\log_{10} t_1} \right\} - 55 \left( \frac{d_{s2}}{\lambda_2} - \frac{d_{s1}}{\lambda_1} \right) \quad (1) \\
 &+ 20 \log_{10} \left\{ \frac{1-e^{-4\pi d_2/\lambda_2}}{1-e^{-4\pi d_1/\lambda_1}} \right\}
 \end{aligned}$$

This expression results from a combination of theoretical and empirical studies and applies essentially to  $\gamma\text{Fe}_2\text{O}_3$  media.<sup>[1]</sup> As a bench-mark, we have for audio mastering tape

$$P(20^\circ\text{C}, 24 \text{ hours}, 15.2 \text{ mils}, .5 \text{ mils}, 1.5 \text{ mils}) = -50 \text{ dB} \quad (2)$$

As a worst case example let us consider computer tape stored at  $20^\circ\text{C}$  for 50 years where  $d = .5 \text{ mils}$ ,  $d_s = 1.5 \text{ mils}$ . We choose a worst case wavelength of that corresponding to ten times the bit density or

$$\lambda = 10 \lambda_b = 10 \times \frac{2}{1600} = 12.5 \text{ mils} \quad (3)$$

which yields

$$P(T = 20^\circ\text{C}, t = 50 \text{ years}, \lambda = 12.5 \text{ mils}, d = .5 \text{ mils}, d_s = 1.5 \text{ mils})$$

$$\begin{aligned} &= -50 + 20 \log_{10} \left\{ \frac{\log_{10} 50 \times 3.15 \times 10^7}{\log_{10} 24 \times 60 \times 60} \right\} - 55 \left( \frac{1.5}{12.5} - \frac{1.5}{15.2} \right) \\ &\quad + 20 \log_{10} \left\{ \frac{1 - e^{-4\pi \times .5/12.5}}{1 - e^{-4\pi \times .5/15.2}} \right\} \\ &= -50 + 5.4 - 1.17 + 1.34 = -44 \text{ dB} \end{aligned} \quad (4)$$

As this example shows, the print-through is increased but is still 14 dB below that considered detrimental to error rates. In this example, the change in storage time from 24 hours to 50 years only increases the print-through 5.4 dB! In addition, the wavelength effect is small since ten times the bit density for 1600 bpi computer application corresponds to a peak print-through wavelength at which audio measurements are made ( $\lambda_{\text{peak}} = 2\pi(d + d_s)$ ). To illustrate the effect of wavelength, we evaluate the print-through for high density 33k bpi at tens times the bit density

$$\text{or } \lambda = 10 \times \frac{2}{33000} = .61 \text{ mils} \quad (5)$$

(and for this application  $d = .2 \text{ mils}$ ,  $d_s = .8 \text{ mils}$ )

Thus we obtain

$$\begin{aligned} P(T = 20^\circ\text{C}, t = 50 \text{ years}, \lambda = .61 \text{ mils}, d = .2 \text{ mils}, d_s = .8 \text{ mils}) \\ = -50 + 5.4 - 55 \left( \frac{.8}{.61} - \frac{1.5}{15.2} \right) + 20 \log_{10} \left( \frac{1-e^{-4\pi \times .2/.61}}{1-e^{-4\pi \times .5/15.2}} \right) \\ = -50 + \underbrace{5.4 - 66 + 9}_{-57} \\ \cong -102 \text{ dB !!} \end{aligned} \quad (6)$$

Thus shortening the wavelength dramatically reduces the print-through. These examples show conclusively why print-through is negligible in digital recording.

### 2.3 Mechanical Studies of Tape Packs

#### 2.3.1 Introduction

As a first step of this work a survey of the literature available on reel packing and relaxation has been made. In addition, experimental and analytical studies have been carried out to supplement the information available in the literature.

Beyond this introduction Section 2.3 is divided into three main parts. The first part (2.3.2) is aimed at giving the reader a qualitative overview of the mechanical phenomena which are significant to tape archivability. This information is based on the literature survey and is supplemented by our work. The second part (2.3.3 - 2.3.6) describes our experimental efforts in detail and finally Section 2.3.7 summarizes the analytical work under this contract.

#### 2.3.2 Survey of Mechanical Effects Significant to Tape Archivability

##### 2.3.2.1 Basic Model

Generally, analyses of tape winding on reels reported in the literature [2, 3, 4] consider the reel to be a continuous solid disc in plane state of stress with some wound-in initial stress distribution. The hub is assumed to be either an elastic or a viscoelastic material. The reel itself is usually assumed to be viscoelastic and anisotropic. The conventionally assumed viscoelastic model for polyester is that of a four-parameter fluid

described in Fig. 3. Results discussed later indicate, however, the modifications in the model are needed for the purpose at hand. The anisotropy of the reel involves different elastic and thermal properties in the longitudinal, lateral and thickness directions. A summary of typical properties is given in Table 4. It should be emphasized that these properties are only typical. Large variations occur between different manufacturers (major brand names: Mylar, Melinex, Celanar) as well as between different products and manufacturing processes.

In the following, the qualitative effects of various environmental and elastic parameters on the stress distribution in the reel are discussed. (Figure 4) At least two basic criteria from an archival storage viewpoint need be kept in mind: reel integrity and time base errors.

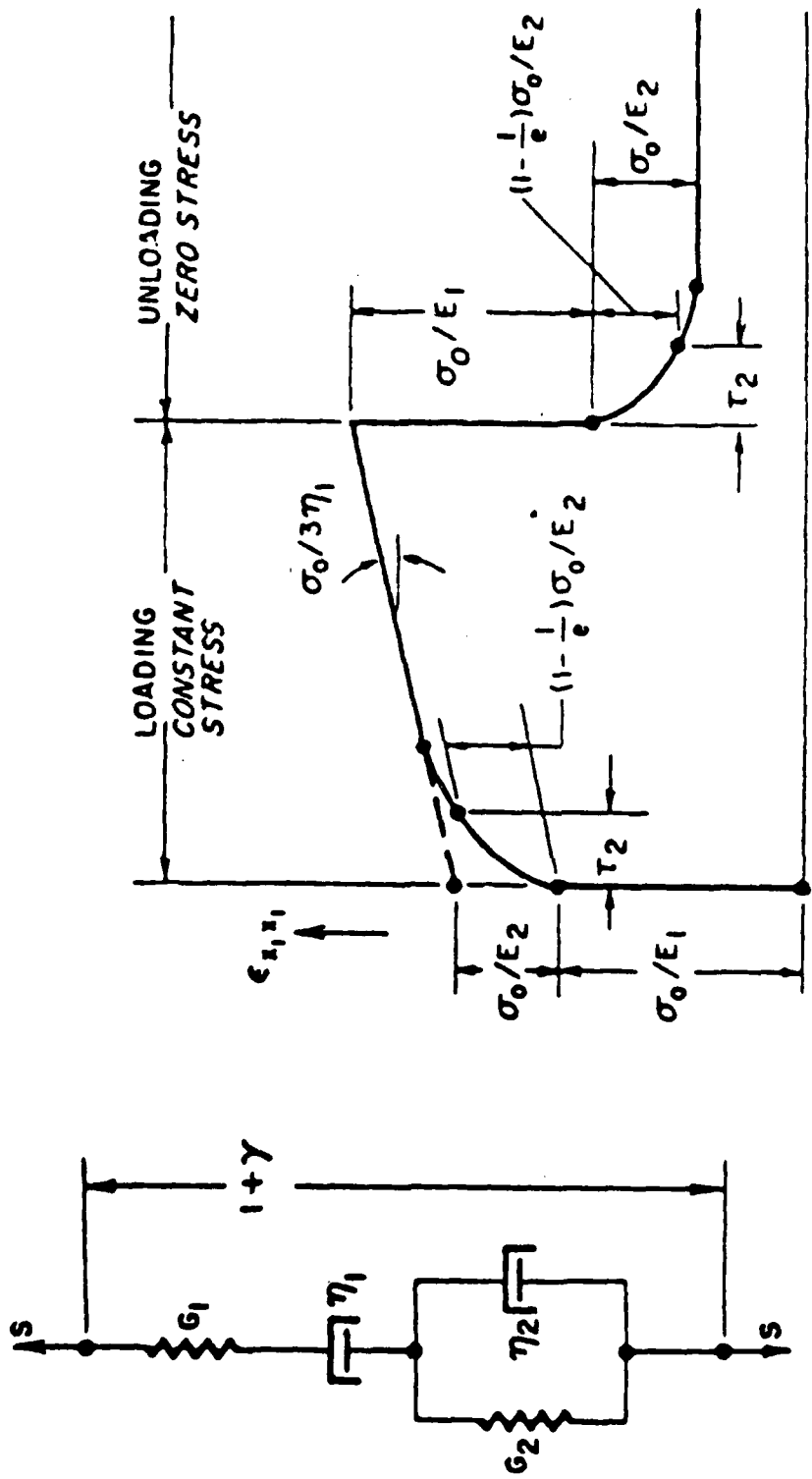
Reel integrity will be adversely affected by stress relaxation in the reel, which may cause mechanical tape damage. Two damage mechanisms may be distinguished. If the interlayer friction is too low, the danger of tape slippage during wind/rewind or transportation arises. If the tension decreases too close to zero or becomes negative, the risks of tape buckling become considerable.

Time base errors may be produced by permanently set strains, reducing the quality of the recorded information. In recent years however, the significance of this factor has been largely eliminated in professional video recording due to modern electronic time base correction techniques as well as accurate tape and head speed servos. Similarly, computer tape drives with self-clocking can successfully avoid this problem.

### 2.3.2.2 Tension and Pressure Distribution in a Wound Reel

During the tape winding process, a stress distribution is induced in the reel. First, the tape winding tension is "remembered" by each layer as it is wound. As more and more layers are wound, their cumulative radial components generate an inwardly growing inter-layer pressure. Due to Poisson's ratio effects, these pressures, in turn, reduce the tensions in the inner layers. Moreover, these tensions may be relieved to the point that the stresses become compressive.

The equations describing the wound-in tensions and pressures in a reel are given in Section 2.3.7.3. [2, 3, 4]. A schematic description of the radial distributions of these variables is shown in Figs. 4a - 4f. Demonstrated are the effects of constant tension winding vs. constant torque winding. Also exhibited is the effect of a compliant hub, which tends to relieve the interlayer pressure. The compliant hub affects the tension level by two opposing effects. On one hand, the relieved pressure contributes less to the



SCHEMATIC OF  
4-PARAMETER MATERIAL  
IN PURE SHEAR

CREEP AND RECOVERY CURVE OF TENSILE  
SPECIMEN.

The model considered is characterized by the following four parameters: Young's Modulus  $E_1$  (of instantaneous elasticity), the modulus of delayed elasticity  $E_2$ , the viscosity  $\eta_1$  (strictly speaking the material is a fluid, it deforms continuously under shear load) and the retardation time  $\tau_2$ . Dilatational response of the material is elastic. Behavior in shear is characterized by the 4-parameter schematic. [4]

Table 4 Typical Properties of Polyester Base Film

(The user of this table is warned that significant variations of properties between different products and manufacturers exist)

	Longitudinal Direction (M.D.)	Thickness Direction (Th.D.)	Lateral Direction (T.D.)
Modulus of Instantaneous Elasticity, E, $E_1$ (psi)	$(5..6) \times 10^5$	$2.5 \times 10^4$ [7]	$(7..8) \times 10^5$ [12]
Modulus of Delayed Elasticity (psi) $E_2$	$20 \times 10^5$ [8,9]		
Asymptotic Creep Strain Rate per Unit Stress * of a Tensile Specimen $(1/\sigma)d\epsilon/dt$ (1/psi x day) = $(1/3\eta_1)$	$0.94 \times 10^{-8}$ [8,9] $1.5 \times 10^{-8}$ [5,6]		
Cumulative Creep Strain per Unit Stress 1/psi *	Tensilized; 1 day [11] $9 \times 10^{-8}$ @ 20°C $45 \times 10^{-8}$ @ 45°C Non Tensilized [11] $14 \times 10^{-8}$ @ 20°C $60 \times 10^{-8}$ @ 45°C $33 \times 10^{-8}$ @ 20°C, 11 day [10] $11 \times 10^{-8}$ @ 45°C, 2 day [13]		
Retardation Time (days) $\tau_2$	2 (@ 70°F) [8,9] 0.5 (@ 113°F)		
Coefficient of Thermal Expansion (1/°C)	$(1.5..1.9) \times 10^{-5}$	$1.5 \times 10^{-4}$ [7]	$1.6 \times 10^{-5}$ [12]
Hygroscopic Expansion Coefficient (1/%RH)	$(3..8) \times 10^{-6}$ [10,11,12]		$7 \times 10^{-6}$ [12]
Poisson's Ratio $\nu$	0.35 [5,6,8,9] 0.23 - 0.27 [13]		
Shrinkage	2.5...4% 190°C [10,12] See Sec. 2.3.4.3		3.5% 5 min. 190°C [12]

\* Linearization of creep rate appears to be too crude for long term storage applications.  
The reader is referred to Sections 2.3.2.3, 2.3.3.3, 2.3.4.3 for further information.

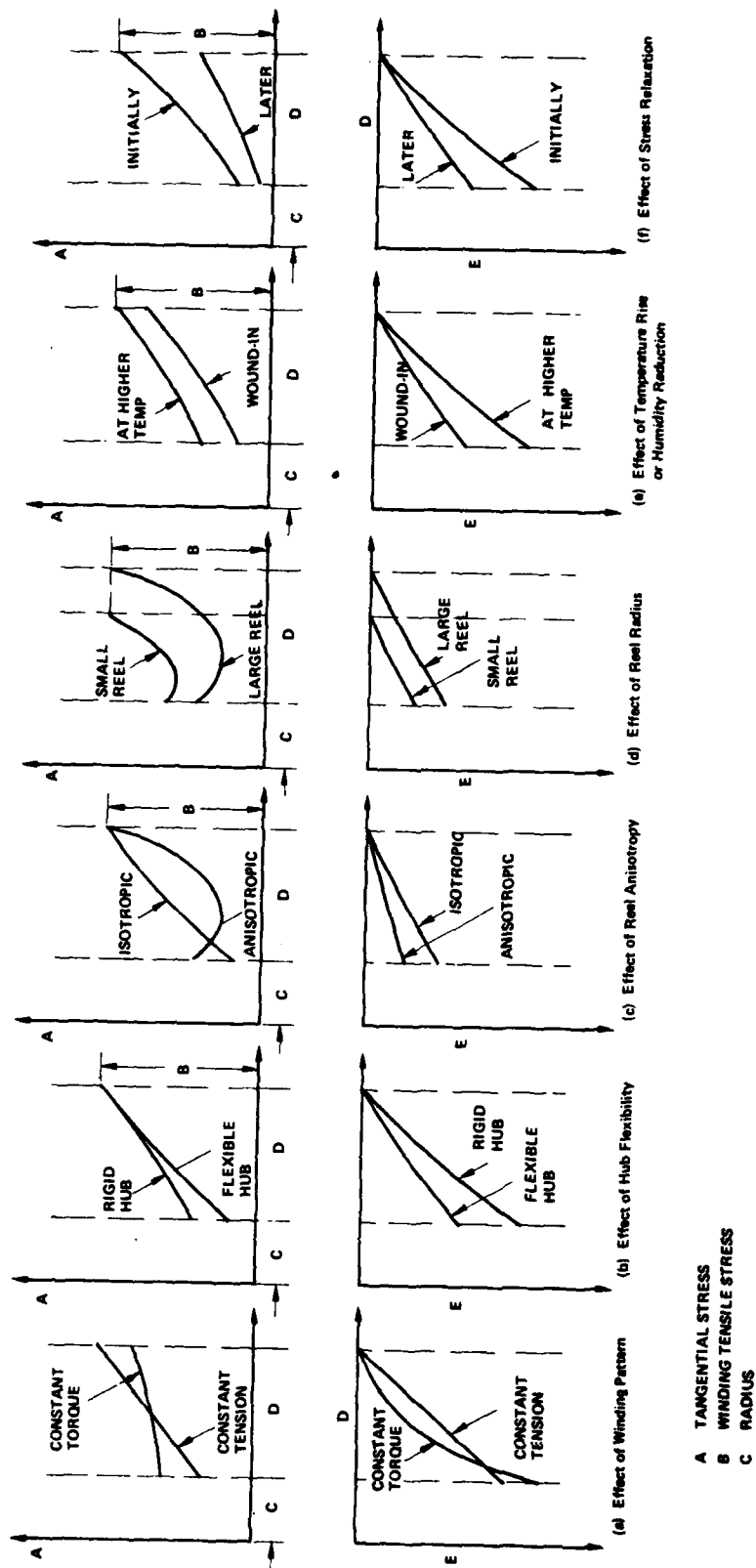


Figure 4 Schematic Description of the Effect of Various Parameters on the Stress Distribution in a Reel. [4,5,6,7,8]

Poisson's ratio effect, keeping the tension high. On the other hand, the inward radial displacement of the tape layers reduces their length and tends to decrease the tension. Usually the latter effect is the dominant one.

### 2.3.2.3 The Relaxation Mechanism

Using the four parameter material model proposed in the literature for polyester films (Figure 3), a film under an imposed tensile stress is expected to creep in time (elongate). Alternatively, a film under an imposed strain will relax. The relaxation rate and the magnitude of unrecoverable creep are proportional to the stress level. Consequently, heavily tensioned films will suffer greater levels of creep than lightly loaded ones. Softer hubs would therefore, prolong relaxation time by initially contracting and reducing the tension level and then expanding and partly replenishing the tension, as relaxation takes place. According to [5] typical relaxation rates would reduce the pressure at the hub to 50% in order of  $100 \tau_2$  (Table 4) and to 10% in approximately  $500 \tau_2$ . If we accept a 50% pressure reduction in the reel as an indication for the need to rewind, a specification of a six months approximate period between rewinds is deduced. (Figure 5)

The analyses in [5,6,8,9] assume a constant asymptotic creep rate with time. It appears that this assumption is not justified for the long term storage required for archivability. Creep vs. time as presented in [13] is schematically depicted in Fig. 6. It indicates that for the long term, creep strain is proportional to time to a small power ( $\approx 0.07$ ). Thus the asymptotic creep rate monotonically decreases and the relaxation times predicted by the above analyses appear to be significantly underestimated. Estimates of relaxation times in reels are given in Section 2.3.7.5.

### 2.3.2.4 Effect of Environmental Cycles

A storage temperature cycle exposing the foil to a temperature above its winding temperature will cause a temporary increase in stress levels if the hub coefficient of thermal expansion is greater than that of the reel [6]. A similar effect will occur if the coefficient of thermal expansion of the oriented polyester is greater in the radial direction than it is longitudinally, [7] (Table 4). An analogous situation might be expected when a humidity cycle exposes a reel to a lower relative humidity than it was wound at. This is owing to the hygroscopic contraction of the tape, in the absence of hygroscopic contraction of the hub.

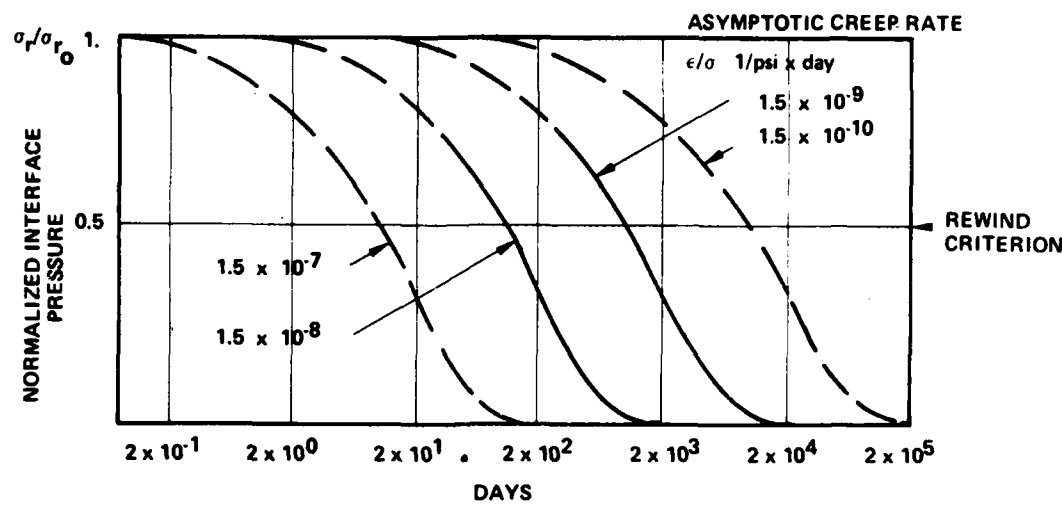


**Figure 5** Basic trends of normalized interface pressure at hub vs. relaxation time.  $\sigma_{r_0}$  is initial value of interface pressure. Solid lines are average values from Ref. [5], Figs. 4(a), 4(b). Broken lines are abstractions. Curves are based on a constant asymptotic creep rate.

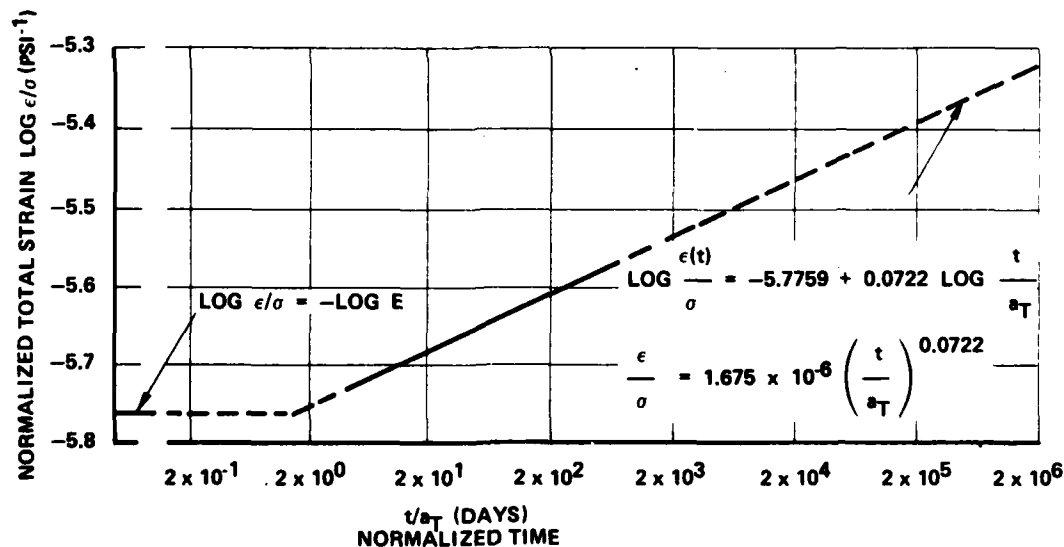


**Figure 6** Essential features of creep data extracted from Ref. [13]. Initial strain is elastic and total strain (creep and elastic) may be extrapolated by a straight line on a log-log plot. The value of  $a_T$  as a function of temperature is given in Fig. 7. Solid lines are based on empirical data. Broken lines are abstractions.

The greater stresses induced by these environmental cycles increase the rate of viscoelastic stress decay. Therefore, when the reel is returned to its original thermal state it would be in a more relaxed state of stress. A typical reel when stored at 120°F, after being wound at 70°F, and when the coefficient of thermal expansion of the hub is three times the value for the tape, will approach stress-free conditions at least 80% earlier than when stored at the winding temperature [6].

#### **2.3.2.5 Effect of Temperature**

It is to be noted that the above mentioned analyses of environmental cycles assume that the basic film properties do not change with temperature (e.g., "viscosity of polyester"). The results of our work as well as the recent publication [13] indicate a substantial change in total creep strain with temperature (a factor of 10 for a 10°C rise) (See Figure 7). Thus the above analyses seem to significantly underestimate the effect of thermal cycles.

#### **2.3.2.6 Effect of Winding Tension**

The stress variations (and consequently, the variations of time base errors) across the reel radius can be reduced by constant torque winding rather than constant tension winding [8]. This may be explained by Fig. 4a. Here, it may be seen that with constant tension winding, the tangential stress decreases radially inwardly. Constant torque winding would tend to counter this non-uniform stress distribution by imposing higher tensions at the inner radius.

Winding tension also affects significantly the amount of interlayer air wound into the reels. (Section 2.3.2.8)

#### **2.3.2.7 Effect of Winding Speed**

Like reduced tension, increased winding speed promotes the establishment of locked-in interlayer air film. (Section 2.3.2.8)

#### **2.3.2.8 Locked-in Air Layers**

A significant degradation of tape reel integrity may be caused by air layers locked in the pack during winding. To a first approximation, tape reeling may be viewed as a lubrication phenomenon in which both the moving tape and the rotating reel team up to pump air into the nip. (Figures 8 , 9 ) Part of the pumped-in air may be

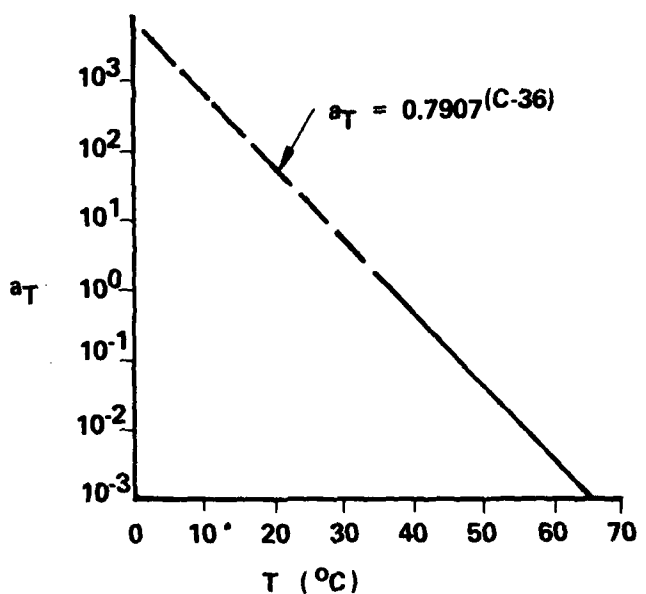


Figure 7 Temperature-Time Interchange Factor  $a_T$  [13]. Solid Line is Empirical. Broken Line is an Abstraction.

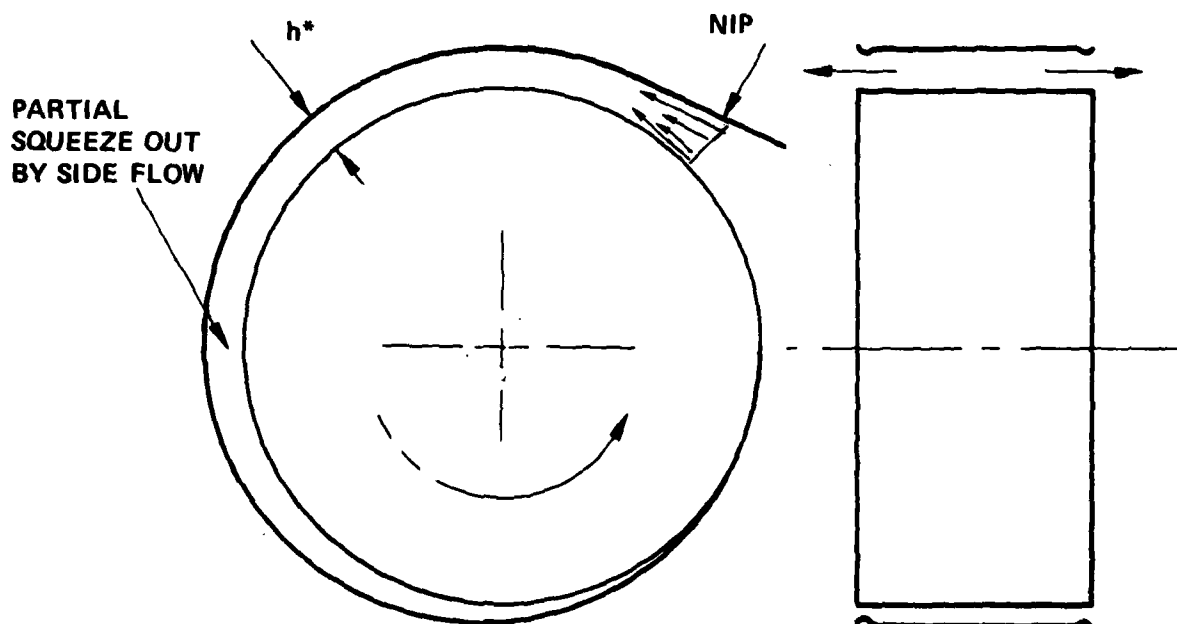


Figure 8 Schematic Description of Interlayer Air Entrapment During Reel Winding.

squeezed sideways, during winding or shortly after. A significant quantity of air tends, however, to be locked in the reel. This air layer undermines reel stability by reducing the interlayer friction and by lowering tape tension owing to delayed leakage.

Based on foil bearing theory [14], in the absence of side flow, air layer thickness tends to be proportional to  $r^{5/3} \left(\frac{\omega}{T}\right)^{2/3}$  where r is the reel radius,  $\omega$  the angular velocity and T the tension. Both experiments and theory (see Section 2.3.6) indicate that if high speed winding is desired, added means such as a packing roller pressure is necessary and is useful to prevent air from being locked in the reel.

### 2.3.2.9 Tape Shrinkage

After manufacturing, polyester films have a tendency to shrink. This tendency increases with temperature. Figure 10 shows a typical experiment in which a base film strip is raised in temperature to a given level and held [15].

The shrinkage characteristics of polyester as a function of time, temperature, stress level, manufacturing process, etc., are not firmly established. This factor obscures tests of tape behavior since the past history of a tape reel from its manufacturing time is difficult to trace. Experiments in [13] attempt to eliminate past history by subjecting each test sample to a preliminary constant temperature period prior to any additional test.

Manufacturers of home video tape have proprietary processes of reducing tape shrinkage [16]. While moderate shrinkage does not appear to have adverse mechanical effects, similar processes may be utilized to eliminate shrinkage of archival storage tapes for the sake of uniformity.

### 2.3.2.10 Effect of Anisotropy

Even if one neglects differences between the polyester film properties across its thickness and along its axis, a wound reel may still exhibit anisotropy of properties in these directions for the following reason. Radial pressure on the reel will cause, depending on its winding stress, interlocking of tape asperities, in addition to the compressive strain in the film. In other words, due to surface roughness effects and locked in air layers, the film appears more flexible radially than it is tangentially [6]. This softness tends to augment the effect of hub flexibility in relaxing the pressure in the interior of the reel. The tangential stress in the foil is also affected by the radial film compliance. Since the effective film compliance is greater than that of the hub, the tension reduction in mid-reel (due to inward radial displacement) may be greatest. (Figure 4c)

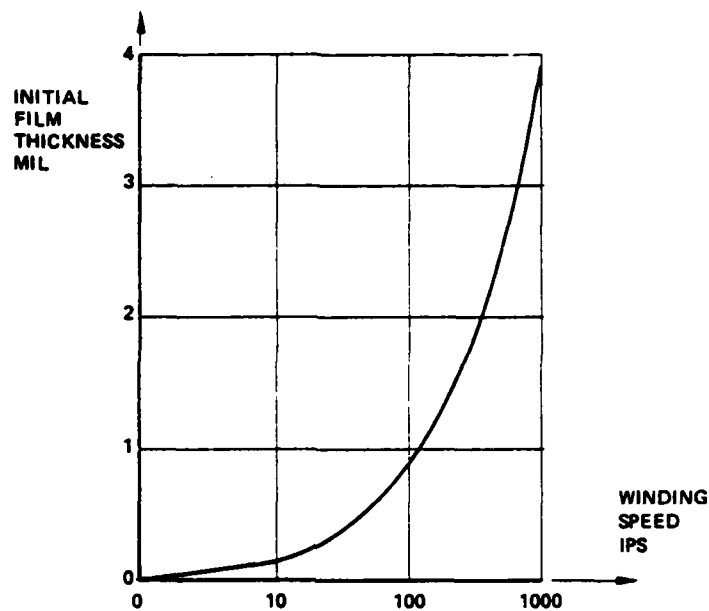


Figure 9 Predicted Air Film Thickness Trapped During Reel Winding in the Absence of Side Flow.

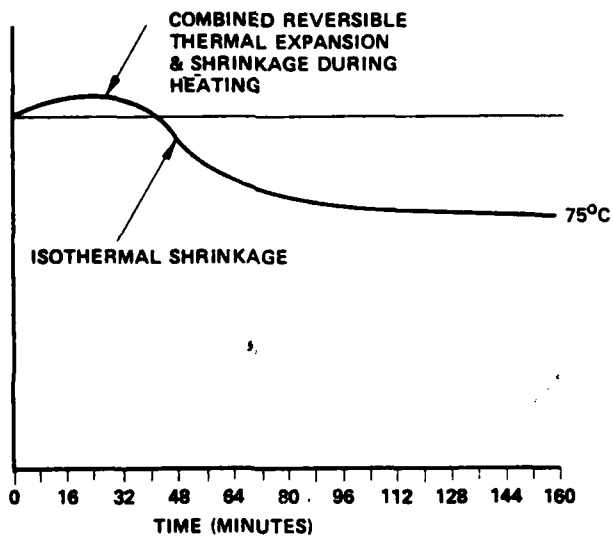


Figure 10 Shrinkage of a Typical Mylar Sample (Sample Heated to Temperature at  $1.5^{\circ}\text{C}/\text{Min}$  and Held) [15]

### 2.3.3 Experiments on Creep Rate at Room Temperature

#### 2.3.3.1 Motivation for the Experimental Work

The simulation models described in Section 2.3.2.3 point to the need for periodic reel rewinds, roughly twice a year, to prevent loss of interlayer pressure. Procedures of this type are costly. Extension of the period between rewinds or its total elimination would be highly desirable.

In contrast with the above recommendation which follows from the computer simulation models, it was found that many computation centers do not have regular rewind procedures. Nevertheless, they indicate that mechanical tape damage does not occur unless the reels have been exposed to considerable environmental adversity.

In an attempt to resolve these two conflicting views, additional consideration had to be given to the creep rates of polyester base film. Questions such as the following had to be answered. How do different makes of polyester film differ from one another? Are the creep rates constant over a prolonged period of time? Would a tensioned film not reach asymptotically a strain limit? These questions are addressed in this section.

Inquiries with the major manufacturers of polyester film yielded, surprisingly, little information. Conflicting measurements of creep levels over only short time periods or at much higher stress levels have been reported (Table 4). Considering an average, the strain rate per unit stress is of the order  $0.4 \times 10^{-7}$  (1/psi · day). Using this figure, a tape strip of 25" x 1" x 0.001" under a typical tension of 0.5 Lbf/in would creep in 200 days an amount of

$$\left( \frac{1}{\sigma} \frac{d\epsilon}{dt} \right) \frac{T \cdot L \cdot t}{d} = 0.4 \times 10^{-7} \frac{0.5 \times 25 \times 200}{0.001} = 0.100'' \quad (7)$$

By comparison the elastic elongation of this tape strip would only be

$$\frac{T \cdot L}{d \cdot E} = \frac{0.5 \times 25}{0.001 \times 6 \times 10^5} = 0.020'' \quad (8)$$

With these results the favorable field experience of people who do not have regular rewind procedures seems contrary to expectation. This apparent contradiction and lack of data has motivated us to perform our own tests on polyester creep.

### 2.3.3.2 Experimental Apparatus

Samples of polyester base film were each loaded and hung as shown in Figs. 11 and 12. A microscope was used to focus on a cross hair marked on the weight used for loading each sample. Using an indicator (1 mil division) the deflection of each sample relative to a fixed reference was measured. The reading reproducibility (due to thread and slide clearance, cross hair thickness, etc.) was within less than 1 mil. In view of the expected order of deflection of 100 mils in half a year this seemed to be rather adequate for the purpose at hand.

The test set up was placed in an air-conditioned laboratory with reported set points of 65°F, 55%RH. Initially, no precautions were taken to record the environmental conditions which were presumed to be more constant than in a typical air-conditioned office or industrial environment. It was discovered later, unfortunately, that an air-conditioning failure did occur and that relative humidity fluctuated between 45% and 65%. Subsequently, humidity and temperature recorders were installed on the 75th day of the experiment.

### 2.3.3.3 Results and Discussion

Fourteen samples of 1" x 24" uncoated polyester base films of various thicknesses and four manufacturers (DuPont, Celanese, ICI, Torray) have been tested for a period of 250 days. Their elongation is recorded in Fig. 13 based on roughly once a week measurement. Two "irregular" events may be observed in the data. First, approximately around the 20% time mark a three day air-conditioning failure occurred in which temperatures are assumed to have reached 80°-90°F (not recorded). Secondly, during the 90-100th days of the experiment, significant humidity fluctuations occurred (64% → 45% → 58%). It may be seen that in this period a major trend in the data was due to reversible humidity extensions and contractions.

While the air-conditioning failures are regrettable, meaningful observations, listed below, can still be based on the data. Moreover, some beneficial information follows from the air-conditioning failures which would not have been obtained otherwise. In the conclusions stated below, the creep strain during the air-conditioning failure period is subtracted from the cumulative strain. It is believed that this is a reasonable approach. It is consistent with the four-parameter viscoelastic model (Figure 3).

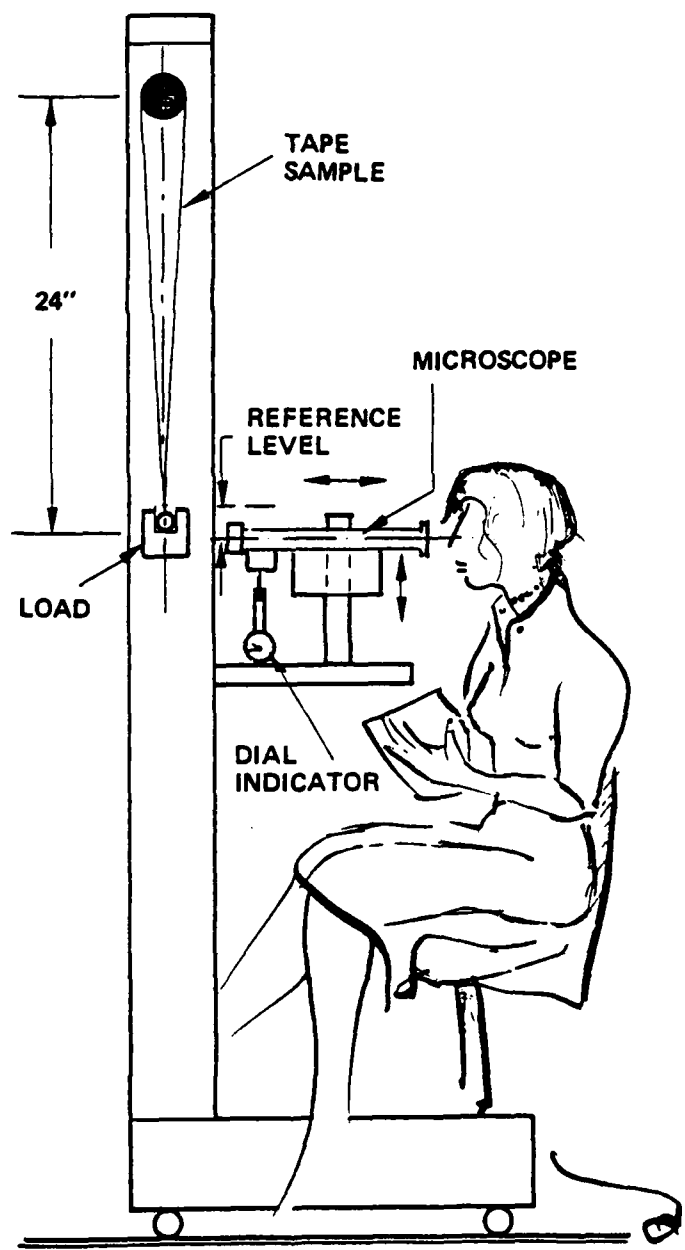


Figure 11 Schematic View of Creep Measurement Apparatus

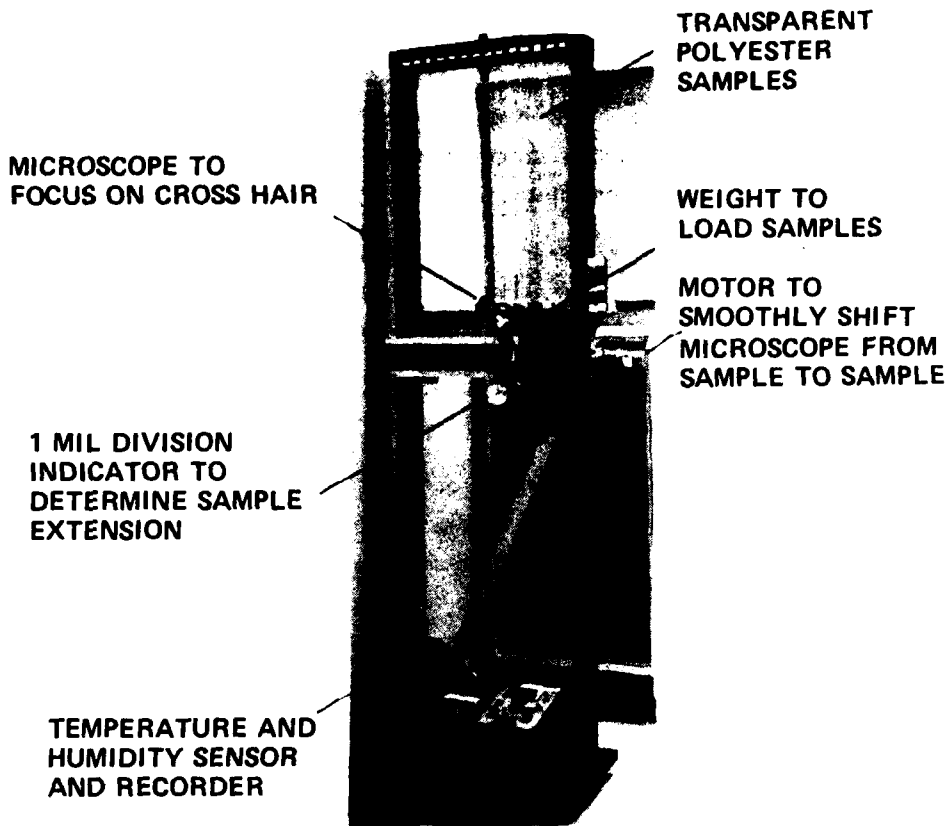


Figure 12 Photograph of Creep Measurement Apparatus

1. Creep rates are highly sensitive to temperature. Strict temperature control appears to be essential for archival storage. During the air-conditioning failure mentioned above, the lowest creep rate observed was for Sample 4 ( $0.25 \times 10^{-7}$  1/psi day). This is by two orders of magnitude more than the average creep rate of this sample and by one order of magnitude greater than the average creep rate of the bulk of the samples at room temperature.
2. Creep rates at constant temperature slow down considerably with time. This should be borne in mind when creep rates are reported. It is perhaps preferable to report creep levels and their corresponding test period.
3. In addition to creep, shrinkage affects length. Creep and shrinkage are opposing mechanisms (e.g., Sample 13, Fig.13).
4. Percentages of samples as a function of inelastic strain (due to creep but modified by shrinkage) are given in Fig. 14 for two long periods (112, 250 days). The worst average creep strain rate per unit stress over 250 days is for Sample 3:  $0.26 \times 10^{-8}$  1/psi day. By comparison to Table 4 and to Fig. 5 , it may be seen that a recommended rewind frequency of twice a year is grossly exaggerated. The much faster creep rates reported in the literature are probably due to the short period of the tests on which they are based and the rapid slow down of creep rate with time.
5. Reversible humidity effects measured during days 90-94 agree with the data in the literature. The range of observed humidity contraction is 2.5 to 5.0 mil. The rate is then  $[(2.5 \text{ to } 5.0) \times 10^{-3}]/[24 \text{ in} \times 19\% \text{RH}] = (5.4 \text{ to } 10.9) \mu\text{in/in}\% \text{RH}$  which compares well with Table 4. Moreover, the similarity between the RH history and extension records over parts of the experimental period indicates that fluctuations in length observed in experiments (except for the air-conditioning failure) were to a great extent due to reversible humidity effects.

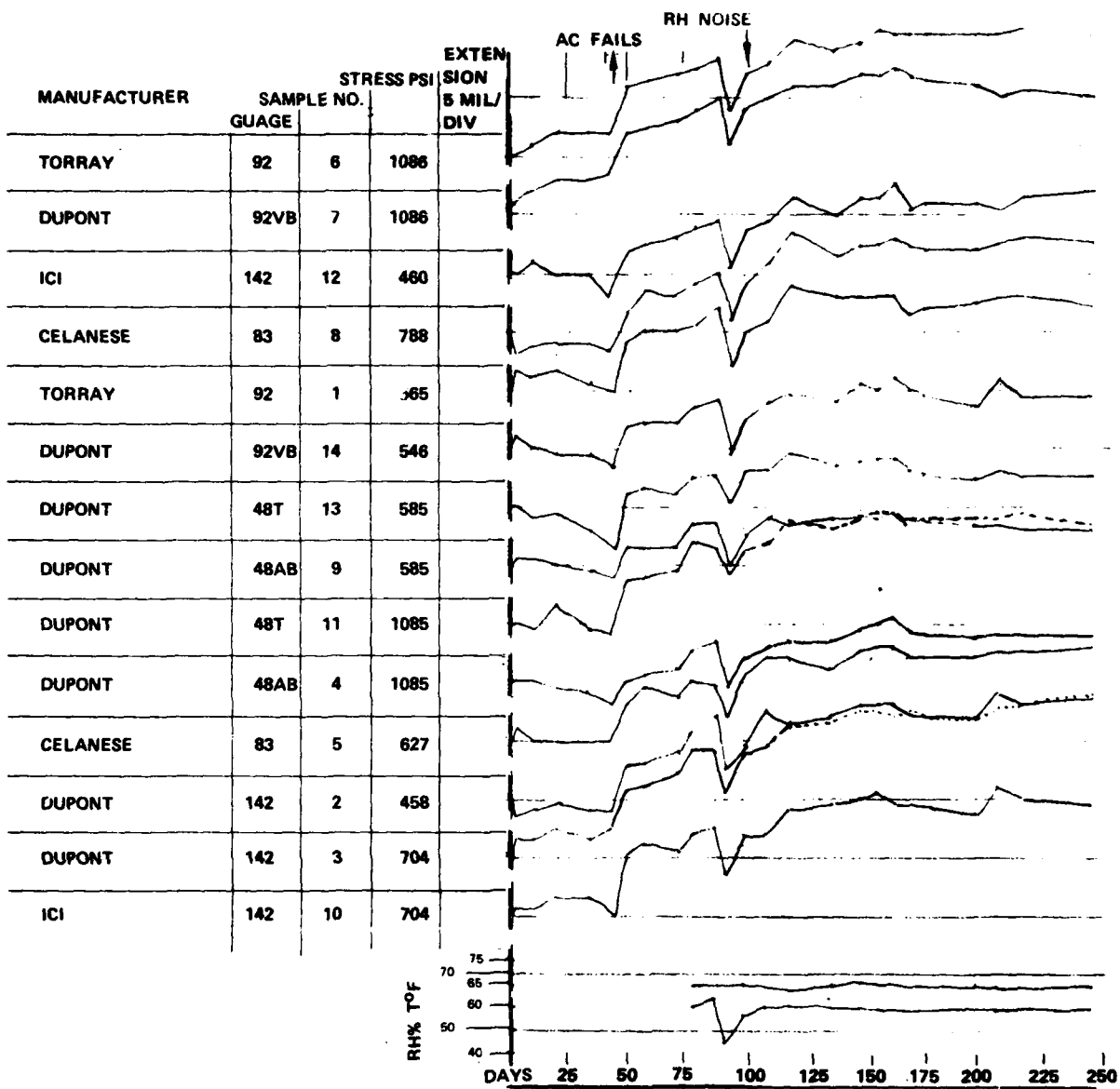


Figure 13 Extension of 24" Samples Nominally at 65°F, 55%RH as a Function of Time.

### **2.3.4 Experiments on Creep Rate and Shrinkage at Moderate Temperatures**

#### **2.3.4.1 Motivation**

Several information items point to the significant adverse effects of even moderate thermal perturbations on tape reels. In the first place, there is an established "folklore" of computation centers that after shipping, tape is prone to mechanical damage such as cinching. Secondly, the experimental results mentioned in 2.3.3.3 indicate that a three-day air-conditioning failure was sufficient to introduce irreversible creep effects significantly greater than those one-hundred days at room temperature had caused. Finally, a recent paper [13] indicates roughly a factor of 10 reduction in time to obtain a given creep level for each  $10^{\circ}\text{C}$  rise in temperature.

Under certain conditions, an opposite effect, i.e., shrinkage may be present and appears to be of significance. One pointer to this effect is our experience with TBM tapes at elevated temperatures (see Section 2.5.4.2). Another data item is given in [16] and discussed in Section 2.3.2.9.

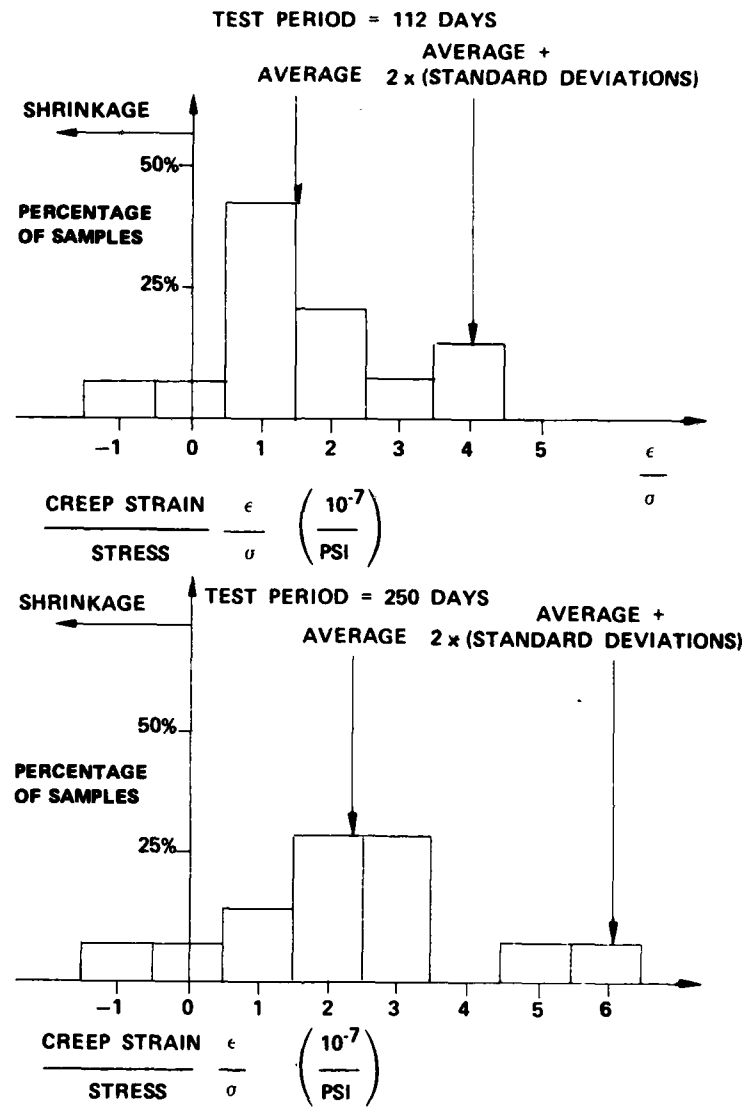
While the information discussed above indicates the significance of the mentioned phenomena, insufficient quantitative information on the subject is available. Our work is intended to fill some of the gaps.

#### **2.3.4.2 Experimental Apparatus**

Studying elastic, creep and shrinkage deformation of foils in an oven while it is subject to a combination of reversible and irreversible thermal and humidity expansion imposes several difficult requirements. Table 5 exhibits some of the orders of magnitude involved. The main requirements are:

1. Usage of sensors without thermal drift over a prolonged period of time.
2. Elimination of the effects of thermal expansion and distortion of the apparatus from the measurement.
3. Remote measuring (outside oven) without disturbing apparatus.

A photographic view of the apparatus constructed for the purpose is shown in Figs. 15a,15b. The measurement principle used was as follows: Suspended tape strips were vibrated each as a pendulum and the accurately read period served to measure the test



BASED ON 14 SAMPLES  
MANUFACTURERS: DUPONT, ICI, CELANESE, TORRAY  
THICKNESS RANGE: 0.5-1.4 MIL  
STRESS LEVEL: 450-1100 PSI  
TEMPERATURE: 66°F NOMINALLY  
(EFFECT OF 3 DAY AIR-CONDITIONING  
FAILURE AT 80°-90°F SUBTRACTED)  
RELATIVE HUMIDITY: 55% ± 10%

Figure 14 Creep Strain of Polyester Base Film for Specified Test Periods.

Table 5

Order of Magnitude of Length Changes Initially Considered  
in Construction of Creep/Shrinkage Measurement Apparatus

Based On:

- Temperature  $20^{\circ}\text{C} \rightarrow 30^{\circ}\text{C}$
- Stress Level - 1000 psi
- Time - 10 days
- Humidity 45%  $\rightarrow$  55%

		$30''$ Sample	$8''$ Sample
Steel Expansion	$12 \times 10^{-6}$ 1/ $^{\circ}\text{C}$	4 mil	1.0 mil
Polyester Expansion	$15 \times 10^{-6}$ 1/ $^{\circ}\text{C}$	5 mil	1.2 mil
Shrinkage	0.02% at $30^{\circ}\text{C}$ (?)	6 mil	1.6 mil
Creep at $20^{\circ}\text{C}$	$3 \times 10^{-9}$ 1/psi day	1 mil	0.2 mil
Creep at $30^{\circ}\text{C}$	$30 \times 10^{-9}$ 1/psi day (?)	10 mil	2.4 mil
Hygroscopic Expansion	$5 \times 10^{-6}$ 1/% RH	1.5 mil	0.4 mil
Elastic Elongation	$0.2 \times 10^{-5}$ 1/psi	60 mil	16 mil

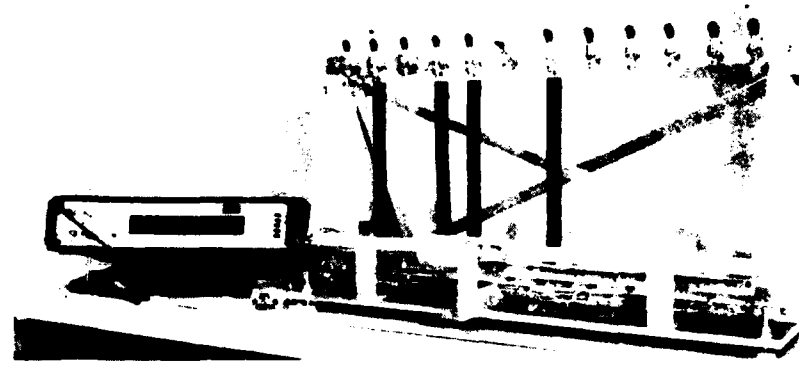


Figure 15a Photographic view of creep/shrinkage measurement apparatus for controlled environments. Period of pendulum is used to measure tape strip length.

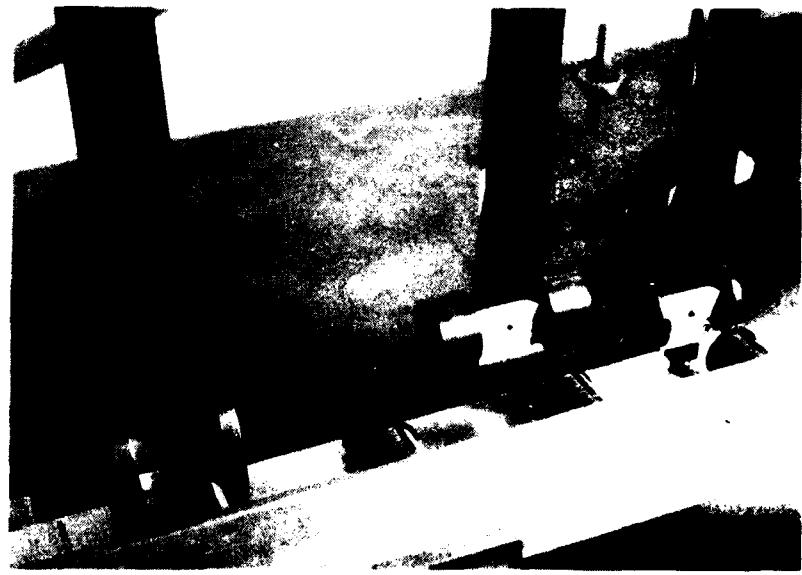


Figure 15b Detail of pendulums for tape length measurement. Note electromagnets used to start vibration of each pendulum. LED used to generate timed pulse train may be seen below pendulums.

sample elongation. Remote control mechanisms to lift each sample independently and release it with a prescribed amplitude were constructed. For most of the 12 eight-inch long samples a period-measurement repeatable within 0.01 ms was achieved. It is to be noted that the counter used for period-measurement was accurate to 0.1  $\mu$ sec. The reason why only 0.01 ms reproducibility was obtained (and not for all samples) is associated with spurious mechanical vibrations and variations in release time, damping, etc.

The pendulum period is:

$$\tau = 2\pi \sqrt{\frac{l}{g}}$$

where  $l$  is the length and  $g$  the acceleration of gravity. The correspondence between period measurement accuracy and length measurement accuracy is thus

$$dl = \frac{\sqrt{gl}}{\pi} d\tau$$

Using  $l = 8"$ , we expect for  $d\tau = 10 \mu s$ , reproducibility within  $dl = 0.2$  mil. Thus we would measure at  $30^\circ C$  (see Table 5) the creep rate to within 10%.

#### 2.3.4.3 Results and Discussion

Twelve 8" long samples were tested in the apparatus shown in Fig. 15. Before inception of the experiment, the apparatus was equilibrated in a preheated oven at  $50^\circ C$ . The experiment was started by hanging the samples in the oven. The need to open the oven door in order to place the samples, caused temperature and humidity fluctuations for approximately one hour. The initial state of each sample was recorded at this time. A set of six histories of creep strain vs. time is shown in Fig. 16. It may be seen that highly loaded samples exhibited creep elongation whereas lightly loaded samples exhibited shrinkage. Figure 17 shows strain data for 10 samples, plotted vs. stress at a few selected time points.

#### 2.3.5 Experiments on Reel Structural Integrity

##### 2.3.5.1 Motivation

As explained in Section 2.3.2 the relaxation of tape reels is a known phenomenon. However, the rate of this relaxation over a prolonged storage time is not well established. To prevent information loss due to mechanical damage associated with relaxed reels, it is sometimes recommended that reels would be rewound twice a year. This procedure is unsatisfactory for two reasons.

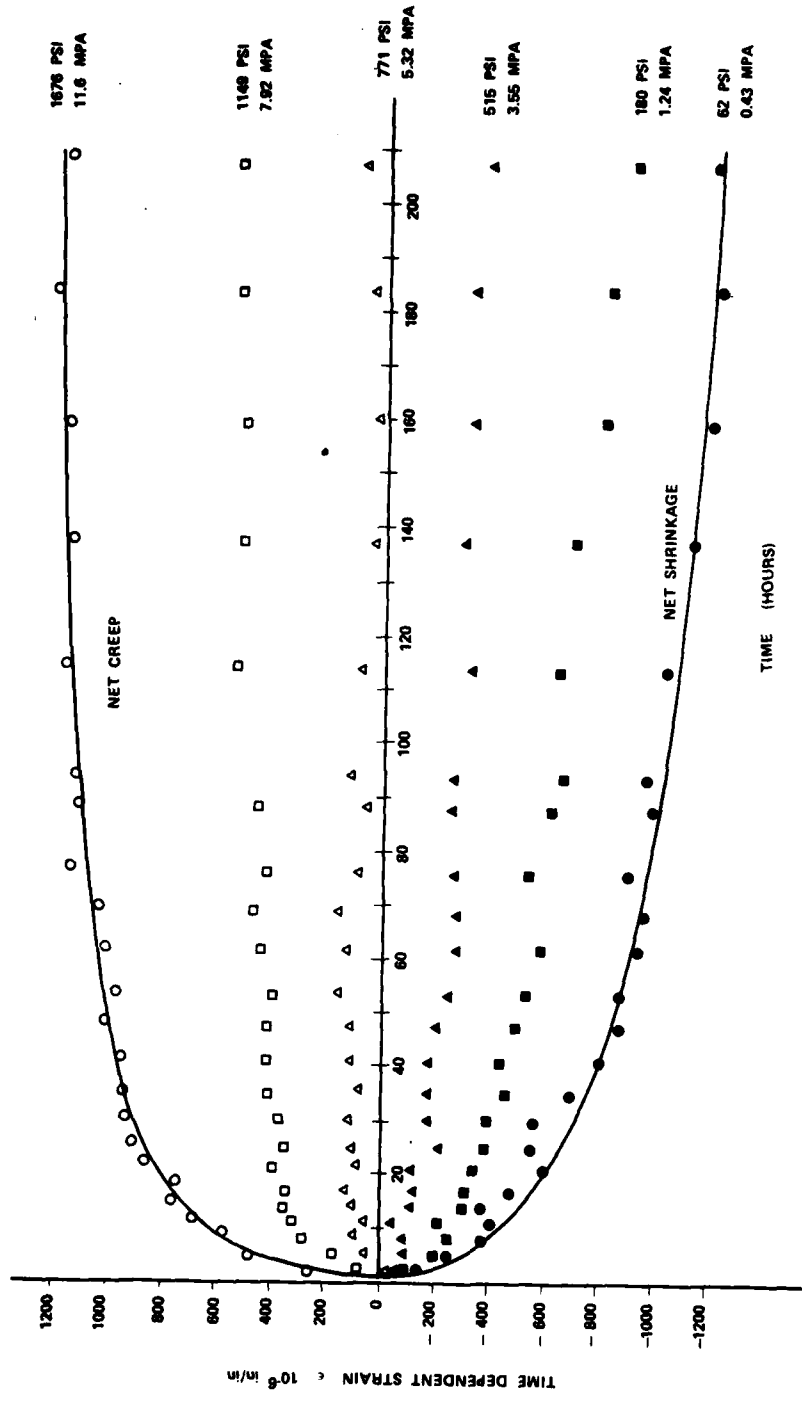


Figure 16 Time Dependent Strain vs. Time for Different Tensile Stress at 500°C, 50%RH.

1. It appears that tape stored under well controlled conditions could be stored significantly longer without rewinding.
2. It appears that for tapes subjected to environmental adversity such as shipping or air-conditioning failures, more frequent rewinds than described above would be necessary.

It follows, that if means were devised to measure the state of tightness of a reel, a safer and more economical procedure could be established. Our concept is as follows. At the archival storage facility (ASF), the last date of rewind would be marked on each tape reel. Additional test reels of the same type and size with no information would be stored in the facility every specified period (e.g., monthly or semi-monthly). These reels will be tested, at given intervals and if indication of looseness is detected, all reels of equal or greater most-recent-winding-time would be subjected to rewind. In a large facility it would be feasible to use a computerized data base to list all tapes due for rewind once their corresponding test tape indicated the desirability of it. This method would serve to wind tapes only as frequently as required.

We considered a number of possible tests to permit an ASF to determine whether a tape reel is due for rewind. The test principles considered and their reasons for rejection or acceptance are listed in the following:

1. Insertion of capacitance probe tabs between layers:  
Tabs were to consist of two conductive layers separated by a compressible dielectric. The tab capacitance would serve as a measure of internal reel pressure.  
  
We concluded that it would be impractical to construct thin enough tabs. In addition, tab damage and dielectric viscoelasticity might affect reproducibility.
2. Correlation of speed of wave propagation through reel with tightness:  
This seems a feasible approach but we felt we would not have sufficient time and funds under the contract to develop the instrumentation for this technique. It probably merits further study.
3. Measurement of hub deformation by an attached strain gage:  
After deliberation, we concluded that this would be a tedious procedure for ASF personnel. In addition, we were apprehensive of long term drifts in indications.

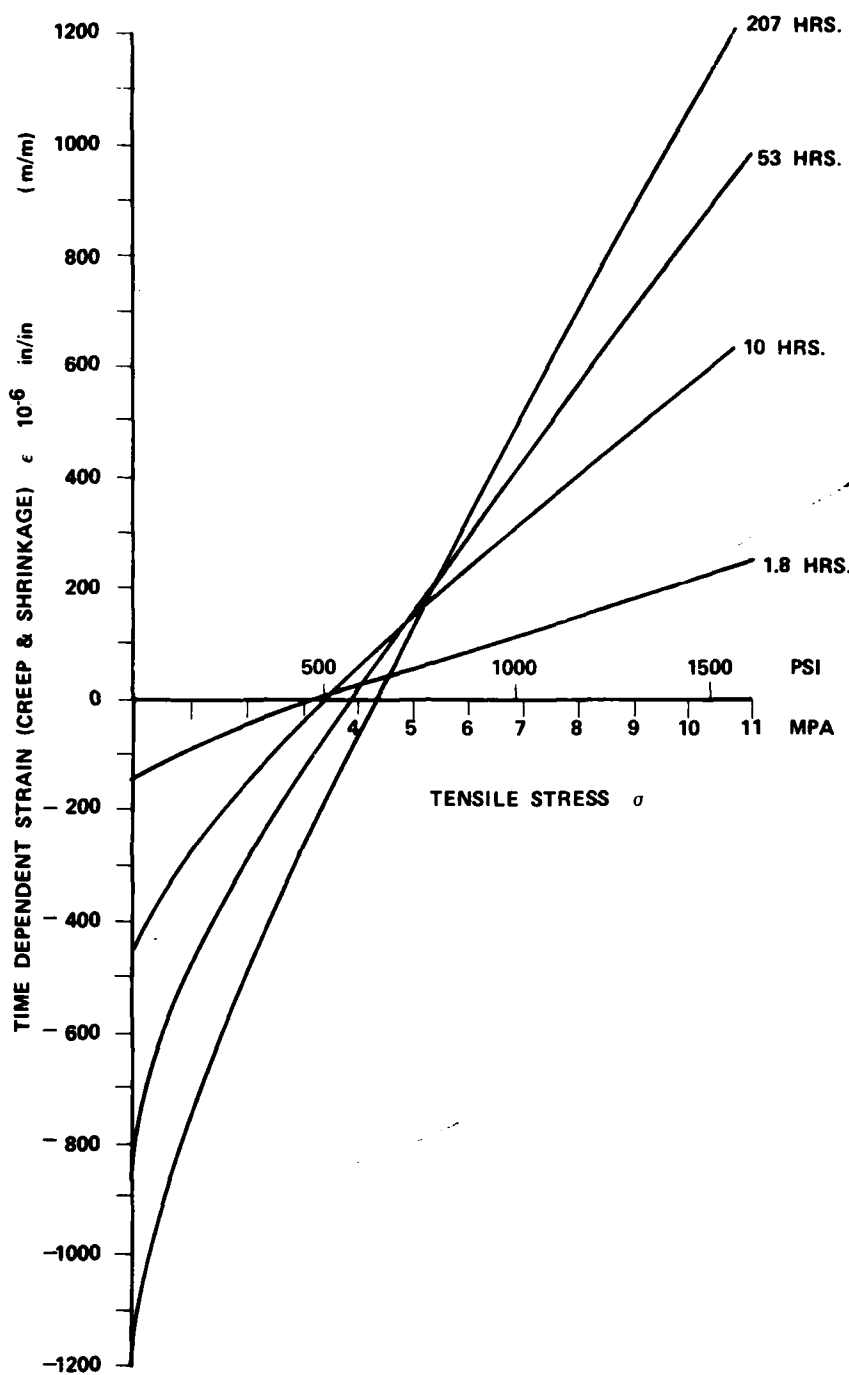


Figure 17 Time Dependent Strain vs. Stress for Different Times at 50°C, 50%RH.  
(Data Points are Shown on Fig. 16.)

4. Friction tabs:

Thin tabs are inserted into the reel during winding. The force required to pull out a tab measures reel tightness. This seemed to us the simplest go/no go technique, and so we concentrated our effort on investigating this approach.

The following two sections describe our experiments with this technique. An additional benefit of the friction tab method is that it permits experimental studies of the complete reel pressure distribution.

**2.3.5.2 Equipment**

Tape Winder:

A tape drive was adapted for the project. Tape may be wound at various capstan controlled speeds and with various tensions. In addition, fast wind/rewind without capstan control is possible.

Deceleration Test Rig:

A second rig was adapted for testing a reel for interlayer slippage by subjecting it to a sudden deceleration. A test reel would be slowly accelerated to a nominal speed of 500 RPM. Then, the reel would be braked while the back EMF generated by the reel motor armature would be displayed on an oscilloscope. Assuming EMF to be proportional to angular speed, the rate of deceleration was monitored. Figures 18 a & b show samples of deceleration of a tight reel and a slipping reel. The rate of deceleration of a slipping reel is greater than that of a tight reel since its effective inertia is lower. The deceleration of a tight reel is  $400 \text{ rad/sec}^2$ .

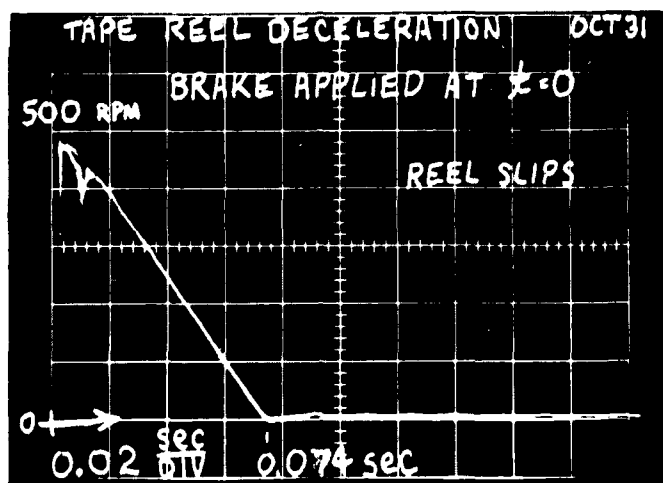
Tabs:

Tab dislodging approach has been by the use of a spring scale to obtain the pull force. It should be noted that for ASF personnel one would design a simple to use, force limited, tab puller which does not dislodge the tab as long as the reel passes.

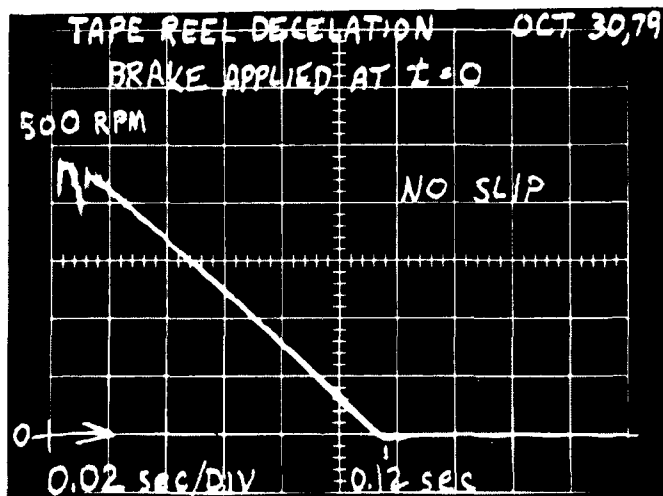
**2.3.5.3 Tests and Results**

Friction Tabs:

After study and experimentation, friction tabs of  $0.25'' \times 2'' \times 0.001''$  stainless steel were selected. Their strength, smoothness, dimensional stability and thinness (to avoid disturbing the reel structure as much as possible) were considerations



(a) REEL SLIPS



(b) REEL DOES NOT SLIP

Figure 18 Armature Back EMF of Reel Motor Owing to a "Sudden" Reel Deceleration.

in this selection. While we envision insertion of a single tab per reel in the ASF, we utilized more tabs for test purposes. It was found that a spiral arrangement of about a dozen tabs per reel was acceptable and yields results not significantly different from those obtained using a single tab at a time (see Figure 19).

#### Effect of Winding Torque:

Figure 19 shows a comparison between constant speed windings at different torques. It indicates that a 20% reduction in winding tension may be responsible for 50% reduction in tab pull forces. This disproportionate relationship hints to the possibility of air trapped between the layers, causing a delayed relaxation of tension as air bleeds out.

#### Correlation of Deceleration and Friction Tab Tests:

Figures 20 & 21 demonstrate that for a given deceleration there is a threshold tab pull force at which slip starts. For lower values of pull force greater slip will occur. For higher values no slip occurs. This would indicate that if a tab imbedded at  $R = 60$  mm (2.4") of a 4000-foot Ampex 799 instrumentation tape reel can be dislodged by a force of 30 N (6.8 lb) or less, it is time to rewind, if decelerations of  $400 \text{ rad/sec}^2$  are required.

#### Effect of Winding Speed:

Figure 22 illustrates the effect of winding speed. The reduced interlayer pressure at higher speeds again hints at the probability of air entrapment in the reels. Fast wound reels slip under the effect of rapid deceleration as described in Section 2.3.6.

#### Effect of Temperature History:

Figure 23 demonstrates the pressure relaxation taking place in the reel due to elevated temperatures. Figure 24 shows corresponding reel pressure distributions.

### 2.3.6 Experiments on Air Locked in Wound Reels

#### 2.3.6.1 Motivation

Results reported in Section 2.3.5.3 indicate that fast winding and/or low tension winding are responsible for reel looseness due to air entrapment. Means to restrict air pumping are therefore, desirable both to prolong the period between rewinds as well as to allow tight fast winding.

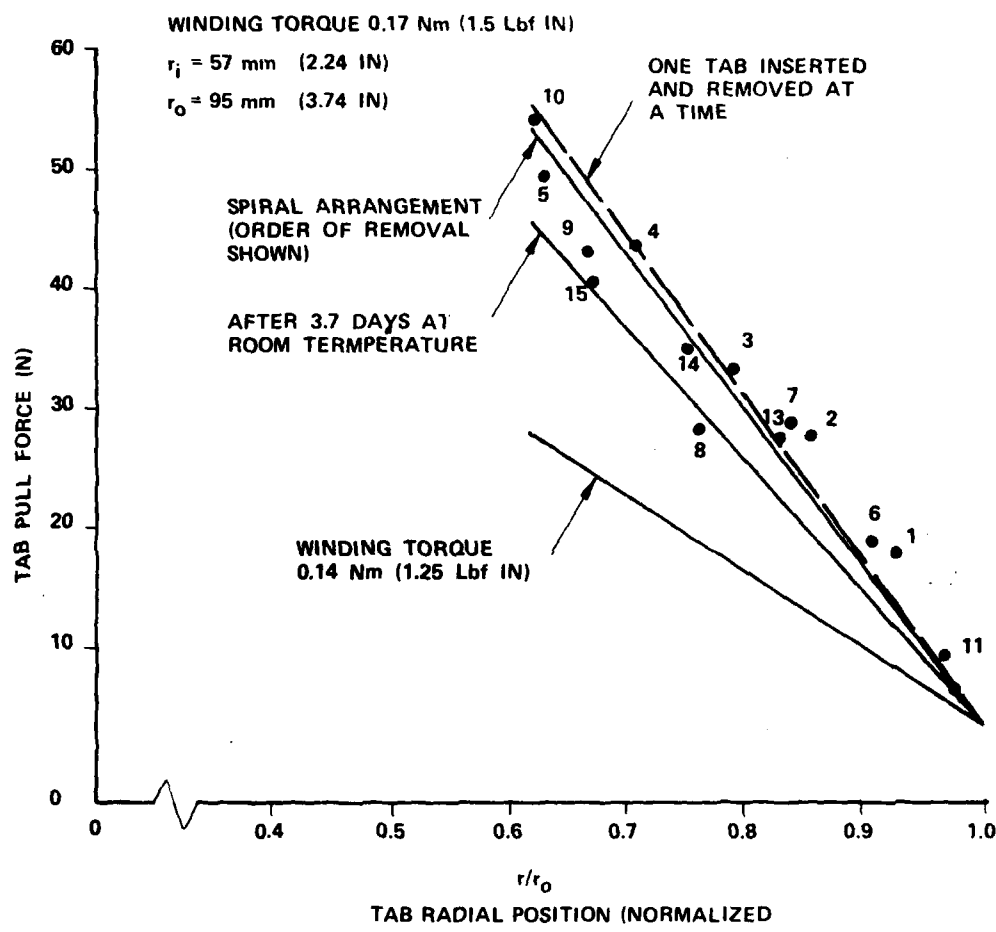


Figure 19 Radial Distribution of Tab Pull Force Showing Various Effects

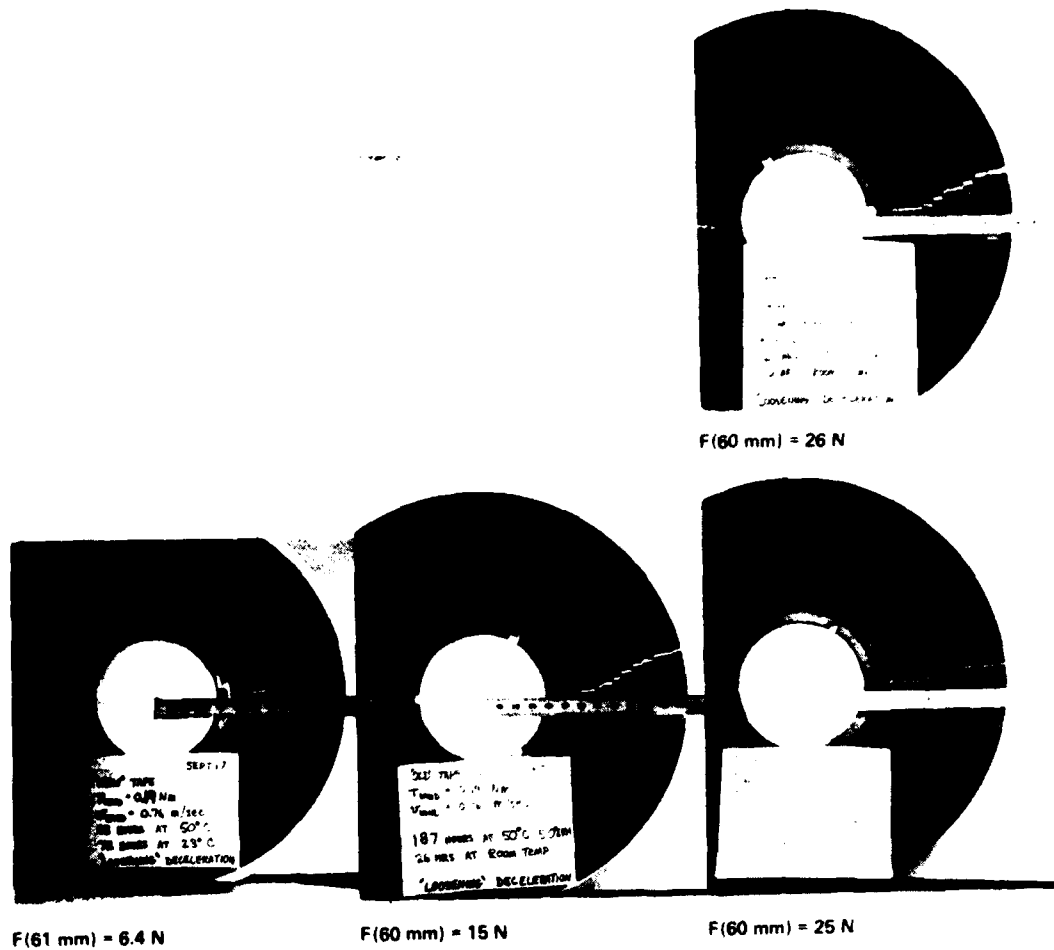
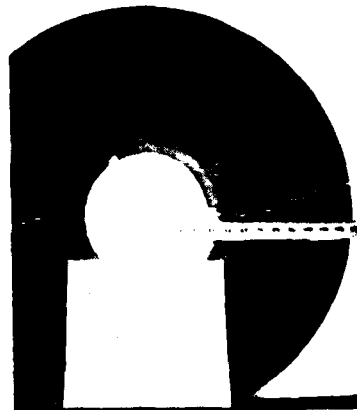


Figure 20

Slippage of Ampex 799 instrumentation tape in response to a  $400 \text{ ra/sec}^2$  deceleration. Prior to deceleration a straight chalk line was marked on each reel. The slippage is shown in the photographs for various environmental histories. The corresponding tab pull force at 60 mm radius for a different reel with same post winding history is shown on each figure.



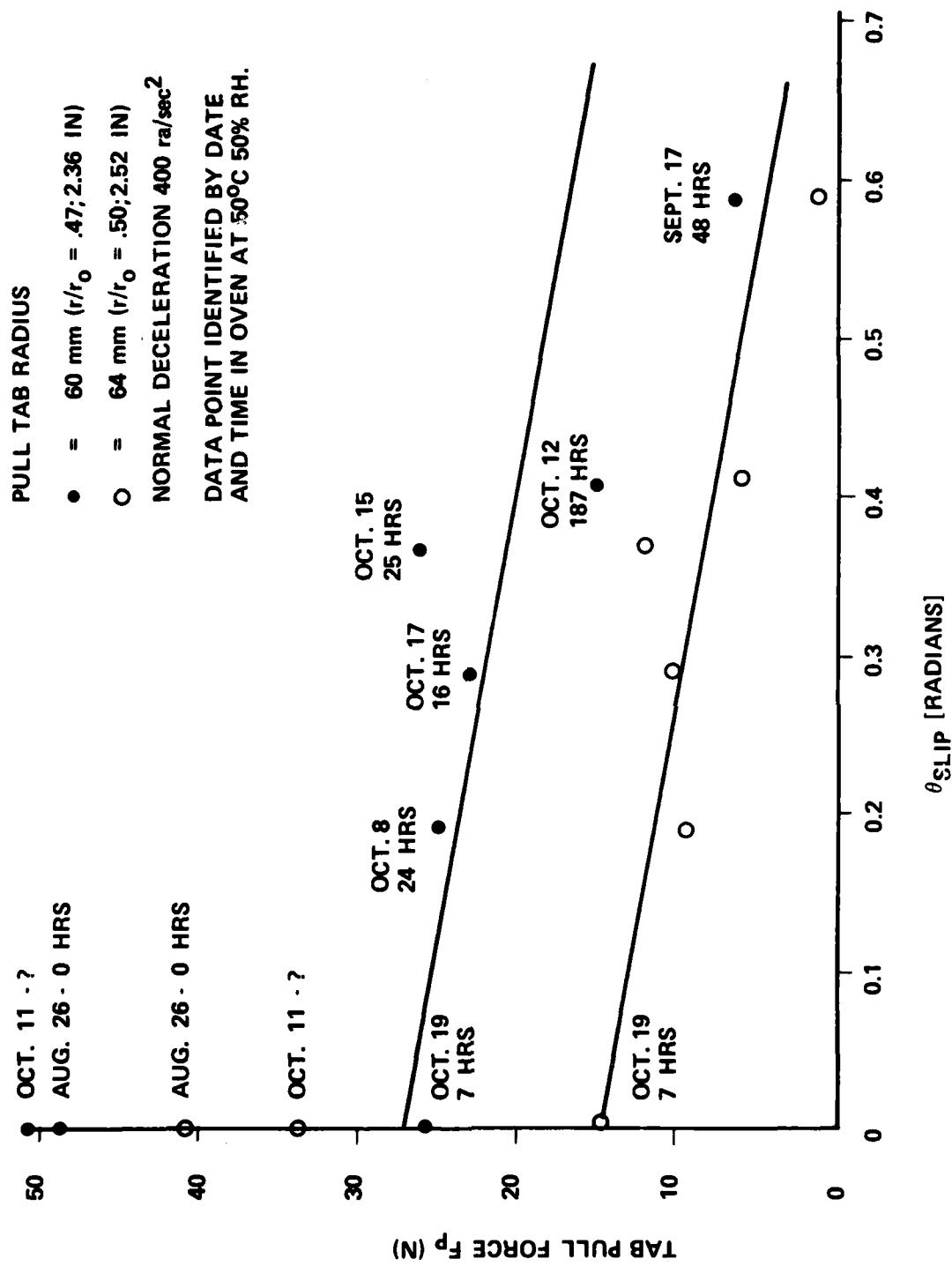


Figure 21 Correlation of Tab Pull Force with Angular Slip During a Sudden Deceleration.

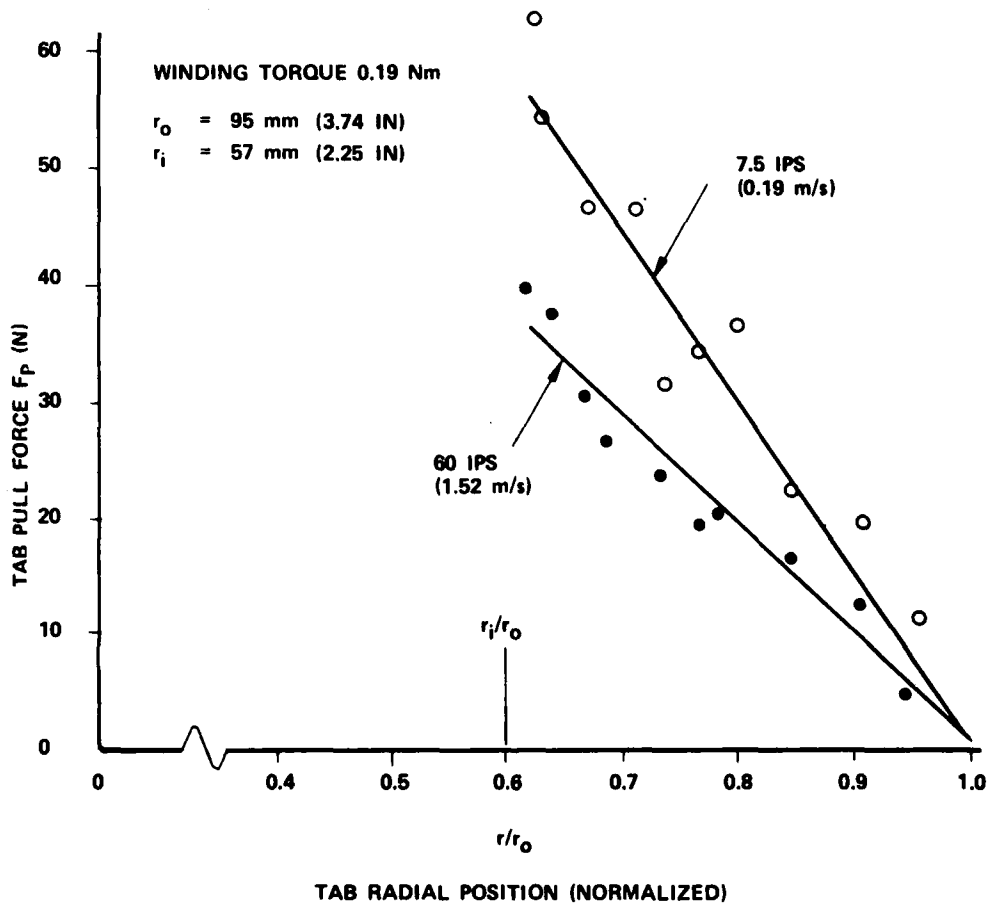


Figure 22 Effect of Winding Speed on Tab Pull Force (Reflecting the Effect of Air Entrapment). Experimental Points Represent Tabs in a Spiral Arrangement.

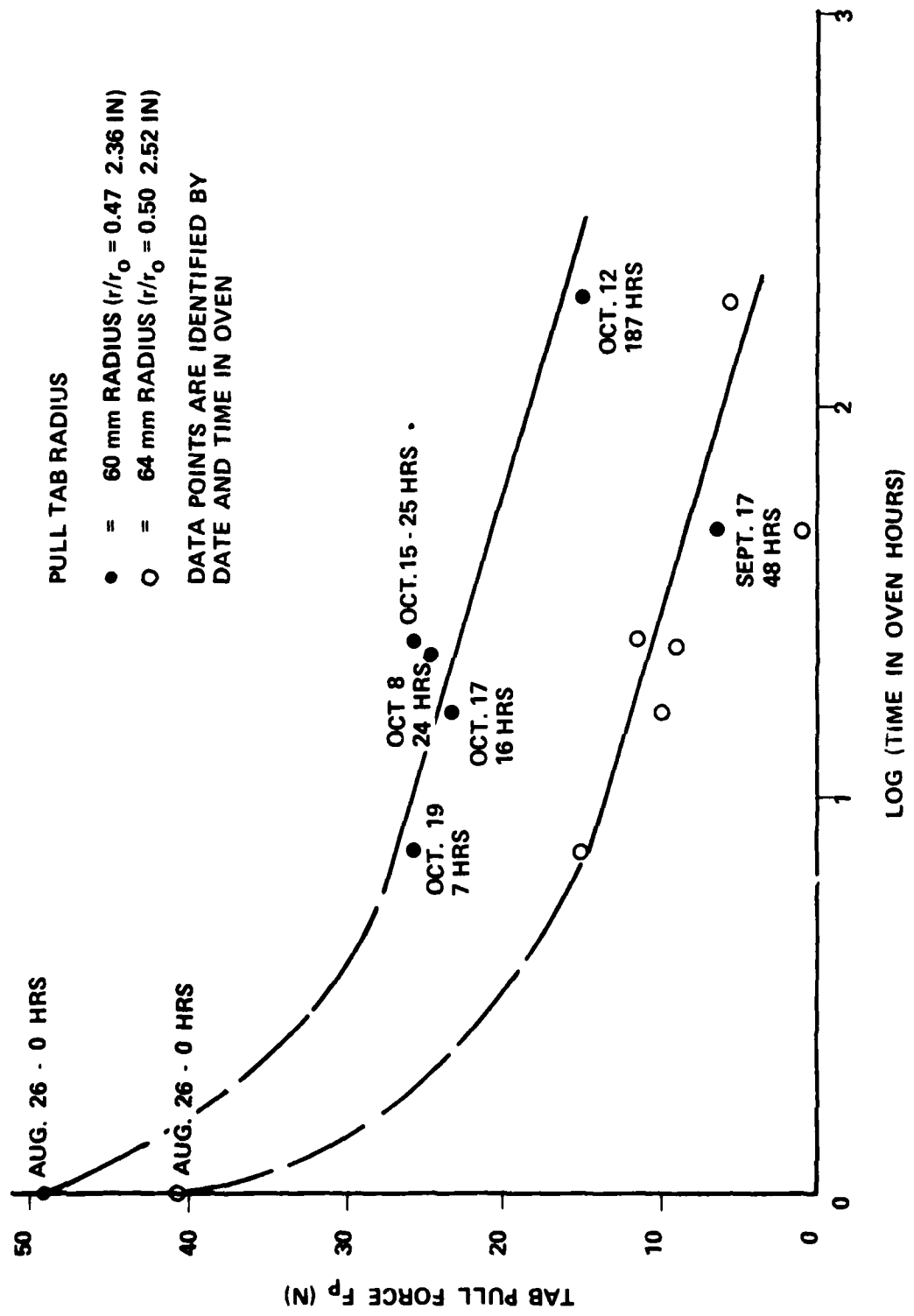


Figure 23 Correlation of Tab Pull Force with Time in Oven at 50°C, 50% RH.

### **2.3.6.2 Equipment**

One possible means to eliminate interlayer locked air is the use of a packing roller to load the tape against the reel during fast winding. To test the effectiveness of this scheme our tape winder was equipped with a packing roller.

### **2.3.6.3 Tests and Results**

#### **Roller Load:**

Fast winding tests using a packing roller (follower) indicate that a relatively small roller load is sufficient to insure a tight reel which can withstand considerable deceleration without slippage, (see Figure 25). This figure shows a correlation between tab pull force and packing roller load for the winding speed distribution shown in Fig. 26. It should be noted that depending on geometry, tape tension force on the follower may add or detract from the net load (Figure 33). In our apparatus the tape tension tended to offset part of the external load. The net load may therefore, be found by subtracting the portion of external load which balanced the tension (see mark in Fig. 25) from the total load.

#### **Reel Speed and Inertia:**

During fast winding reel speed usually varies. In order to report the speed conditions under which tests were performed as well as to keep these conditions independent of roller load, reel speed vs. radius was monitored (Figure 26).

As a result of the above measurements, it was concluded that roller loads in the range tested adds insignificantly to motor torque requirements. It was also observed that reel inertia is a significant variable and tape tension during free fast winding cannot be quasi statically estimated on the basis of motor torque and radius. Analysis of tape tension as a function of reel radius is given in Section 2.3.7.2.

## **2.3.7 Analytical Studies**

### **2.3.7.1 Introduction**

The theoretical works reported herein were intended to enhance physical insight and help explain and extrapolate observations. In addition, the analyses were aimed at building an arsenal of predictive tools for designers of future archival storage systems. These analyses may be divided into two groups.

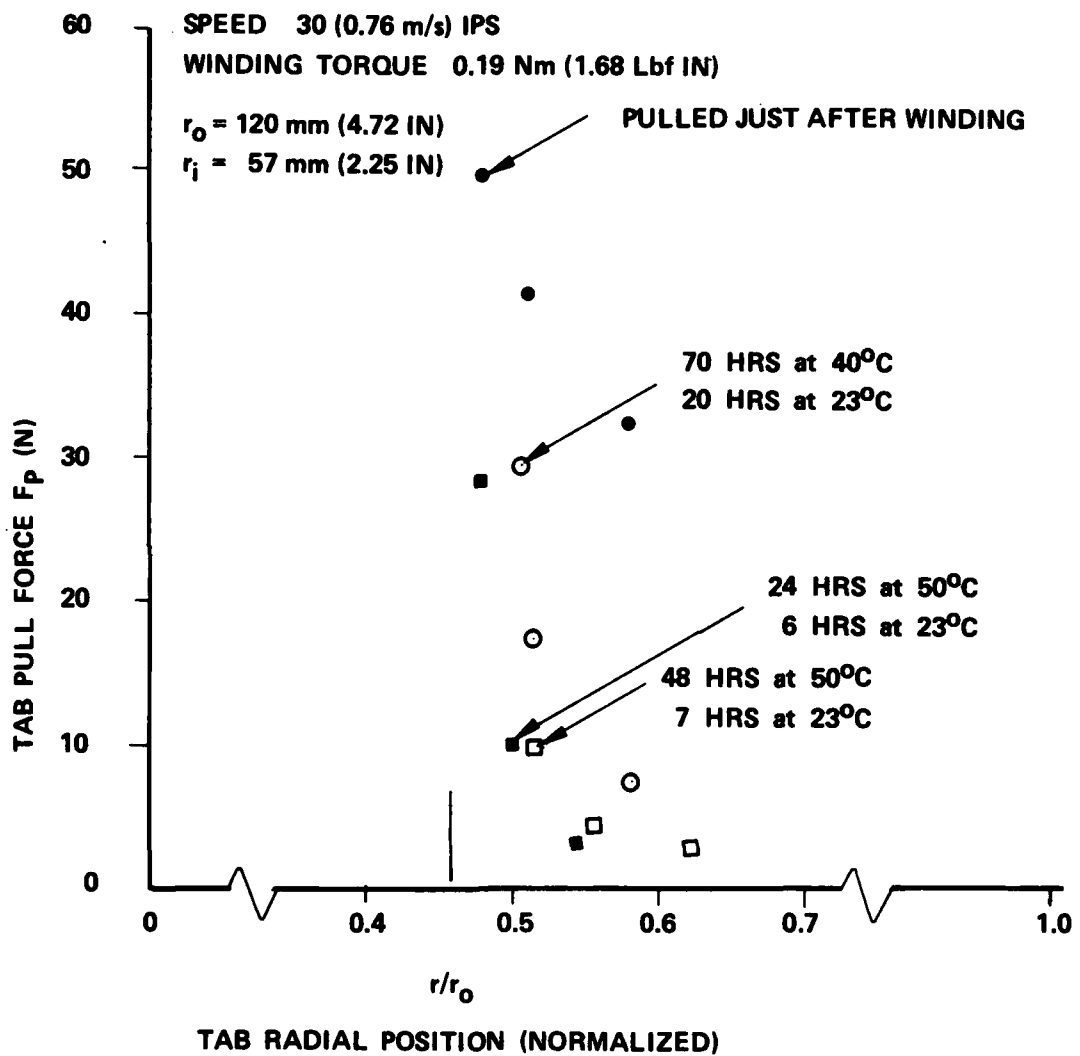


Figure 24 Effect of Environmental Conditions on Tab Pull Force

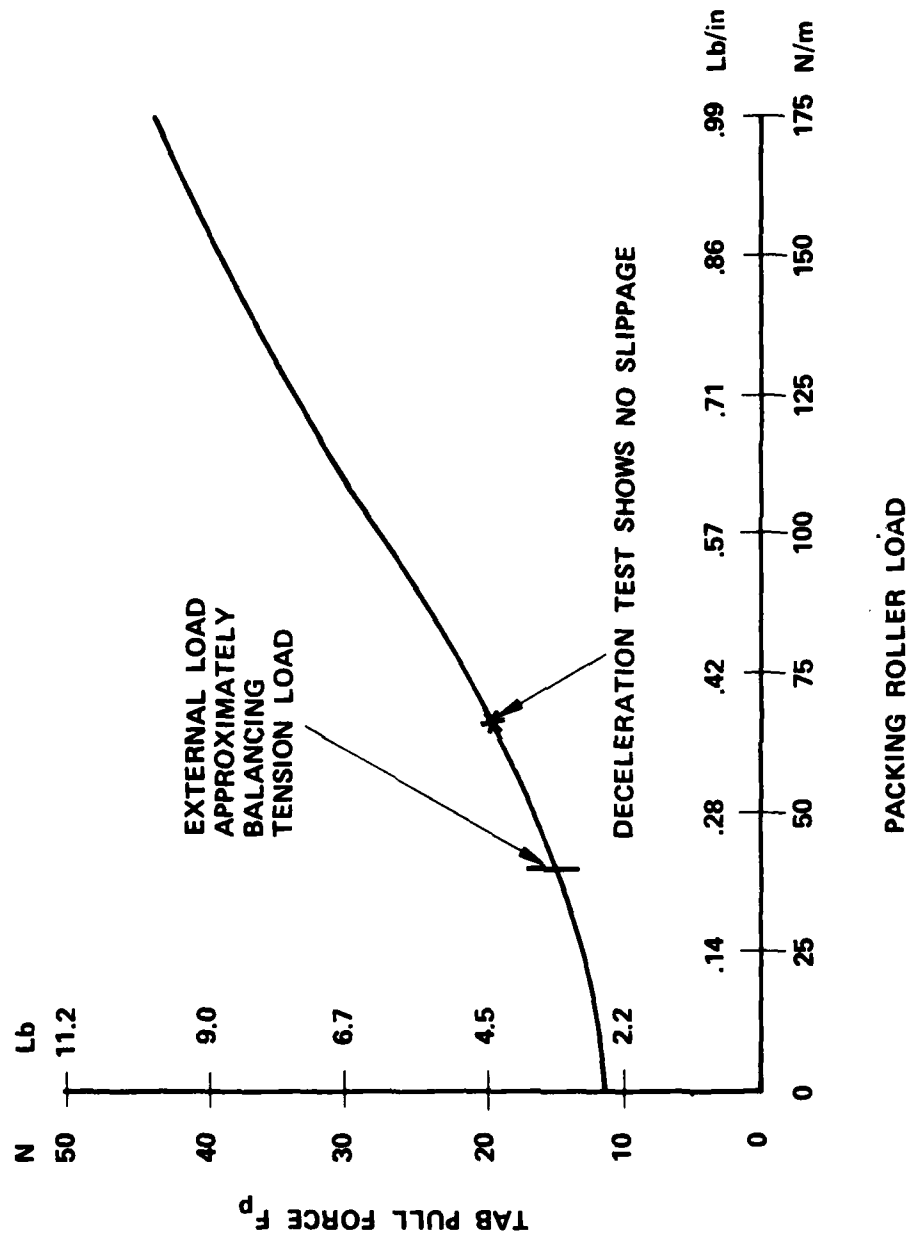


Figure 25 Tab Pull Force vs. Average Packing Roller Load. Readings were taken after a fast wind at the angular speed shown in Figure 26.

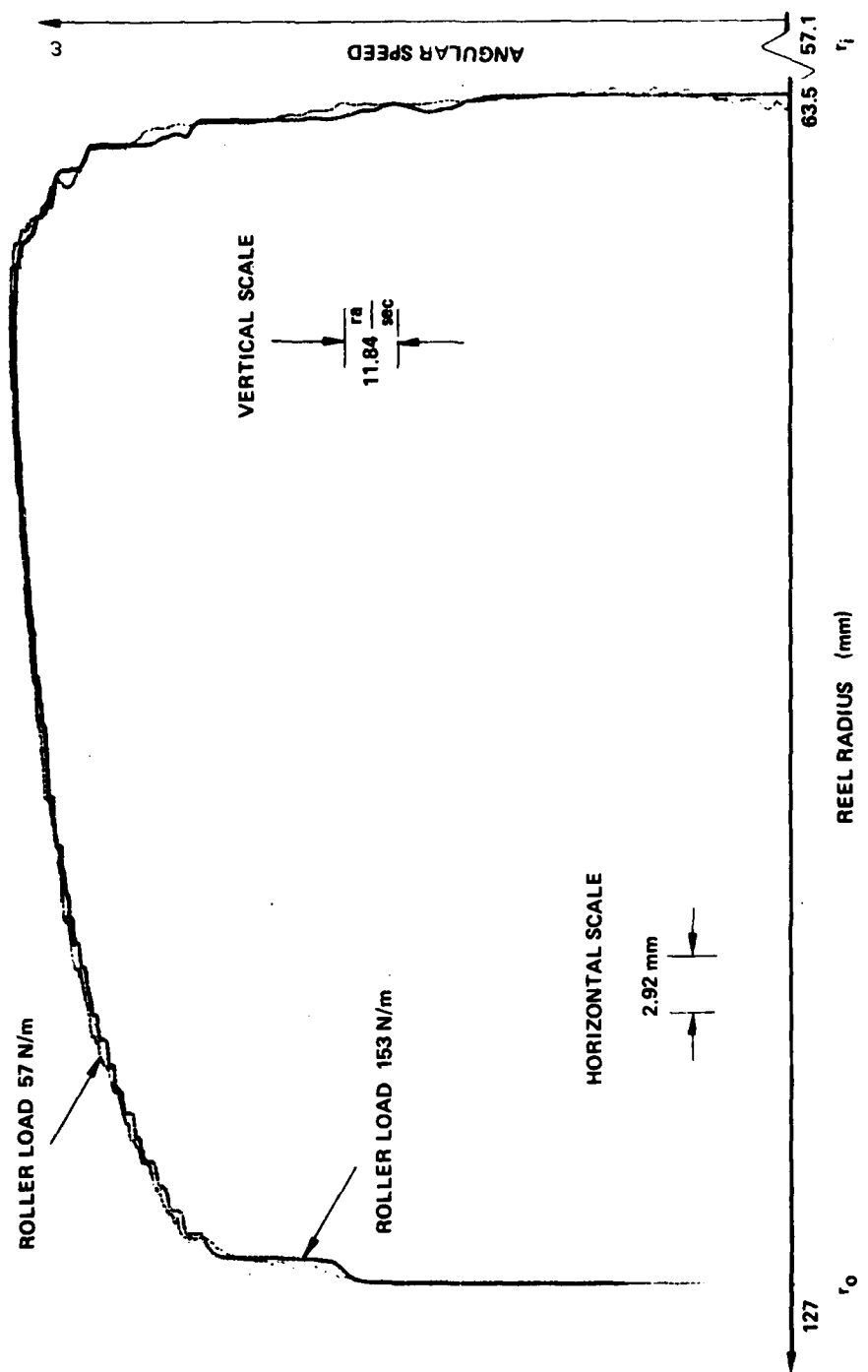


Figure 26 Angular Speed of Take Up Reel as a Function of Radius for Two Values of Roller Load.

One group of analyses is aimed at the estimation of time between rewinds. Several steps have been formulated. The first step consists of an analysis of the winding tension and reel speed in a fast winding process (Section 2.3.7.2). Secondly, using the winding tension, the equations provided may be used further to find the wound-in tension and pressure in the reel. Furthermore, on these, the effects of centrifugal forces and thermal perturbations may be superposed (Section 2.3.7.3). Finally, a model is described for slip during deceleration or acceleration of a reel with a given speed and a given pressure and tension distribution (Section 2.5.7.4). A desirable extension, which is recommended as a future task is the utilization of the logarithmic creep model to simulate the time history of pressure and tension in a reel subjected to thermal and humidity cycles. Since such a simulation was beyond the scope of the contract, cruder estimates were provided (Section 2.3.7.5).

The second area of analytical effort was motivated by the realization that air entrapment in reels needed to be eliminated. The parameters controlling air entrapment when a packing roller is used are analyzed in Section 2.3.7.6. Some insight into the dynamics of a packing roller is provided in Section 2.3.7.7.

### 2.3.7.2 Winding Speed and Tension During Fast Winding

In the interest of achieving tight fast winding we set out to analyze the following problem. Given the torques of the supply and take-up reel motors respectively,  $M_1$ ,  $M_2$  (possibly programmable, or varying with radius and speed), find the reel angular speeds  $\omega_1$ ,  $\omega_2$  and tension  $T$  as a function of reel radius. With empty reel inertia  $I$ , the equations below formulate the problem.

$$\dot{\omega}_2 = \frac{M_2 - (T + D)r_2}{I + \frac{\pi w P}{2}(r_2^4 - r_i^4)} \quad (1)$$

$$\dot{\omega}_1 = \frac{-M_1 + Tr_1}{I + \frac{\pi w P}{2}(r_1^4 - r_i^4)} \quad (2)$$

$$\omega_1 = \frac{r_2}{r_1} \omega_2 \quad (3)$$

$$\dot{r}_1 = -\frac{d}{2\pi} \omega_1 \quad (4)$$

$$\dot{r}_2 = \frac{d}{2\pi} \omega_2 \quad (5)$$

The boundary conditions are:

$$\begin{aligned} \text{at } r_2 &= r_i & r_1 &= r_o \\ \omega_1 &= 0 & & \\ \omega_2 &= 0 & & \end{aligned}$$

where

- $d$  = tape thickness
- $D$  = frictional drag on tape
- $r$  = instantaneous reel outer radius
- $r_i, r_o$  = inside and outside reel radii
- $w$  = tape width
- $\rho$  = tape density

For the particular case that  $M_1$  and  $M_2$  are constant, the problem may be formulated in dimensionless form as

$$\frac{\omega}{\sqrt{\frac{2\pi r_i}{d} \frac{M_2}{I}}} = f\left(\frac{r_o}{r_i}, \frac{M_1}{M_2}, \frac{\pi w \rho r_i^4}{2I}, \frac{D}{M_2 r_i^2}, \frac{r_o}{r_i}\right)$$

Similarly,  $T/(M_2/r_i)$  is expressible in terms of the same variables.

A typical plot of angular velocities and tension vs. radius is shown in Fig. 27 for constant holdback and take-up reel motor torques. It may be observed that upon starting, both reels accelerate rapidly. As the take-up reel gains inertia and its radius increases, its angular acceleration decreases until the reel reaches a peak angular velocity. On the other hand, the moment of inertia and radius of the supply reel continuously decrease and therefore its angular speed monotonically increases. Figure 28 shows a series of sample runs designed to qualitatively illustrate the effects of drag, torque ratio, hub inertia and reel radius. The case shown on top is a reference case. The other cases differ from the reference case by one parameter at a time.

### 2.3.7.3 Stresses in a Heated and/or Rotating Reel Modeled by a Disk

The first analysis of tangential and compressive stresses in wound reels known to the authors is given in [2]. Following some improvement, e.g. [3], the exposition in [4] seems best. The results of this analysis are described here with the addition of anisotropic thermal expansion and centrifugal effects.

Consider a reel of outer radius  $r_f$  rotating at an angular velocity  $\omega_f$  and temperature change  $\Delta T_f$  relative to its winding temperature. Consider it to be an orthotropic solid disk with some unknown initial stress distribution. The reel is wound around a hub (core) of a different material. The reel has anisotropic elastic moduli  $E_t$ ,  $E_r$ , Poisson's ratio  $\nu_t$ ,  $\nu_r$  and thermal expansion coefficients  $\alpha_t$ ,  $\alpha_r$ , (where the subscripts t, r denote the tangential and radial directions respectively). The stress distribution may be described as a superposition of the thermal stresses (due to  $\Delta T_f$ ) and the centrifugal stresses due to  $\rho\omega_f^2$  on the initial stresses (due to winding). The terms corresponding to each contribution are shown in the following paragraphs.

#### Thermal and Centrifugal Stresses:

In this paragraph we denote the increments in radial and tangential stresses and the radial displacement over their corresponding initial values at  $\omega_f = 0$ ,  $\Delta T_f = 0$  by  $\sigma_r$ ,  $\sigma_t$ ,  $u$  respectively. These functions must satisfy.

$$\frac{d}{dr}(\sigma_r r) - \sigma_t = -\rho\omega_f^2 r^2 \quad (\text{Equilibrium})$$

$$\frac{du}{dr} - \frac{1}{E_r} \sigma_r + \frac{\nu_t}{E_t} \sigma_t = \alpha_r \Delta T_f \quad (\text{Stress Displacement})$$

$$\frac{u}{r} - \frac{1}{E_t} \sigma_t + \frac{\nu_r}{E_r} \sigma_r = \alpha_t \Delta T_f \quad (\text{Stress Displacement})$$

with boundary conditions

$$\text{at } r = r_i \quad u - \frac{\sigma_r}{K_c} = \alpha_c r_i \Delta T_f \quad (\text{Core Stiffness})$$

$$\text{at } r = r_f \quad \sigma_r = 0$$

where  $K_c$  denotes an effective core stiffness defined as the pressure per unit radial displacement of the outer core (see below).

The solution of the problem may be found by superposing the solution of the homogeneous differential equations on particular solutions associated with the centrifugal effects (subscript  $\omega$ ) and the heating effects ( $h$ ). With the boundary conditions satisfied the pressure, tension and displacement in a reel owing to thermal and centrifugal effects are:

$$\begin{aligned} p = -\sigma_r &= -\rho \omega_f^2 (a_r a_\omega r^\alpha + b_r b_\omega r^{-\beta} + A_\omega r^3) \frac{1}{r} \\ &\quad - \Delta T_f (a_r a_h r^\alpha + b_r b_h r^{-\beta} + A_h r) \frac{1}{r} \end{aligned}$$

$$\begin{aligned} T/d = \sigma_t &= \rho \omega_f^2 (a_t a_\omega r^\alpha + b_t b_\omega r^{-\beta} + B_\omega r^3) \frac{1}{r} \\ &\quad + \Delta T_f (a_t a_h r^\alpha + b_t b_h r^{-\beta} + B_h r) \frac{1}{r} \end{aligned}$$

$$u = \rho \omega_f^2 (a_\omega r^\alpha + b_\omega r^{-\beta} + C_\omega r^3) + \Delta T_f (a_h r^\alpha + b_h r^{-\beta} + C_h r)$$

where

$$a_r = \frac{E_r}{1-\nu_t \nu_r} (\nu_t + \alpha) \quad b_r = \frac{E_r}{1-\nu_t \nu_r} (\nu_t - \beta)$$

$$a_t = \frac{E_t}{1-\nu_t \nu_r} (1 + \alpha \nu_r) \quad b_t = \frac{E_t}{1-\nu_t \nu_r} (1 - \beta \nu_r)$$

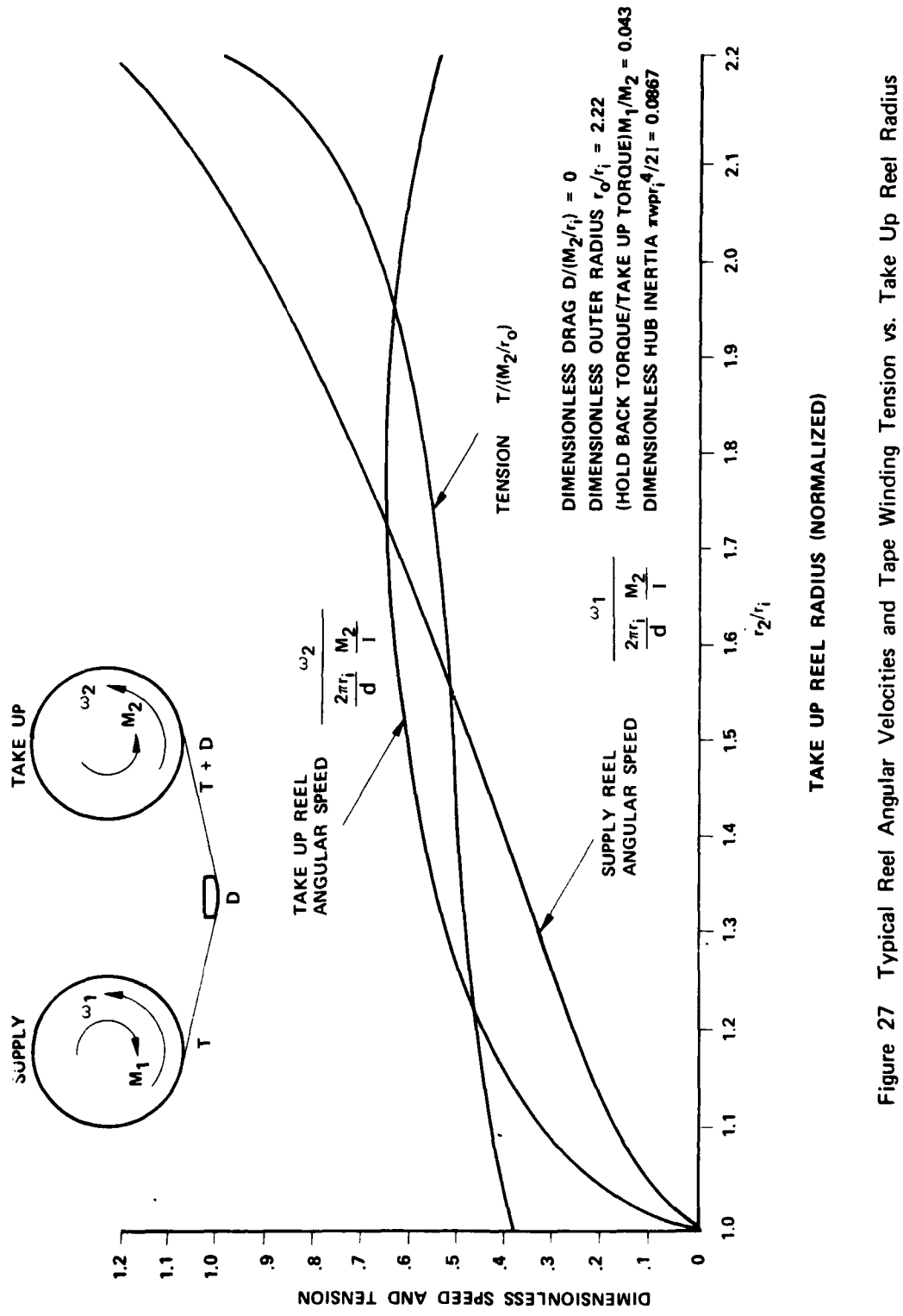


Figure 27 Typical Reel Angular Velocities and Tape Winding Tension vs. Take Up Reel Radius

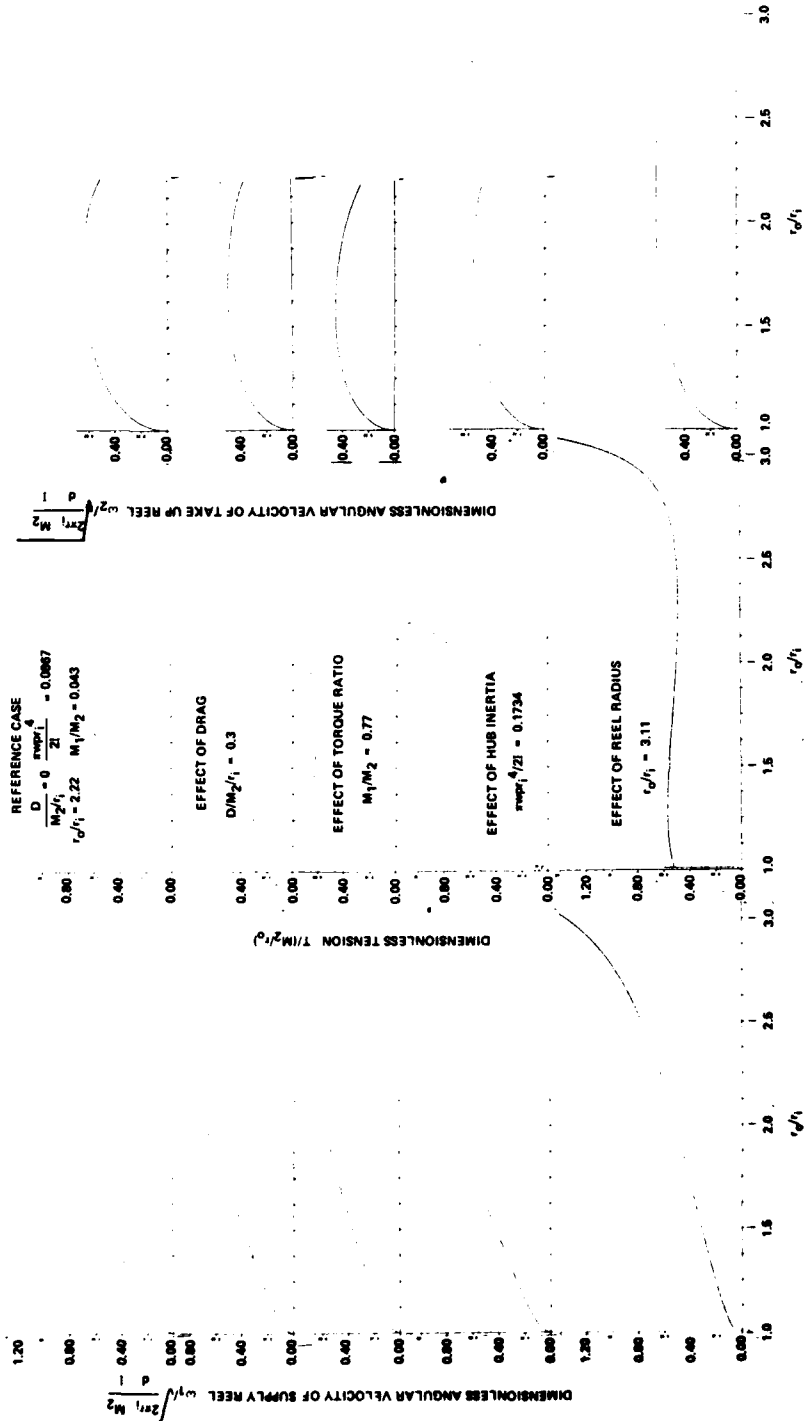


Figure 28 Qualitative Effect of Various Parameters on Angular Speed and Tension  
During Constant Torque Wind With No Capstan Control.

In addition, the coefficients of the particular solution associated with the centrifugal effects are:

$$A_w = \frac{\frac{1}{3} \frac{3+\gamma_t}{E_t}}{\frac{1}{3} + \frac{\gamma_r}{E_r} - \frac{3+\gamma_t}{E_t}}$$

$$B_w = \frac{\frac{1}{3} + \frac{\gamma_r}{E_r}}{\frac{1}{3} + \frac{\gamma_r}{E_r} - \frac{3+\gamma_t}{E_t}}$$

$$C_w = \frac{\frac{1}{E_t E_r} \left( \frac{(1-\gamma_r \gamma_t)}{3} \right)}{\frac{1}{3} + \frac{\gamma_r}{E_r} - \frac{3+\gamma_t}{E_t}}$$

and the coefficients of the particular solution associated with the thermal expansion are:

$$A_h = B_h = \frac{\alpha_t - \alpha_r}{\frac{1+\gamma_r}{E_r} - \frac{1+\gamma_t}{E_t}}$$

$$C_h = \frac{\alpha_t \left( \frac{1}{E_r} - \frac{\gamma_t}{E_t} \right) - \alpha_r \left( \frac{1}{E_t} - \frac{\gamma_r}{E_r} \right)}{\frac{1+\gamma_r}{E_r} - \frac{1+\gamma_t}{E_t}}$$

The determination of the integration constants from the boundary conditions yields:

$$a_{\omega} = \frac{\begin{vmatrix} C_{1\omega} & a_{12} \\ C_{2\omega} & a_{22} \end{vmatrix}}{\Delta}$$

$$b_{\omega} = \frac{\begin{vmatrix} a_{11} & C_{1\omega} \\ a_{21} & C_{2\omega} \end{vmatrix}}{\Delta}$$

$$a_h = \frac{\begin{vmatrix} C_{1h} & a_{12} \\ C_{2h} & a_{22} \end{vmatrix}}{\Delta}$$

$$b_h = \frac{\begin{vmatrix} a_{11} & C_{1h} \\ a_{21} & C_{2h} \end{vmatrix}}{\Delta}$$

$$\Delta = \begin{vmatrix} a_{11} & a_{12} \\ a_{21} & a_{22} \end{vmatrix}$$

$$a_{11} = a_r r_f^{\alpha-1}$$

$$a_{21} = r_i^{\alpha} - \frac{a_r r_i}{K_c} r_i^{\alpha-1}$$

$$a_{12} = b_r r_f^{-(\beta+1)}$$

$$a_{22} = r_i^{-\beta} - \frac{b_r r_i^{-(\beta+1)}}{K_c}$$

$$C_{1\omega} = -r_f^{\alpha} A_{\omega}$$

$$c_h = -A_h$$

$$C_{2\omega} = \frac{A_{\omega} r_i^2}{K_c} - C_{\omega} r_i^3$$

$$c_{2h} = a_c r_i + \frac{A_h}{K_c} - C_h r_i$$

Initial Winding Stresses in a Reel:

In this paragraph  $\sigma_r$ ,  $\sigma_t$ ,  $u$  denote respectively the increments in radial and tangential stresses and the radial displacement due to a stretched ring pressing on a disk of radius  $r_0$  as a tight sleeve. The ring simulates a newly wound layer of tape. The disk plays the role of the already wound portion of the reel. In this paragraph the disk is assumed to be at the winding temperature and at zero angular velocity. Therefore, the pressure assumed to be exerted by the newly wound layer of thickness  $dr_0$  at  $r_0$  is

$$dQ = \frac{\sigma_w - u_0(\omega) \cdot E_t / r_0}{r_0} dr_0$$

Here  $\sigma_w$  and  $\omega$  denote, respectively, the winding tensile stress and the winding angular velocity, both of which are prescribed functions of reel radius.  $u_0$  denotes the displacement of an inner disk of radius  $r_0$  due to centrifugal effects, which causes a reduction in the outer layer pressure when the disk is brought to rest. From the previous paragraph

$$u_0(\omega) = \rho \omega^2 (a_w r_0^\alpha + b_w r_0^\beta + c_w r_0^\gamma)$$

The following equations must be satisfied

$$\frac{d}{dr} (\sigma_r r) - \sigma_t = 0 \quad (\text{Equilibrium})$$

$$\frac{du}{dr} - \frac{1}{E_r} \sigma_r + \frac{\gamma_r}{E_t} \sigma_t = 0 \quad (\text{Stress Displacement})$$

$$\frac{u}{r} - \frac{1}{E_t} \sigma_t + \frac{\gamma_r}{E_r} \sigma_r = 0 \quad (\text{Stress Displacement})$$

with boundary conditions:

$$\text{at } r = r_i \quad u - \frac{\sigma_r}{K_c} = 0$$

$$\text{at } r = r_0 \quad \sigma_r = -dQ \quad (\text{outer layer pressure})$$

$K_c$  denotes the effective core stiffness. If the core is considered to be an isotropic thick shell with outer radius  $r_i$ , inside radius  $r_c$  and Young's modulus  $E_c$ , then the core stiffness is:

$$K_c = -\frac{E_c}{r_i} \frac{\left(\frac{r_i}{r_c}\right)^2 - 1}{(v-1)\left(\frac{r_i}{r_c}\right)^2 - (v+1)}$$

If the hub may be considered a thin shell of thickness  $d_c$ , the expression simplifies to

$$K_c = \frac{E_c d_c}{r_i^2}$$

The initial interlayer pressure in a roll is found [4] to be:

$$p(r) = -\zeta_r = \frac{1 + \alpha(r/r_i)^{-2\beta}}{(r/r_i)^b} \int_r^{r_o} \frac{(r_o/r_i)^b}{1 + \alpha(r_o/r_i)^{-2\beta}} \cdot dQ$$

and the tangential wound-in tension per unit width is:

$$T(r) = T_w - u_f \frac{E_t}{r_o} d - d \cdot \frac{\alpha - \alpha \beta(r/r_i)^{-2\beta}}{(r/r_i)^b} \int_r^{r_o} \frac{(r_o/r_i)^b}{1 + \alpha(r_o/r_i)^{-2\beta}} \cdot dQ$$

where

$$\alpha = \frac{r - \mu - E_t/(K_c r_i)}{\delta + \mu + E_t/(K_c r_i)}$$

$$b = 1 - \alpha$$

$$\alpha = \gamma - \delta$$

$$\beta = \gamma + \delta$$

$$\gamma = \sqrt{\delta^2 + E_t/E_r}$$

$$\delta = 0.5 (\nu_t - \nu_r E_t/E_r)$$

$$\mu = 0.5 (\nu_t + \nu_r E_t/E_r)$$

$$u_f = P \omega_f^2 (a_w r_f^\alpha + b_w r_f^{-\beta} + c_w r_f^3)$$

### Comparison of Theory and Experiment:

A tab pull force distribution obtained experimentally has been compared with the theoretical initial pressure distribution for constant torque winding obtained by the equations described in this section. The conversion of the tab pull force to pressure was done assuming the combined friction coefficient between the tab, and both the oxide and the back coating to be 0.59. This value was, obtained independently by loading a tab between several layers of foil on a flat table, applying a load and measuring the force required to pull the tab. The result presented in Figure 29 shows a remarkably good agreement between theory and experiment.

#### 2.3.7.4 A Model for Reel Slippage During Deceleration

Consider a reel rotating at an angular speed  $\omega_f$  with a known tension and pressure distributions  $T(r, \omega_f), p(r, \omega_f)$ . If this reel is subjected to an angular deceleration  $\alpha = \dot{\omega}$ , the reel is expected to slip if there exists some value of the radius  $r$  in the range  $r_i \leq r \leq r_f$  such that:

$$\int_s p(r, \omega_f) 2\pi r^2 \pm T(r, \omega_f) r \leq \rho \frac{\pi (r_f^4 - r^4)}{2} \cdot \alpha$$

Here the plus applies when the deceleration tends to tighten the reel (as shown in Figure 30) and the minus applies when the deceleration tends to loosen the reel.

Since the information about deceleration propagates from the hub outwards, one would expect the lowest value of  $r$  satisfying the above equation to be the point where slip would start. Once slip started, the stress distribution in the reel is changed and the above analysis is not expected to be valid.

To obtain a qualitative physical feel of the above equation, refer to Fig. 31. The right hand side of the equation is shown by broken lines for a range of  $\alpha = \dot{\omega}$  values. In the left hand side, the tension contribution is usually small and the pressure  $p$ , usually increases from zero at  $r_0$  to some maximum value close to the interior. A typical form of the left hand side is shown as a solid line. Thus, for small  $\alpha$  the slip condition is never fulfilled.

For greater  $\alpha$  values slip will start at  $r_i$ . For some other forms of pressure distribution, slip may conceivably start at some larger radius but presumably not too far from the hub.

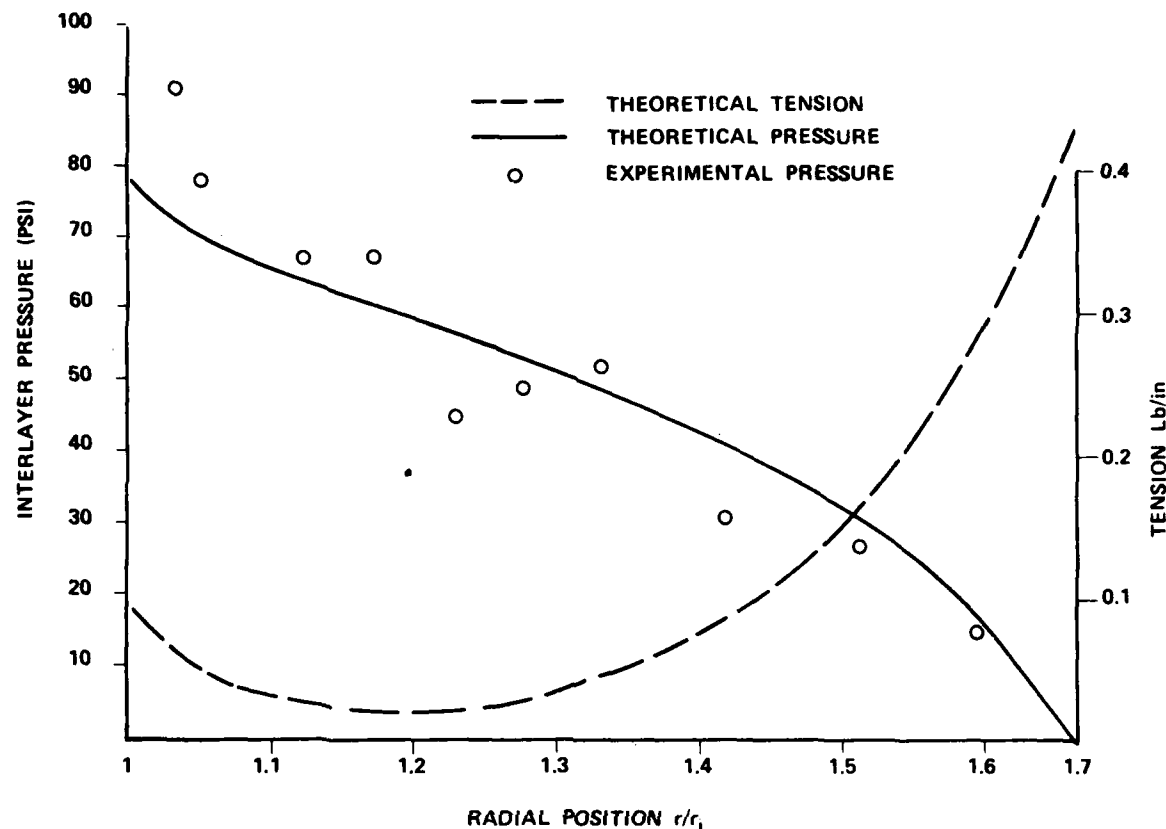


Figure 29 Comparison of theoretically predicted pressure distribution in a reel with experimental results obtained by friction tabs. (Tab pull force was converted into pressure by using an independent measurement of composite friction coefficient between tab and two adjacent tape layers of 0.59.)

Core

$r_c = 1.74''$   
 $r_i = 2.25''$   
 $E_c = 1.06 \times 10^7$  psi (Aluminum)  
 $\nu_c = 0.33$

Reel

$E_t = 6 \times 10^5$  psi  
 $E_r = 2 \times 10^4$  psi  
 $\nu_t = \nu_r = 0.3$   
 $r_f = 3.74$   
 $M = 1.68$  in Lb (Constant torque)  
 $d = 0.92$  mil

### Comparison of Theory and Experiment:

Referring to Figs. 20 & 21, we find that a tab pull force of 25 N (5.6 lb) at  $r = 2.36''$  is the threshold value for slippage at  $\alpha = 400 \text{ rad/sec}^2$ . Using a friction coefficient of tab to tape of 0.59 the threshold interlayer pressure is:

$$\frac{5.6 \text{ lb}}{0.59 \times 0.25 \text{ in}^2} = 38 \text{ psi}$$

Assuming that this pressure is the same as the pressure at the hub, assuming that the tension is equal to the winding tension, i.e., 0.75 lb/in, and the interlayer friction coefficient is 0.3, the predicted threshold  $\alpha$  is:

$$\begin{aligned} \alpha &\geq \frac{f_s p 2\pi r_i^2 - Tr_i}{\rho \pi \frac{(r_f^4 - r_i^4)}{2}} = \\ &= \frac{0.3 \times 38 \times 2\pi \times 2.25^2 - 0.75 \times 2.25}{0.0484 \cdot \pi (5.14 - 2.25^4)} = 2815 \frac{\text{rad}}{\text{sec}^2} \end{aligned}$$

Thus the predicted threshold angular deceleration is an order of magnitude greater than the actual one, indicating that the above model is not correct. This is an area which merits further investigation.

#### 2.3.7.5 Estimates of Periods Between Rewinds

As indicated earlier in this report, the relaxation of a stored wound reel necessitates rewinding to re-establish reel tension and protect reel integrity. In this section estimates of the period between rewinds as a function of temperature are provided. The assumptions underlying these estimates are delineated below and then the conclusions are presented.

The first assumption made is that the time to rewind occurs when reel interlayer pressure relaxes to 50% of the original interlayer pressure. Figure 21 indicates that for the typical reels used in our experiments, accelerated pressure reduction to 50% of the original level brought the reels to the threshold of slippage for deceleration of  $400 \text{ rad/sec}^2$ . Since this is a high deceleration, the 50% figure is a conservative one.

Secondly, it is assumed that interlayer pressure relaxes proportionally to tension level.

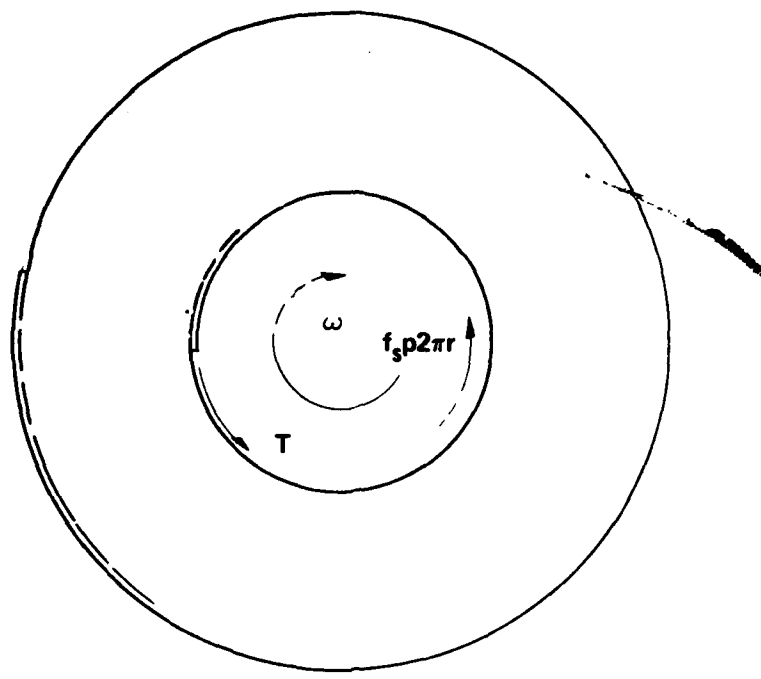


Figure 30 Free Body Diagram of a Decelerating Reel (Tightening Direction)

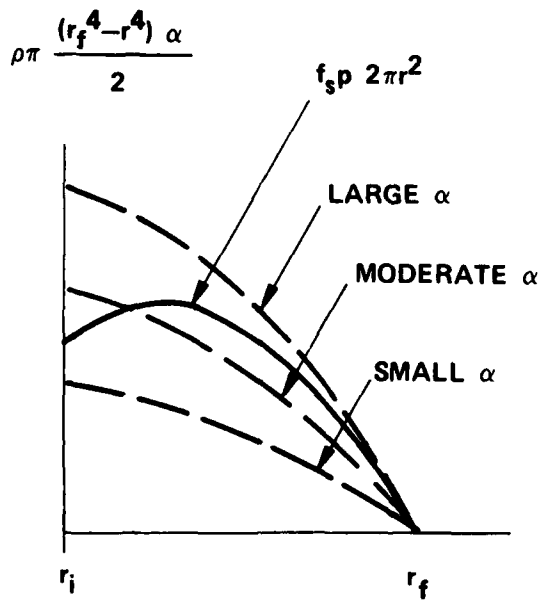


Figure 31 Schematic Comparison of Terms in the Slip Condition

The third assumption is that the time for the tension to relax 50% to its original value is roughly the same as the time for creep strain in a constant-tension creep-test to reach 50% of the elastic strain. Since creep rates are proportional to stress, the above assumption is also a conservative one.

Finally, it is assumed that asymptotically, total strain behaves with time as shown in Fig. 6, namely  $\epsilon \sim t^{0.0722}$ .

Using the above and assuming that if the creep strain  $\Delta\epsilon_1$  is known at a given time  $t_1$ , then the time  $t_{50\%}$  for the creep strain to reach 50% of the elastic strain, at the same temperature, may be found by the extrapolation:

$$t_{50\%} = t_1 \left( \frac{\frac{1}{E} + \frac{0.5}{E}}{\frac{1}{E} + \frac{\Delta\epsilon_1}{G}} \right)^{1/0.0722}$$

Various experimental results have been extrapolated according to this formula. The resulting (conservative) estimates are shown in Fig. 32.

The Ampex results indicated on the graph have been described in detail in Section 2.3.3, 2.3.4. The average creep level measured in these tests with the addition of two standard deviations was extrapolated as described above and forms one point of our recommended period between rewinds at 65°F. The slope of the recommendation curve is based on the values of  $a_T$  (Figure 7). Thus it is safe to retain a reel wound at 65°F for at least 3.5 years without rewinding provided that the environment is maintained at 65°F and constant relative humidity. At 75°F the safe period is reduced to 10.5 months approximately.

The effect of a winding temperature higher than the storage temperature, or a lower winding humidity compared to the storage humidity, is to prolong the allowable period between rewinds. The reason is that these effects reduce reel tensions and lower creep rates. Though favorable, only small differences of this type are recommended (up to perhaps 5°F and 10%RH) since larger differences would conceivably bring about a need to equilibrate the tapes when carried from the storage area to the computer room. This small variation would pose no real danger of bringing the reels close to an imminent slip condition, while providing a beneficial effect. The following estimate is given to prove this point. If we accept as a criterion for imminent slip, 50% reduction in elastic strain, then one of the following environmental effects is sufficient to cause such a state.

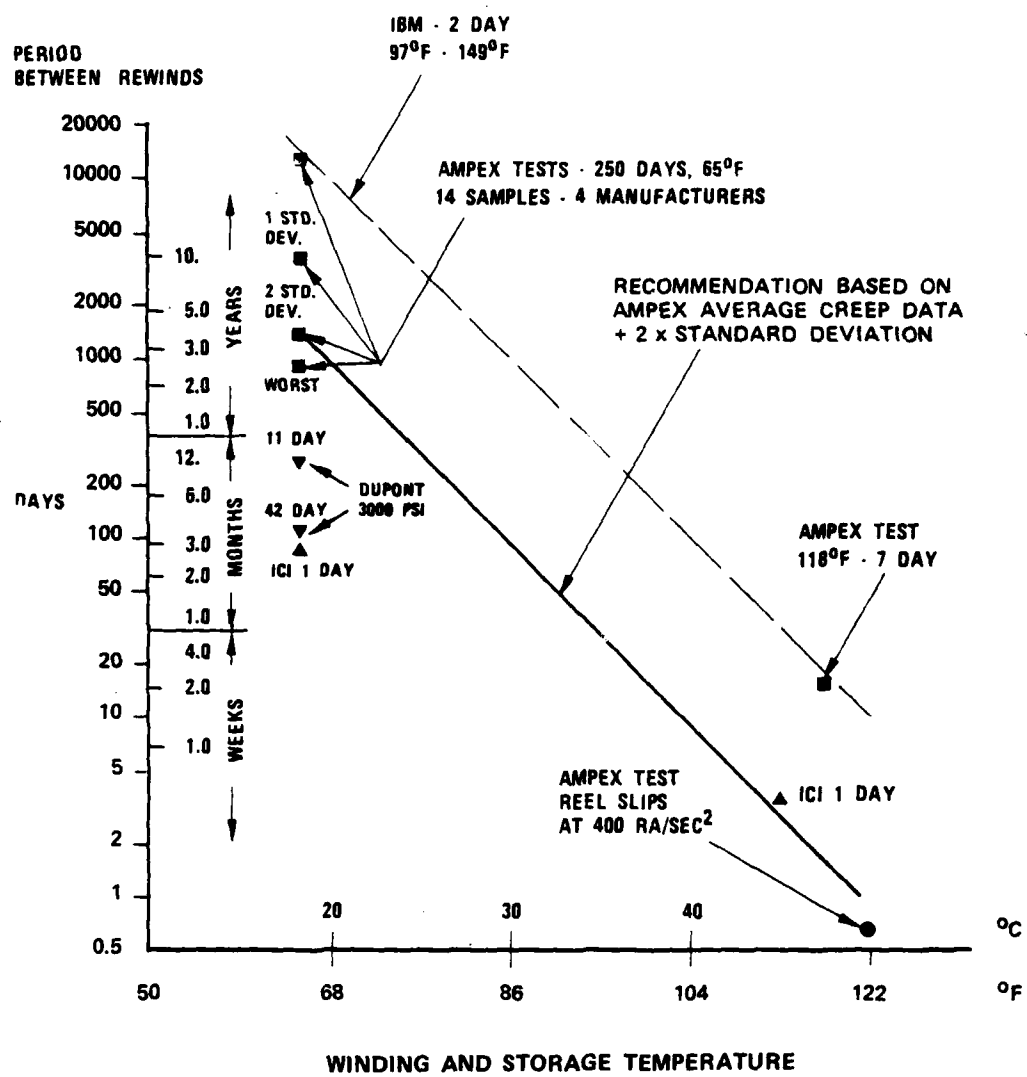


Figure 32 Estimated Period Between Rewinds as a Function of Storage Temperature. Based on a Non-linear Extrapolation of Time for Total Strain to Reach 150% of Elastic Strain ( $\epsilon \sim t^{0.07}$ ).

For an elastic strain of  $1 \times 10^{-3}$ , a radial temperature expansion coefficient of  $1.5 \times 10^{-5} \text{ } 1/\text{ }^{\circ}\text{C}$  for the foil and  $4.5 \times 10^{-5} \text{ } 1/\text{ }^{\circ}\text{C}$  for the hub, a temperature reduction of the order

$$\Delta T = \frac{0.5 \times 10^{-3}}{4.5 \times 10^{-5} - 1.5 \times 10^{-5}} \approx 17^{\circ}\text{C} (30^{\circ}\text{F})$$

is needed to halve the strain. Similarly, for a humidity expansion coefficient of  $10.9 \times 10^{-6} \text{ } 1/\% \text{RH}$  for the foil and zero for the hub, 50% reduction in strain would occur due to an increased RH of:

$$\Delta RH = \frac{0.5 \times 10^{-3}}{10.9 \times 10^{-6}} = 45\%$$

A similar reasoning would indicate that an increase in temperature relative to the winding temperature or decrease in RH relative to the winding RH, accelerates the creep rate by increasing the stress level in the reel, (this is in addition to the fact that the creep rate itself increases with temperature as indicated earlier). Avoiding stress increments of more than 5% of the elastic strain dictates approximately 3°F upward tolerance on temperature and 5%RH downward on humidity. No estimates on the effect on time to rewind of these bounds is given here. Some information about this issue is provided in [6,8]. [6] states; "A typical reel when stored at 120°F after being wound at 70°F, and when the coefficient of thermal expansion of the hub is three times the value of the tape, will approach stress free conditions at least 80% earlier than when stored at the winding temperature". It is to be noted that this conclusion is arrived at in [6] only on the basis of thermal stresses in the reel with the creep rate itself assumed constant with temperature.

### 2.3.7.6 Air Entrapment During Packing Roller Assisted Winding

Winding a reel with a packing roller loading the nip has been shown to be beneficial in eliminating interlayer air (Section 2.3.6). The following paragraph provides a simplified model of the air entrapment process. A prediction formula is derived and a qualitative description of the effects of various parameters is given.

Referring to Figure 33, the pressure distribution in the nip is controlled by Reynold's equation

$$\frac{dp}{dx} = -6\mu(U+V) \frac{h_0 - h^* + \frac{x^2}{2r_0}}{(h_0 + \frac{x^2}{2r_0})^3}$$

with boundary conditions

$$p = p_a + \frac{T}{r_0} \quad \text{at} \quad x = 0$$

$$p = p_a \quad \text{at} \quad x \rightarrow \infty$$

where  $h^*$  is a constant to be determined.

Integration in closed form yields the pressure distribution:

$$\frac{p-p_a}{T/r_0} = 1 - \frac{12\mu U}{T} \frac{r_0}{h_0} \sqrt{\frac{2r_0}{h_0}} \left[ f_1(\xi) - \frac{h^*}{h_0} f_2(\xi) \right]$$

where

$$f_1(\xi) = \int_0^\xi \frac{d\xi}{(1+\xi^2)^2} = \frac{\xi}{2(1+\xi^2)} + \frac{1}{2} \arctan \xi$$

$$f_2(\xi) = \int_0^\xi \frac{d\xi}{(1+\xi^2)^3} = \frac{\xi}{4(1+\xi^2)^2} + \frac{3}{4} f_1(\xi)$$

$$\frac{h^*}{h_0} = \frac{4}{3} \left( 1 - \frac{1}{\frac{\pi}{4} \frac{12\mu U}{T} \frac{r_0}{h_0} \sqrt{\frac{2r_0}{h_0}}} \right)$$

The load capacity per unit width required to overcome air bearing effects is:

$$L = \int_0^\infty p dx = 2\mu U \frac{r_0}{h_0} + \frac{4}{3\pi} \frac{T \sqrt{2r_0 h_0}}{r_0}$$

It is to be noted (Figure 33) that depending on geometry an additional (and possibly larger) component of load  $L_T = 2T \sin \Theta/2$  is required to overcome the tape tension components.  $L_T$  acts along the bisector of the wrap angle.

The dependence of  $L$  on various parameters is shown in Fig. 34. It may be seen that generally the magnitude of the required net load is quite small and is insensitive to tension and reel radius though roughly proportional to speed and guide radius. It may be observed, however, that while a small load will eliminate most of the air film, considerable load is required to eliminate its last few microinches.

### 2.3.7.7 Dynamics of a Packing Roller Follower

The purpose of this section is to answer the following question: under what conditions will a packing roller follow a reel with a runout without losing contact.

The model being considered is sketched in Fig. 35. The reel surface may be simulated by a perturbation  $x = x_{\max} \sin \omega t$  where  $\omega$  is the angular velocity of the reel and  $x_{\max}$  is the radial runout. The displacement of the packing roller  $m_1$  from the average position is  $x$  and the displacement of a lumped packing roller arm mass  $m_2$  is  $y$ . Assuming constant preload  $F_0$  and a spring constant  $k$ , one may write

$$\begin{aligned} m_1 \ddot{x} &= k(y-x) + F_R \\ m_2 \ddot{y} &= k(x-y) - F_0 \end{aligned}$$

where  $F_R$  is the reaction force of the reel surface on the packing roller.

It may be concluded that

$$F_R = F_0 + \left[ 1 - \left( \frac{\omega}{\sqrt{k/m_1}} \right)^2 - \frac{1}{1 - \left( \frac{\omega}{\sqrt{k/m_2}} \right)^2} \right] \cdot k x_{\max} \sin \omega t$$

$$y = - \frac{F_0}{k} + \frac{1}{1 - \left( \frac{\omega}{\sqrt{k/m_2}} \right)^2} x_{\max} \sin \omega t$$

The condition for no loss of contact between the packing roller and reel is  $F_R > 0$ . Figure 36 shows schematically the frequency response of the system.

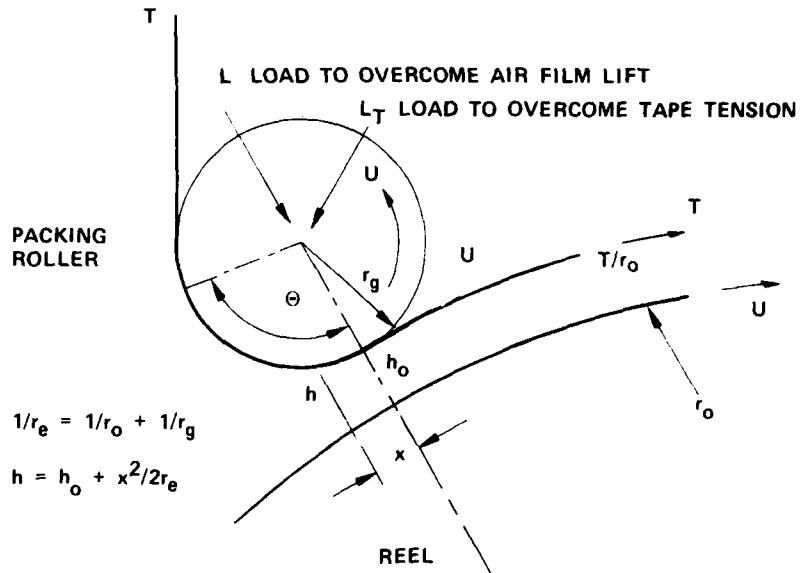


Figure 33 Schematic View of Packing Roller Assisted Winding

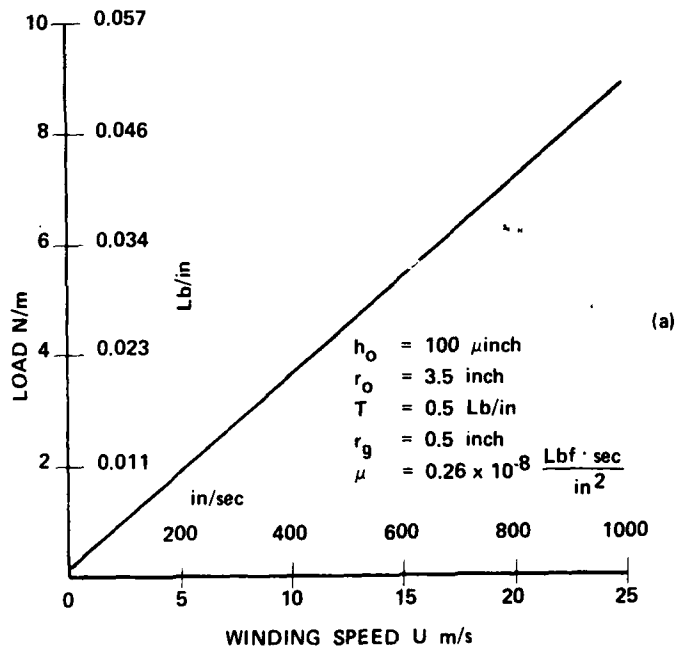
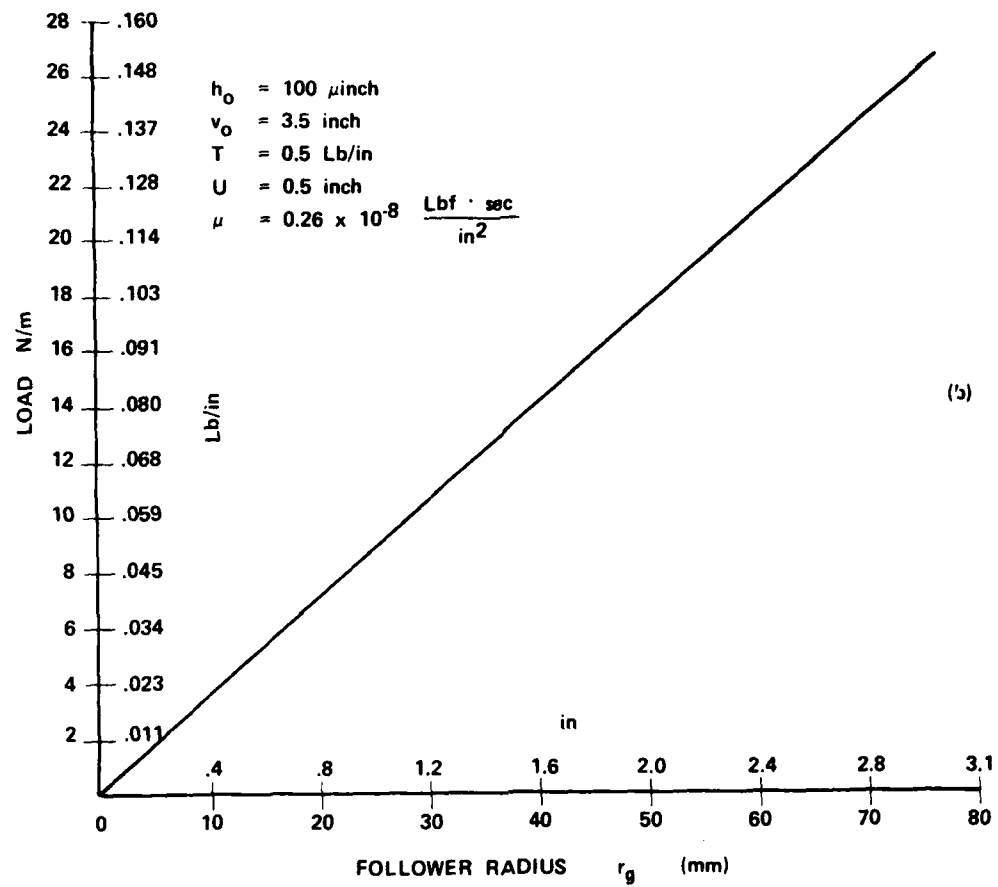
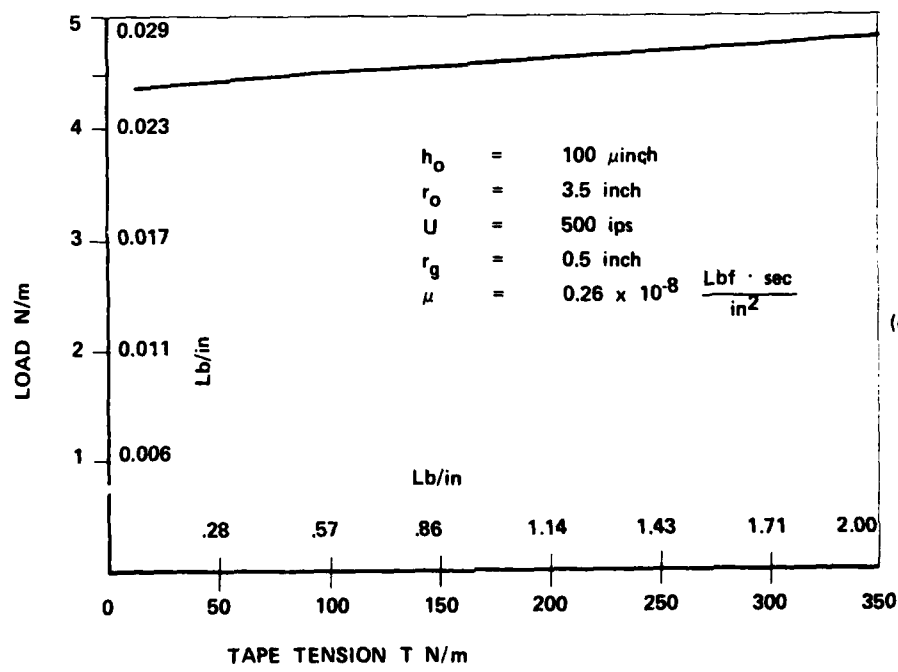


Figure 34 Sample Curves Showing Effect of Various Parameters on Lead Required per Unit Width to Reduce Air Film to 100  $\mu\text{in}$ .



(b)



(c)

Figure 34 (Continued)

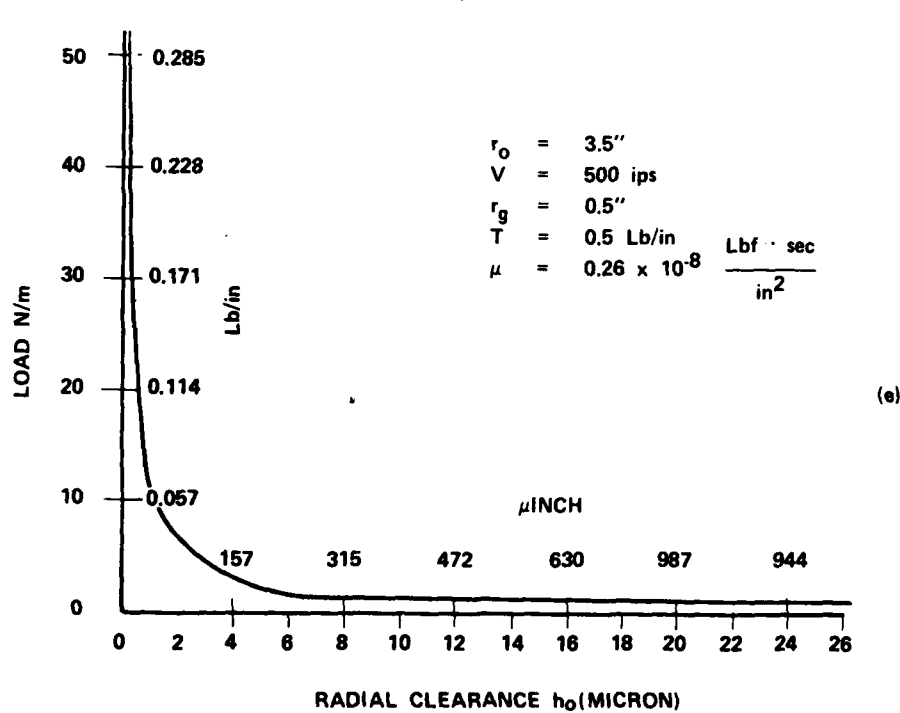
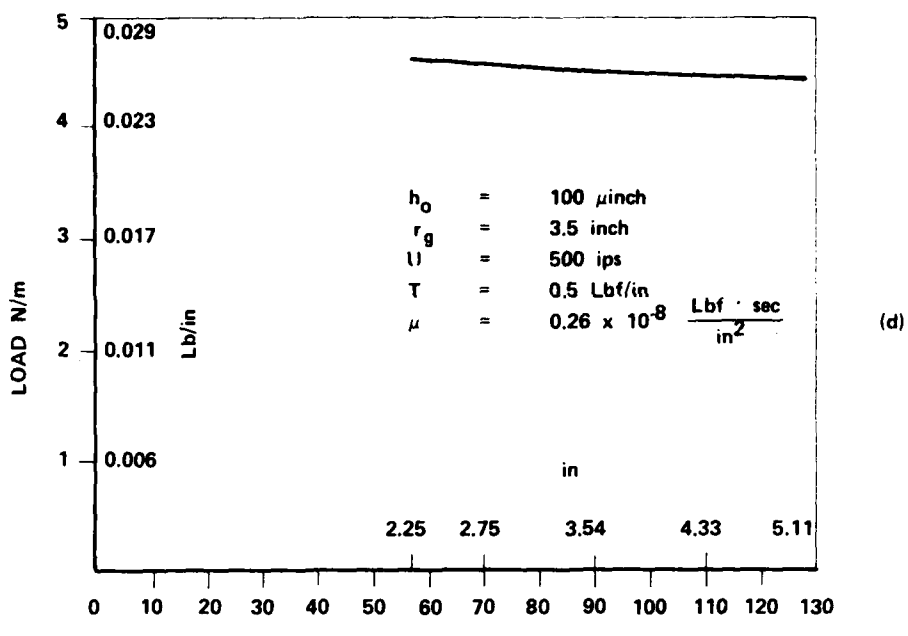


Figure 34 (Continued)

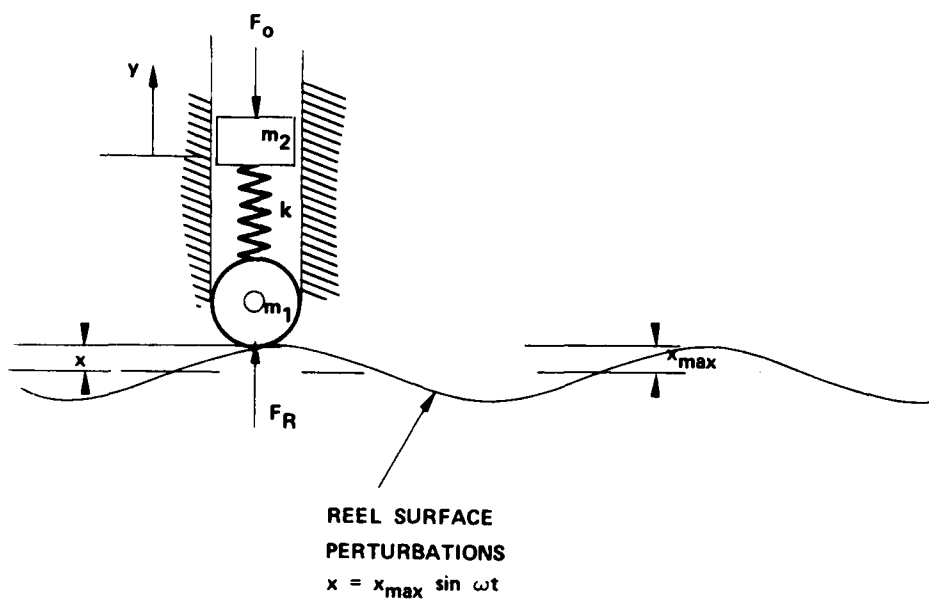


Figure 35 Model of Packing Roller Following a Reel with Runout

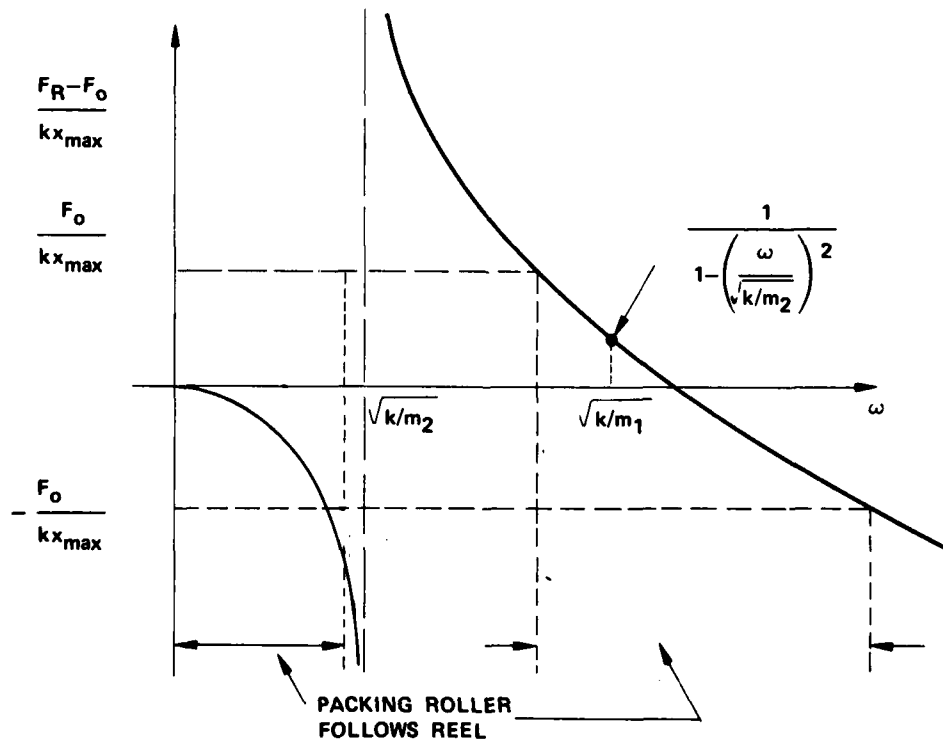


Figure 36 Frequency Response of a Typical Packing Roller Follower with Respect to Reel Runout of Form  
 $x_{\max} \sin \omega t.$

## 2.4 Chemical Kinetics of Tape Binder Degradation

Virtually all magnetic recording tape consists of a polyester urethane binder which contains the magnetic particle suspension to form a dense, uniform, smooth, magnetic coating surface. The substrate which supports the coating is also a polyester polymer for most magnetic tapes and chemically is polyethylene terephthalate (PET). All polyesters are, in general, susceptible to degradation by hydrolysis which is the chemical reaction of water with the polymer. In a paper by E. Cuddihy, "Aging of Magnetic Tape", [17] it is argued that hydrolysis of the substrate is negligibly slow as well as oxidation and pyrolysis of the binder. In this section, we will review the hydrolysis process, summarize measured rates from Ref. 17 and present a mathematical analysis which leads to reasonable archivability criteria for magnetic tape. It should be noted that hydrolysis rates depend on the binder constituents so that the conclusions drawn here are restricted to apply only to binders composed of polyester urethanes. In addition, the rates derived in Ref. 17 were from studies on a 3M900 tape. Although it is likely that these rates apply generally to all polyester urethane binders, there may be some variation since there is a wide variation in additives which different manufacturers use in binder formulation.

The hydrolysis process consists essentially of water plus ester combining to form carboxic acid and alcohol. Since the ester is part of the coupling network which forms the binder, hydrolysis weakens the tape and can lead to the hydrolysis products which cause tape shed and dropouts. Experimental evidence indicates that hydrolysis is a reversible process; thus it may be expressed as



where E, W are respectively the ester and water, C, A are respectively the carboxic acid and alcohol. For the purpose of this analysis it is sufficient to express the process in terms of one product:



The rate equation which may be formulated from this reaction is

$$\frac{d[C]}{dt} = K_f [E][W] - K_r [C] \quad (11)$$

where [ ] denotes concentration.

In Eq. 11 the rate of production of [C] is equal to a forward rate constant  $K_f$  times the product of the ester concentration [E] and water concentration [W] minus a reverse rate  $K_r$  times the concentration [C]. The essence of the interpretation is that the hydrolysis process will not proceed indefinitely. Not only is reversibility included in Eq. 11, but a definite final process equilibrium is entailed which depends on the relative humidity (via [W]) and temperature (via  $K_f$  and  $K_r$ ). Thus, as will be discussed in some detail, the proper way to state tape longevity is to give a table in which regions are denoted where tape storage in a range of temperatures and humidities yields a usable tape after the hydrolysis process has come to equilibrium.

The essential points of Eq. 11, therefore, are the final equilibrium state and the initial rate of reaction. Whatever the initial concentrations, equilibrium occurs when the process is stationary or

$$\frac{d[C]}{dt} = 0 \quad (12)$$

Thus, equilibrium is given by

$$K_f [E][W] = K_r [C] \quad (13)$$

If it is assumed that the tape (binder) is in a fixed water atmosphere of concentration  $[W_o]$  and that the total binder  $[B_o]$  represents the fixed sum of [E] and [C], then Eq. 13 may be written as

$$K_f ([B_o] - [C_{eq}]) [W_o] = k_r [C_{eq}] \quad (14)$$

so that the equilibrium concentration of hydrolysis product  $[C_{eq}]$  is given by

$$[C_{eq}] = \frac{K_f [B_o] [W_o]}{K_f [W_o] + K_r} \quad (15)$$

(An analysis of the time to reach equilibrium is given in the addendum of this section.)

The other important concept is the initial rate of reaction. If the initial rate is defined as

$$K_i = \left[ \frac{1}{[C]} \frac{d[C]}{dt} \right]_{t=0} \quad (16)$$

then from Eq. 11 one obtains

$$K_i = K_f [W_o] \frac{[E_o]}{[C_o]} - K_r \quad (17)$$

But  $[E_o] = [B_o] - [C_o]$

and  $[W_o]$  may be written as

$$[W_o(T, RH)] = [W_o(T, 100\%)] RH \quad (18)$$

where the relative humidity RH is expressed as a fraction. Thus a simple form is

$$K_i = K_f' RH - K_r \quad (19)$$

where

$$K_f' \equiv K_f [W_o(T, 100\%)] \left\{ \frac{[B_o]}{[C_o]} - 1 \right\} \quad (20)$$

Now from Cuddihy's work [17] the rates for tape aging in air (at least the tape he used) may be summarized as

$$K_r = e \left( 16.1 - \frac{4790}{T(^{\circ}K)} \right) \times 10^{-2} \text{ weeks}^{-1}$$

$$K_f' = e \left( 25.7 - \frac{7310}{T(^{\circ}K)} \right) \times 10^{-2} \text{ weeks}^{-1} \quad (21)$$

Using this information with Eq. 19 yields a curve in the temperature-humidity plane along which the initial rate  $K_i$  is zero. The curve is given by

$$T(^{\circ}\text{K}) = \frac{2520}{9.6 + \ln \text{RH}} \quad (22)$$

In Eq. 22 T is the temperature in degrees Kelvin, RH is the fractional humidity and ln denotes the natural logarithm to base e. The curve given by Eq. 22 is plotted in Fig. 37 where it is labeled  $K_i = 0$ . For convenience, the temperature axis is labeled in degrees Fahrenheit. Along this curve there is no hydrolysis. For temperatures and humidities below the curve, the rate is negative; presumably ester bonds are regenerated. For higher temperatures and humidities, hydrolysis proceeds and the binder is consumed.

Using Eq. 17 (with 18, 20 and 21) a curve of fixed hydrolysis level can be obtained.

The result is

$$(T^{\circ}\text{K}) = \frac{2520}{9.6 + \ln \text{RH} + \ln \left[ \left( \frac{[B_0]}{[C_{eq}]} - 1 \right) / \left( \frac{[B_0]}{[C_0]} - 1 \right) \right]} \quad (23)$$

This expression yields [14] when  $[C_{eq}] = [C_0]$  (the meaning of  $K_i = 0$ ). For Cuddihy's tapes,  $[C_0]/[B_0] = 6.7\%$  so that, for example, if a final equilibrium  $[C_{eq}]/[B_0] = 14\%$  is chosen, it is possible to plot a storage condition curve in Fig. 37 which yields 14% of the binder hydrolysed (from an initial 6.7%). This is shown in Fig. 37. For any storage condition along that curve hydrolysis will yield 14% of the binder consumed.

Archival storage (and operation) conditions can be determined from Fig. 37 immediately. Although this will be discussed in Section 3.1.2 a reasonable, safe choice which is not uncomfortable for personnel would be  $65^{\circ}\text{F}$  and 40%RH.

#### ADDENDUM: Time to reach Equilibrium and Binder Rejuvenation

From Eq. 11 of this section, the basic rate equation is

$$\frac{d[C]}{dt} = K_f [E] [W] - K_r [C] \quad (24)$$

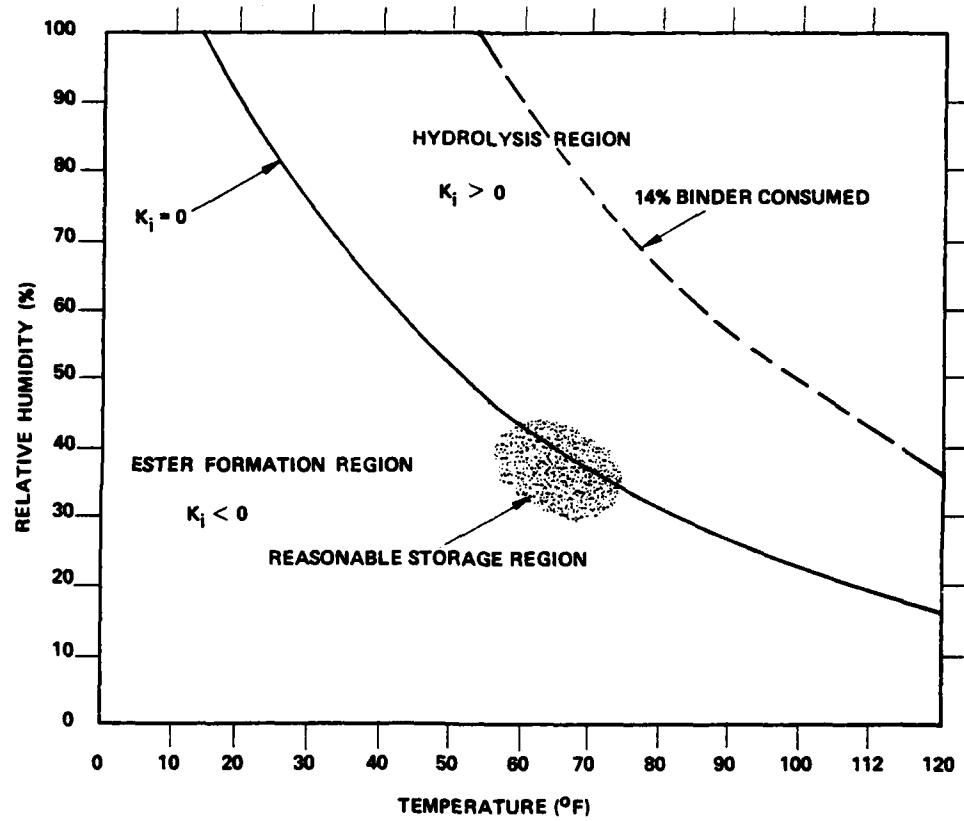


Figure 37 Hydrolysis equilibrium curves vs humidity and temperature.  
 $K_i = 0$  indicates initial equilibrium. Dashed curve denotes 14% binder hydrolysed from an initial 6.7%.

In the process considered here, the water concentration is fixed

$$[W] = [W_0] \quad (25)$$

and also the total binder

$$[B_0] = [E] + [C] \quad (26)$$

From Eq. 15 the final equilibrium state is

$$[C_e] = \frac{K_f[B_0][W_0]}{K_f[W_0] + K_r} \quad (27)$$

Combining Eq. 24 and 25 yields

$$\frac{d[C]}{dt} = K_f[B_0][W_0] - [C](K_r + K_f[W_0]) \quad (28)$$

Combining Eq. 27 and 28 yields

$$\frac{d[C]}{dt} = R([C_e] - [C]) \quad (29)$$

where

$$R \equiv K_f[W_0] + K_r \quad (30)$$

the solution to Eq. 29 is

$$[C] = [C_e] + ([C_0] - [C_e]) e^{-Rt} \quad (31)$$

where  $[C]$ ,  $[C_0]$ ,  $[C_e]$  are respectively the hydrolysis product (proportional to the resent extractables), at time  $t$ , at the beginning of the reaction ( $t = 0$ ), and at equilibrium ( $t = \infty$ ). A reasonable definition of "time to reach equilibrium" is when the reaction is 90% to completion. This yields

$$t_e = \frac{\ln 10}{R} \quad (32)$$

Using Eqs. 18, 20 yields

$$t_e = \frac{2.3 \left( \frac{[B_o]}{[C_o]} - 1 \right)}{K_f' RH + K_r \left( \frac{[B_o]}{[C_o]} - 1 \right)} \quad (33)$$

For example, let storage be at  $T = 55^{\circ}\text{C}$ , 100%RH ( $RH = 1$ ). (34)

Using the data summarized in Eq. 21 of Cuddihy's experiments [17] (and  $[C_o]/[B_o] = 6.7\%$ ) yields

$$t_e = 35 \text{ weeks} \quad (35)$$

This time is virtually the period of the tape storage for this contract so that storage at  $55^{\circ}\text{C}$ , 100%RH provides a partial test of these ideas.

The essential reversibility of the hydrolysis process as determined from the experiments of Cuddihy [17] entail the possibility of tape rejuvenation. A tape stored at an extreme environment resulting in a weakened binder could have the binder strengthened by subsequent storage in a 'cool-dry' environment. Such a regenerative environment would be one whose 'temperature-humidity' fell below the  $K_i = 0$  curve in Fig. 37. The analysis in this addenda, in particular Eq. 31, can be used to calculate the binder state for any temperature-humidity storage sequence. Here the results of two scenarios are presented so that an indication of rejuvenation times may be obtained.

Suppose a tape has been exposed for one year to an environment of  $80^{\circ}\text{F}$  and 80%RH. According to Eq. 15 the hydrolysis will proceed to 16% binder consumption (the time to reach equilibrium is less than one year). As a rejuvenation environment consider storage at 0%RH,  $80^{\circ}\text{F}$ . Utilizing Eq. 31 yields 76 weeks or about 1.5 years to reach the original state (6.7% binder consumed). This is an extremely long time. Consider a less extreme example of a tape stored for 3 months (a summer) at 80%RH,  $80^{\circ}\text{F}$ . This short a time allows the hydrolysis to proceed only to 9% binder consumption. Rejuvenation at 0%RH,  $80^{\circ}\text{F}$  would still require about 25 weeks or .5 years to return the tape to its original state.

The conclusion from an examination of rejuvenation times is that, in general, they are in the one year range and thus are fairly impractical. Recommendations based on this analysis must be somewhat conjectural since it is not known at what stage binder

degradation will effect error rates. Such knowledge probably depends on the recording system (i.e., linear density, detection scheme, error correction technique). As such, then, in Section 3 reasonable general procedural recommendations are given for tapes which have experienced environmental extremes.

## 2.5 System Storage Investigation

In this section the results of a study of the storage of magnetic tape specifically recorded on a variety of standard digital recording systems which span a wide range of recording densities are discussed. The basic plan of the experiments was to record random data on several systems and then store these tapes at several environmental conditions for the duration of this contract. The end result then would be plots of error rates versus time. The systems utilized are summarized in Table 6.

### 2.5.1 System Description

The density regime is spanned by a low, medium and high density system. The low density is represented by a PDP11/55 computer (Digital Equipment Corporation) operating at 1600 bpi. The medium density testing was performed on Ampex's TBM<sup>tm</sup> mass storage system which operates at a linear density of 7575 bpi. The high density recorder was an Ampex 3010 HBR instrumentation recorder operating at 33k bpi. The tapes utilized for the study were standard for the particular system since it would have been extremely difficult to provide a common oxide-binder system for each tape. The tapes utilized are listed in Table 6.

Table 6 System Summary

	<b>Low Density</b>	<b>Medium Density</b>	<b>High Density</b>
<b>Recording System</b>	PDP11/55 Computer (Digital Equipment Corp.)	Ampex TBM	Ampex FR3010 HBR
<b>Linear Density</b>	1600 bpi	7575 bpi	33000 bpi
<b>Tape</b>	Memorex 'MRX IV' ( $\gamma\text{Fe}_2\text{O}_3$ Oxide)	Ampex Certified 3M TBM Tape ( $\gamma\text{Fe}_2\text{O}_3$ )	Ampex '799' Instrumentation Tape ( $\gamma\text{Fe}_2\text{O}_3$ )
<b>Recording Format</b>	Unbiased, Longitudinal $10^8$ Bits per Reel	Unbiased, Transverse in 5,1000 Block Sections, $10^6$ Bits per Block	Biased, Longitudinal Recording, 6 Tracks (1, 2, 7, 8, 13, 14) Recorded, $10^9$ Bits per Track, Miller Squared Encoded
<b>No. of Reels</b>	9	3	3

### **2.5.1.1 Computer**

Table 6 gives a brief description of the recording format. On each tape random data was recorded in a manner according to the particular system. The computer low density system records an unbiased longitudinal data stream at 1600 bits. A 'C' language program was utilized to record 30,000 records each with 512-8 bit bytes. This yielded 122 Mbits per reel of tape so that 9 reels were recorded with 3 reels each (366 Mbits) designated for each storage environment. Upon readback of the tape, each reproduced bit was compared with an exact calculated value.

### **2.5.1.2 TBM**

The TBM system is a transverse rotary recorder recording tracks across the 2" tape width orthogonal to the tape motion direction. The 3.5 mil wide tracks (1.8 mil guard band) are recorded redundantly alternating every half track length. The final system error rates are extremely low since a direct "geometrical" signal comparison upon replay is made between these two redundant channels. The TBM tape is recorded in 43,800 blocks where each block spans one longitudinal inch and contains approximately  $10^6$  bits of redundant information. For these tests the random data was recorded in five 1000 block sections spaced uniformly along the tape (specifically blocks 1000-1999, 10,000-11,999, 19,000-19,999, 28,000-28,999, 37,000-37999) yielding approximately  $5 \times 10^9$  bits recorded per tape. A rotary head set was retained to be used solely for this study.

### **2.5.1.3 Instrumentation**

The Ampex FR3010 HBR Instrumentation Recorder is a longitudinal, AC biased recorder which for these tests record at 33k kpi. A 2500 foot recording thus represents  $10^9$  bits per track. A random sequence was Miller squared encoded and then recorded on six (1, 2, 7, 8, 13, 14) of the fourteen possible longitudinal tracks. For this study a specified set of electronics was reserved guaranteeing fixed equalization and thus, comparable error rates from test to test. Although the same head set was utilized for all measurements, the set could not be reserved solely for this study and, unfortunately, was used continuously throughout the period of this contract.

### **2.5.2 Storage Conditions**

It was decided to span a relatively broad range of environmental conditions even with the relatively small sample of tapes. The first condition chosen was nominal room environment, i.e., 20°C, 50%RH which corresponds to a specific controlled room at Ampex. (Fluctuations are typically  $\pm 1^{\circ}\text{C}$ ,  $\pm 5\%\text{RH}$ .) Two other environments were chosen which represented practical extremes which might test binder degradation. An accelerated environment was chosen to be 55°C, 100%RH. According to the hydrolysis analysis of Section 2.4, this environment corresponds at equilibrium to a tape binder degraded to an unusable state (Fig. 37, Section 2.4). According to Eq. 33, Section 2.4, the time to reach this state is approximately 35 weeks which falls within the scope of this contract (in fact an unusable condition is probably reached in a shorter time since according to Fig. 37, Section 2.4, an unusable condition is felt to be when approximately 14% of the binder is consumed by hydrolysis and at equilibrium 55°C, 100%RH yields approximately 33% hydrolyzed. Since from Cuddihy's study humidity is felt to play an important role, the third storage condition was chosen to be 20°C in a hermetically sealed environment. Such a storage condition should absolutely not allow for hydrolysis and, according to Cuddihy, permit tape rejuvenation.

### **2.5.3 Storage Periods**

An attempt was made to read the tapes every three months. The tapes were recorded and initially read in July 1978. They were placed in their respective storage environments about August 1, 1978 and removed three months later at the beginning of November. The tapes were read during November and re-stored at the end of the month. This period is referred in the following tables as NOVEMBER 1978. Three months later at the end of February 1979, the tapes were removed and measured during the month of March. This period is denoted as MARCH 1979. The tapes were re-stored near the middle of March and removed and measured at the end of May for a slightly shorter third period storage of 2.5 months. The final read period is labeled NOV 1979.

For all the tapes stored at 55°C, 100%RH, a 3 day equilibrating period at nominal room conditions was allowed before measuring after removal from storage so that the high temperature and humidity would not effect results during measurement.

AD-A088 187

AMPEX CORP REDWOOD CITY CA ADVANCED TECHNOLOGY DIV  
RECORDING MEDIA ARCHIVAL ATTRIBUTES (MAGNETIC).(U)  
APR 80 N BERTRAM, A ESHEL

F/G 14/3

F30602-78-C-0181

UNCLASSIFIED

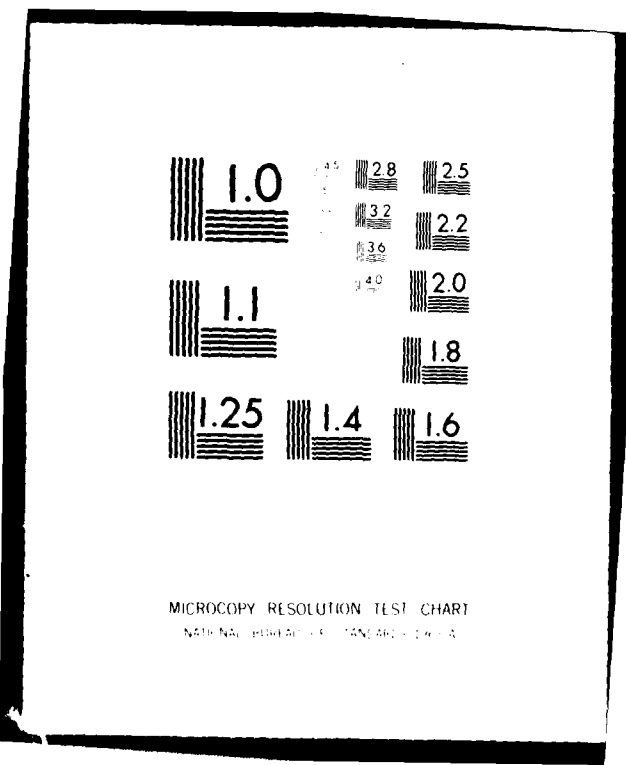
RR-80-01

RADC-TR-80-123

NL

2 02  
40  
AUG 19 1980

END  
DATE FILMED  
0-80  
DTIC



## **2.5.4 Storage Results**

### **2.5.4.1 Low Density Computer**

The results of the computer tape storage are relatively easy to summarize since the error activity was either non-existent or catastrophic. Since the linear density is low on these tapes (1600 bpi) corresponding to 122 Mbits per reel, three reels were recorded for each storage condition and perhaps this low density is the reason for the low error activity. The summary is as follows:

#### **20°C, 50%RH and Hermetic Seal Storage**

No errors at all were measured over the entire storage period. By errors, hard errors are meant which entails retry if errors are measured. In fact, for most of the study, these tapes were virtually error free on a 'first pass' error measurement. The retry provision is reasonable since it not only is a standard computer operating practice, but it is good measure of 'permanent' tape defects.

#### **55°C, 100%RH**

This storage condition produced tape degradation by the end of the contract period. At the end of the first storage period (November 1978), the three tapes stored at this extreme environmental condition exhibited no errors. After the second storage period, (March 1979), degradation was evident. Of the three tapes stored at 55°C, 100RH, one broke, another gave approximately 3800 errors, and the third yielded no errors. At the end of this second period, it does appear that the computer tape is showing signs of deleterious behavior from two months storage at this extreme condition. With regard to the tape which broke, it is not clear whether it was due to a freak machine failure or in fact was due to increased friction from a weakened, shedding binder. The latter seems more plausible since "time to rub" tests were performed on this tape and another which was not heated. The heated tape gave a "time to rub" (in number of strokes) of about 8 whereas a tape stored at room temperature, 20°C, 47%RH, gave a value of 30 strokes. Thus, it is clear that some binder degradation is occurring. However, the other two tapes did not measure extreme error rates. As just mentioned, one tape yielded no errors and the other exhibited approximately 3800 errors which occurred uniformly in the first 1000 records (about 212 feet of tape).

At the end of the fourth period, the remaining two tapes were placed on the transport for a final reading. It was found that both of these were unreadable. It was apparent that storage at this environment resulted in a completely degraded binder by the end of the 12 month storage period.

### Conclusion

Storage at room temperature ( $20^{\circ}\text{C}$ , 50%RH) for 15 months or in a hermetically sealed chamber yields no errors.

Storage at  $55^{\circ}\text{C}$ , 100%RH for 15 months yields catastrophic failure.

#### 2.5.4.2 TBM

Measurements of the TBM tapes are summarized in Table 7. The error rates given are 'hard' errors (with retry) for one channel only. The system eventually compares the two channel outputs to achieve extremely low total system error rates. In Table 7 the measured error rates are given for each of three storage conditions before and after each storage period. The data is for a fourth pass measurement which yields the lowest error rate. The error rates are given in three ways. First, all recorded bits are averaged; second, the average is taken over the data minus the worst 500 block section; third, the data is averaged over the bits minus the worst 1000 blocks. The initial rates (July 1978) are reasonably close considering tape variability. For comparison, a 'best' and 'worst' 500 block error rate data is shown. Even though some arbitrary decision must be made when distilling the raw data, this mode of presentation appears to give a reasonable summary of the tape errors. The error rates measured after the first storage period are given next under the heading NOVEMBER 1978. For the two room temperature measurements, the error rates did not change significantly. All were close to  $10^{-7}$  errors per bit recorded. The third tape was subjected to the extreme environmental condition of  $55^{\circ}\text{C}$ , 100%RH for three months. At the end of this storage period, it was found that the tape shrunk by approximately .15% both in length and width. This shrinkage\* was enough to overcome the range of the time base corrector so that the tape guide had

\* Shrinkage is a normal property of the tape substrate and occurs when all tape is heated and then cooled. The amount of shrinkage is in accord with measurements of the phenomenon.<sup>[18]</sup> TBM is susceptible to shrinkage since redundant channels are recorded in exact time synchrony by an external clock.

Table 7  
Bit Error Rate  
TBM

DATE		20°C, HERMETIC	20°C, 50%RH	55°C, 100%RH
JULY 1978				
ALL BITS		$3 \times 10^{-7}$	$3.3 \times 10^{-7}$	$8.3 \times 10^{-8}$
MINUS WORST 500 BLOCKS		$1.1 \times 10^{-7}$	$1.3 \times 10^{-7}$	$5.6 \times 10^{-8}$
MINUS WORST 1000 BLOCKS		$7.1 \times 10^{-8}$	$7.7 \times 10^{-8}$	$4.5 \times 10^{-8}$
BEST 500 BLOCKS		$2.8 \times 10^{-8}$	0	0
WORST 500 BLOCKS		$2.0 \times 10^{-6}$	$2 \times 10^{-6}$	$3.5 \times 10^{-7}$
NOVEMBER 1978				
ALL BITS		$3.6 \times 10^{-7}$	$5 \times 10^{-7}$	*
MINUS WORST 500 BLOCKS		$1.4 \times 10^{-7}$	$1.9 \times 10^{-7}$	*
MINUS WORST 1000 BLOCKS		$7.1 \times 10^{-8}$	$1.5 \times 10^{-7}$	$7.1 \times 10^{-7}$
BEST 500 BLOCKS		$3.6 \times 10^{-8}$	$2 \times 10^{-9}$	$1.0 \times 10^{-8}$
WORST 500 BLOCKS		$2.2 \times 10^{-6}$	$3 \times 10^{-6}$	*
MARCH 1979				20°C, 50%RH
ALL BITS		*	$5.6 \times 10^{-7}$	*
MINUS WORST 500 BLOCKS		*	$2.8 \times 10^{-7}$	*
MINUS WORST 1000 BLOCKS		$3.3 \times 10^{-7}$	$2 \times 10^{-7}$	$2.2 \times 10^{-7}$
BEST 500 BLOCKS		$2.4 \times 10^{-8}$	$2 \times 10^{-9}$	$6 \times 10^{-9}$
WORST 500 BLOCKS		*	$3 \times 10^{-6}$	*
JUNE 1979				55°C, 100%RH
ALL BITS		$6.8 \times 10^{-6}$	$5.5 \times 10^{-7}$	**
MINUS WORST 500 BLOCKS		$2.1 \times 10^{-6}$	$2.2 \times 10^{-7}$	**
MINUS WORST 1000 BLOCKS		$5.4 \times 10^{-7}$	$1.4 \times 10^{-7}$	**
BEST 500 BLOCKS		$5.8 \times 10^{-8}$	$8 \times 10^{-9}$	$1.5 \times 10^{-7}***$
WORST 500 BLOCKS		$5 \times 10^{-5}$	$3.5 \times 10^{-6}$	$1.5 \times 10^{-6}***$
NOVEMBER 1979				
ALL BITS		*	$4.8 \times 10^{-7}$	
MINUS WORST 500 BLOCKS		*	$2.0 \times 10^{-7}$	
MINUS WORST 1000 BLOCKS		$5.0 \times 10^{-7}$	$1.2 \times 10^{-7}$	NOT MEASURED
BEST 500 BLOCKS		$6.7 \times 10^{-8}$	$4.0 \times 10^{-8}$	
WORST 500 BLOCKS		$3.0 \times 10^{-6}$	$2.2 \times 10^{-6}$	

NOTE: 1) ERROR RATE MEANS ERRORS PER BIT  
 2) DATA IS FOURTH PASS MEASUREMENT  
 3) JULY MEASUREMENT IS IMMEDIATELY AFTER RECORDING  
 \* TAPE EXHIBITED AN UNREADABLE 500 BLOCK SECTION  
 \*\* SEVERE OXIDE SHED OVER MOST OF TAPE  
 \*\*\* DATA IS FOR TWO READABLE 1000 BLOCK SECTIONS

to be set manually to stretch the tape. In fact, the percentage transverse shrinkage varied from .05% at the inside of the reel to .15% at the outside so that separate settings had to be made for each 1k block section. However, in spite of this shrinkage, the error rate remained surprisingly good: all bits gave an error rate of  $10^{-6}$  and discounting a 1000 block section which had particularly high errors, an error rate as low as  $7.1 \times 10^{-7}$  was achieved.

For the second storage period, it was decided to store the heated tape at nominal room conditions ( $20^{\circ}\text{C}$ , 50%RH) as noted in Table 7. It would then be possible to see if the shrinkage might be reduced in a moderate environment so that the tape guide would not need to be reset for each 1000 block section along the tape.

The error rates listed under MARCH 1979 in Table 7 denote a reading of the tapes after six months of storage. It should be noted that during the measurements, the head failed so a replacement head assembly was obtained. By repeating measurements on tape sections just read with the old head it was ascertained the comparable error rates could be measured. In this series of data, there was some error activity. For the hermetically stored tape, there was significant error increase due to a virtually unreadable state in the first 1000 blocks (at the beginning of the reel). The tape which was stored at  $55^{\circ}\text{C}$ , 100%RH exhibited synchronization errors in the last 1000 block section (37,000-37,999) so that it could not be read there. In spite of this difficulty, neglecting the worst 1000 blocks, the error rates were virtually unchanged from the previous readings. The tape which previously shrunk appeared to stretch about 20% back to its original size. It was decided to store this tape at  $55^{\circ}\text{C}$ , 100%RH for the final period to see what dimensional changes or degradation might occur.

At the end of the third storage period the tapes were re-read (June 1979 in Table 6). The tape stored in the hermetic environment still exhibited a large error rate in the first 1000 blocks as in the November reading. However, the error rate was improved considerably. The room temperature/room humidity environment ( $20^{\circ}\text{C}$ , 50%RH) gave error rates with virtually no change from the previous period. The tape which was stored at  $55^{\circ}\text{C}$ , 100%RH after this second period at the elevated temperature and humidity exhibited severe oxide degradation when measured at this final period. As in the case of the computer tapes, the oxide was virtually falling off sections of the tape (even though the storage at elevated conditions was for six instead of the full nine months). Due to this degradation, the first 3000 block section (1000-1999, 10,000-10,999, 19,000-19,999) were unreadable. However, the last two sections (28,000-28,999, 37,000-37,999) did not exhibit severe degradation and as the entry in Table 6 shows, the error rates are reasonably good. It is possible that if this tape had experienced the full 12 months at  $55^{\circ}\text{C}$ ,

100%RH, it might have been totally unreadable.

The results of this study of TBM tape storage are summarized in a convenient way in Fig. 38. This figure is a plot of error rate versus storage time for the three storage conditions. It was decided that a representative plot would be to discount the worst 1000 block sections. It is easy to see in this plot that for the room temperature storage conditions, the error rates hardly change over the storage period. The heated tape, apart from a small anomaly, after three months, shows reasonable error rates until the shedding catastrophe after nine months.

#### Conclusion

This study of the TBM system tapes yields virtually the same conclusion as for the computer system. After 1.5 month's storage at room temperature ( $20^{\circ}\text{C}$ ) there was virtually no error increase with no major differences between 50% humidity and a hermetically sealed environment; storage at  $55^{\circ}\text{C}$ , 100%RH produced tape shedding.

#### 2.5.4.2A Addendum - Seven Year Old TBM Tape

It was decided to include in this report the results of measurements on a seven year old TBM tape. This tape was recorded in standard TBM format and then stored in a normal lab environment with no environmental control. However, it is likely that the tape never experienced any extreme environmental changes. Unfortunately, the raw error rate was not measured when the tape was first recorded. Instead a total system (including redundant recording error correction) 'blocks' in error was measured initially and subsequently. The tape performed well initially and recently (March 1979), when it was read. It exhibited a few 'blocks in error' initially and at the end of seven years, although the blocks in error was not the same at each measurement. This result is especially significant when the single channel current error rates for this tape are considered.

Average:	$3 \times 10^{-4}$
Best 200 Block Section:	$2.7 \times 10^{-7}$
Worst 200 Block Section:	$1.8 \times 10^{-3}$

Unfortunately, there was no raw error rate measurement when the tape was initially recorded. There is no absolute knowledge of the error rates for this tape at time of recording. However, it is generally felt that tapes of that generation exhibit "as new" error activity close to the  $10^{-4}$  average measured seven years later on this tape. The TBM redundant scheme was designed to totally correct such an error rate level. Current production tapes have extremely low initial error rates (less than  $10^{-7}$ ) as the tapes used in this study indicate.

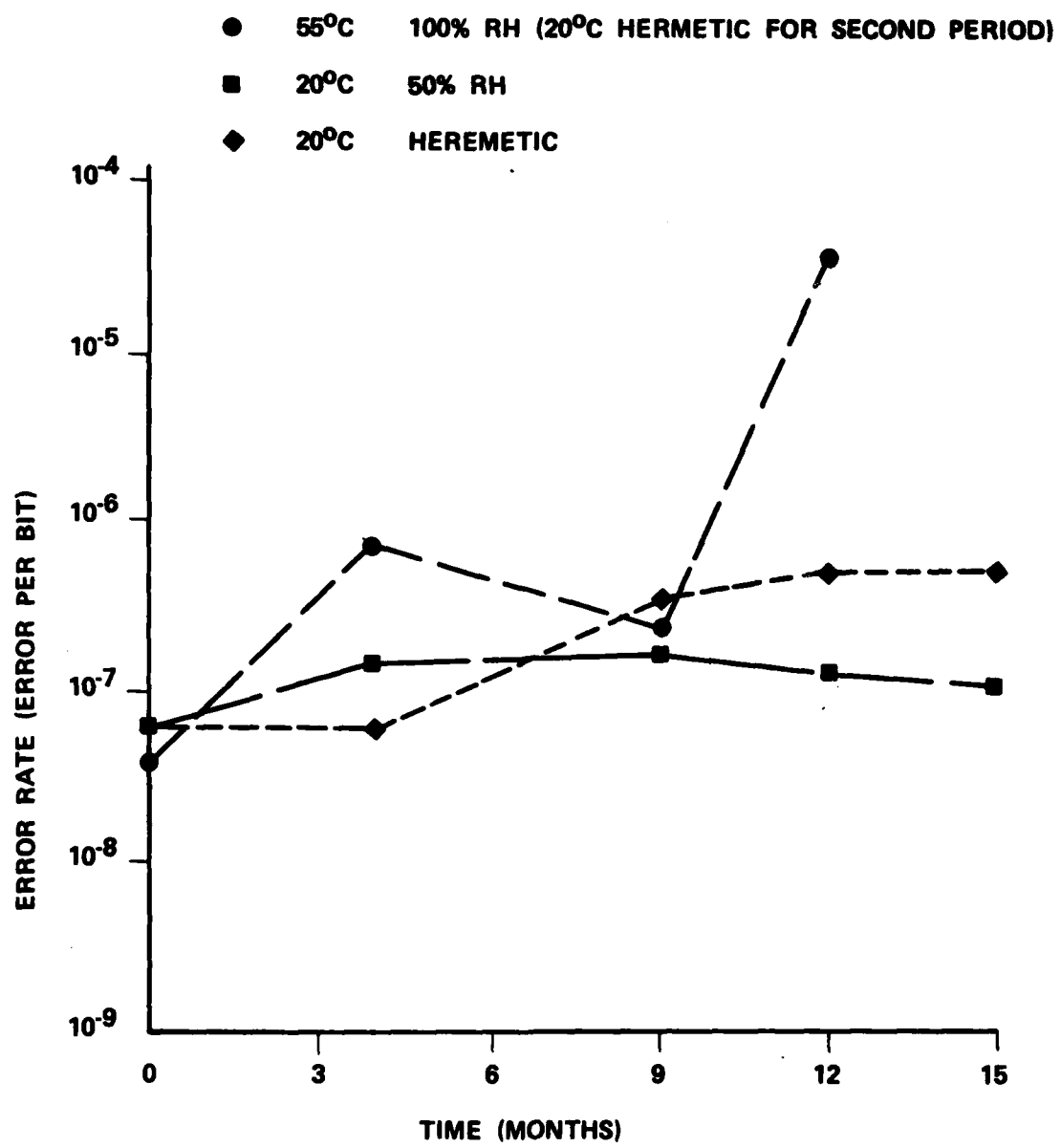


Figure 38 Error Rates vs Storage Time for TBM Tape  
for Three Different Storage Conditions. Error  
Rate Determination Discounts Worst 1000  
Block Sections.

Table 8  
Bit Error Rate  
High Density Instrumentation

DATE	20°C, HERMETIC	20°C, 50%RH	55°C, 100%RH
JULY 1978			
ALL BITS	$2.8 \times 10^{-7}$	$4.5 \times 10^{-8}$	$1 \times 10^{-6}$
MINUS WORST TRACK	$1.3 \times 10^{-7}$	$2.7 \times 10^{-8}$	$4.3 \times 10^{-7}$
MINUS TWO WORST TRACKS	$7.7 \times 10^{-8}$	$7.1 \times 10^{-9}$	$1.1 \times 10^{-7}$
WORST TRACK	$1.0 \times 10^{-6}(\#1)$	$1.4 \times 10^{-7}(\#14)$	$3.9 \times 10^{-5}(\#1)$
BEST TRACK	0(#13)	0(#2,#8)	$2 \times 10^{-8}(\#7)$
NOVEMBER 1978			
ALL BITS	$8.3 \times 10^{-7}$	$6.3 \times 10^{-7}$	$3.3 \times 10^{-6}$
MINUS WORST TRACK	$2.3 \times 10^{-8}$	$3.3 \times 10^{-8}$	$1.1 \times 10^{-6}$
MINUS TWO WORST TRACKS	$7.1 \times 10^{-9}$	$1 \times 10^{-9}$	$1.6 \times 10^{-7}$
WORST TRACK	$4.8 \times 10^{-5}(\#14)$	$3.5 \times 10^{-5}(\#14)$	$1.4 \times 10^{-5}(\#14)$
BEST TRACK	0(#1,#8)	0(#7,#8)	0(#8)
MARCH 1979			
ALL BITS	*	*	$1.4 \times 10^{-5}$
MINUS WORST TRACK	$3.9 \times 10^{-7}$	$1.9 \times 10^{-7}$	$9.0 \times 10^{-6}$
MINUS TWO WORST TRACKS	$3.3 \times 10^{-7}$	$8.6 \times 10^{-8}$	$4.5 \times 10^{-6}$
WORST TRACK	$6.6 \times 10^{-7}(\#7)**$	$6.0 \times 10^{-7}(\#14)**$	$3.5 \times 10^{-5}(\#2)$
BEST TRACK	$3 \times 10^{-9}(\#1)$	0(#7,#8)	$1.6 \times 10^{-8}(\#8)$
JUNE 1979			20°C HERMETIC
ALL BITS	*	*	*
MINUS WORST TRACK	$4.5 \times 10^{-6}$	$2.1 \times 10^{-7}$	$3.6 \times 10^{-5}$
MINUS TWO WORST TRACKS	$5.9 \times 10^{-7}$	$1.5 \times 10^{-7}$	$7.2 \times 10^{-6}$
WORST TRACK	$2.0 \times 10^{-5}(\#14)**$	$4.4 \times 10^{-7}(\#14)**$	$1.5 \times 10^{-4}(\#14)**$
BEST TRACK	$9.0 \times 10^{-9}(\#1)$	$1.3 \times 10^{-8}(\#7)$	$2.0 \times 10^{-7}$
NOVEMBER 1979			55°C, 100%RH
ALL BITS	*	*	$> 10^{-3}$
MINUS WORST TRACK	$3.2 \times 10^{-6}$	$1.28 \times 10^{-6}$	(After 'Pellon')
MINUS TWO WORST TRACKS	$1.9 \times 10^{-6}$	$7.8 \times 10^{-7}$	wipe:
WORST TRACK	$8.5 \times 10^{-6}(\#14)$	$5.1 \times 10^{-6}(\#1)$	$2.0 \times 10^{-6}(\#7)$
BEST TRACK	$2.3 \times 10^{-8}(\#7)$	$6.0 \times 10^{-9}(\#13)$	

- NOTE: 1) ENTRY MEANS ERRORS PER BIT  
 2) DATA IS THIRD PASS MEASUREMENT  
 3) JULY MEASUREMENT IS IMMEDIATELY AFTER RECORDING  
 4) DATA HAS BEEN MILLER-SQUARED ENCODED  
 \* TAPE EXHIBITED AN UNREADABLE TRACK (#2 IN EACH CASE)  
 \*\* DENOTES WORST TRACK OF THE READABLE TRACKS  
 ( ) DENOTES SPECIFIC TRACK

The significant conclusion is that a TBM tape stored at nominal conditions for seven years does not degrade when the signal is processed in the full system. It is also noteworthy that after seven years storage this tape exhibited no evidence of shed or binder degradation.

#### 2.5.4.3 High Density Instrumentation System

The results for the instrumentation tape storage are summarized in Table 8. The error rate is given considering all recorded bits, discounting the worst track and, then again, neglecting the two worst tracks. Both the worst and best track error rates are given with a designation of the specific track. Tracks No. 1 and No. 14 are both edge tracks with No. 7 and No. 8 denoting the mid tape tracks. There seemed to be some variation in error rate between the three instrumentation tapes when all bits are considered. However, neglecting the worst track, the initial error rates are quite comparable. After the first storage period it was found that track No. 14 gave enormously high error rates for all the tapes and this was attributed to head difficulties. In spite of this, the error rates for the two tapes stored at room temperature did not change appreciably after three months. The tape which was stored at 55°C, 100%RH on the other hand, exhibited a definite increase in error rate (neglecting the worst track). Nonetheless, each tape exhibited tracks which were error-free during this measurement period.

After the end of the second storage period (March 1979), the room temperature error rates (less the worst track) had increased a little only to a level slightly exceeding the initial storage rate. The error rate of the heated tape increased by almost an order of magnitude. During this period, track No. 2 gave enormously high rates and was virtually unreadable, and No. 14 did not yield such high rates. This difficulty persisted throughout the remainder of the study and could have arisen from utilization of a head-set under continual use.

Since the error rate for the heated tape was so high after two storage periods, it was decided to store the tape in the hermetically sealed environment during the last three (2.5) month period to see if binder "rejuvenation" might occur. The results of error rate measurements during the final period are listed under JUNE 1979 in Table 8. Again, track No. 2 was unreadable due to exceedingly high errors. The tape stored at 20°C, 50%RH again exhibited little change in error rate. The tape which was stored continuously at 20°C, in a hermetic environment exhibited a large increase. The cause is not clear. It may be due to the instrumentation recorder's sensitivity to low humidity during replay. The third tape, which has been stored at 55°C, 100%RH, for the first two storage periods and then stored at 20°C in a hermetically sealed environment for the final period, did not improve its error rates. In fact, track No. 14 yielded an extremely high rate. Thus the error rate (less the worst track (No. 2) ) increased over the previous period.

In the final period measurement (Nov. 1979) the error rates of the room temperature tapes seem to have increased a little although the best track error rates are still excellent. For the tape heated at 55°C for this period the error rate was immeasurably high. Evidence of severe binder degradation was noticed when a short section of tape was stretched by hand. Normally, a tape will deform but the binder will follow. In this instance the binder completely crumbled so that the oxide could be removed with a gentle finger wiping. At this point the tape was wiped by a "Pellon" roll\* which is part of the Ampex Tape Division burnishing equipment. The remarkable result was that the error rate dropped to a reasonable  $2 \times 10^{-6}$ . Simple wiping of one of the other tapes produced no change.

In Fig. 39 error rate vs. time is plotted for the three tapes where the error rates denote all readable tracks minus the edge tracks. From this, it is evident that nominal room environment yields only slight error increases. It is felt that this slight increase is due to head deterioration over the contract period. The head set was in constant use and in fact, calibration tests indicated a deterioration especially at the edge tracks. Again, the incredible effect of a 'Pellon' wipe is shown which gives almost a  $10^{-6}$  error rate for a tape stored virtually continuously for over a year at 55°C, 100%RH.

### Conclusion

The overall trend is similar to that reported for the other tapes. The low temperature storage yields only slight increases in error rate over the 15 month period. The heated tape exhibited significant increases in error rate although no severe oxide shedding occurred and a 'Pellon' wipe caused the error rate to fall dramatically.

## 2.6 Summary and Recommendations for Further Work

### 2.6.1 Summary

A brief summary is given of the significant results of the previous studies in a brief numeric form.

- 1) Magnetic tape composed of  $\gamma\text{Fe}_2\text{O}_3$  oxide does not exhibit long term demagnetization or print-through when used in digital recording applications of up to 33k bpi and stored at nominal environments.

\* A lint and static free wiping tissue (Pellon Corp., Lowell, Mass). No comparative examination of commercial wiping tissue was made during this study.

- 2) Hydrolysis of polyester urethane binder is insignificant for tape storage at nominal environments ( $65^{\circ}\text{F}$ , 40%RH) as predicted by an analysis of measured hydrolysis rates.
- 3) Storage of a medium density tape at nominal environments with minimal replay for at least seven years appears to yield slight increases in error rates which are within the capacity scope of simple EDAC.
- 4) Tape rejuvenation of degraded tape to recover the signal by storage in a hermetically sealed chamber appears impractical since the rates are too low.
- 5) Measurements of tape stress relaxation indicate that tapes may be stored for approximately 3.5 years without rewind if the environmental temperature is maintained at  $65 \pm 3^{\circ}\text{F}$  and the relative humidity fluctuation is within  $\pm 5\%$ RH.
- 6) It is feasible to monitor tape pack relaxation by the use of friction tabs imbedded in test reels. This can account for deviations from nominal conditions.

#### **2.6.2 Recommendations for Further Study**

- 1) Measure non-accelerated (room temperature) long term demagnetization loss on tape composed of oxide (such as  $\text{CrO}_2$ ,  $\text{Co}-\gamma\text{Fe}_2\text{O}_3$ ) which exhibit large decreases in coercivity with increasing temperature to test for archivability.
- 2) Study hydrolysis process in greater depth to examine a) the effects of various binders or binder additives on the hydrolysis rates, b) the possibility of tape rejuvenation, c) the correlation between theory and experiment to improve understanding of the process and its effect on system performance.
- 3) Continue studies of viscoelastic behaviour of magnetic tape substrates so that a) reel stress relaxation could be predicted exactly from a history of a changing storage environment, (e.g., a microcomputer may simulate in real time the relaxation development and indicate time for rewind) b) various manufacturers' substrates could be distinguished and characterized in order to better specify rewind frequencies, c) develop a standard creep test as an acceptance criterion for archival storage tape.
- 4) Study tape cleaning, both simple wiping and complete burnishing, as a means of recovering data after adverse environmental changes during storage.
- 5) Improve model for reel slippage (see Section 2.3.7.5).

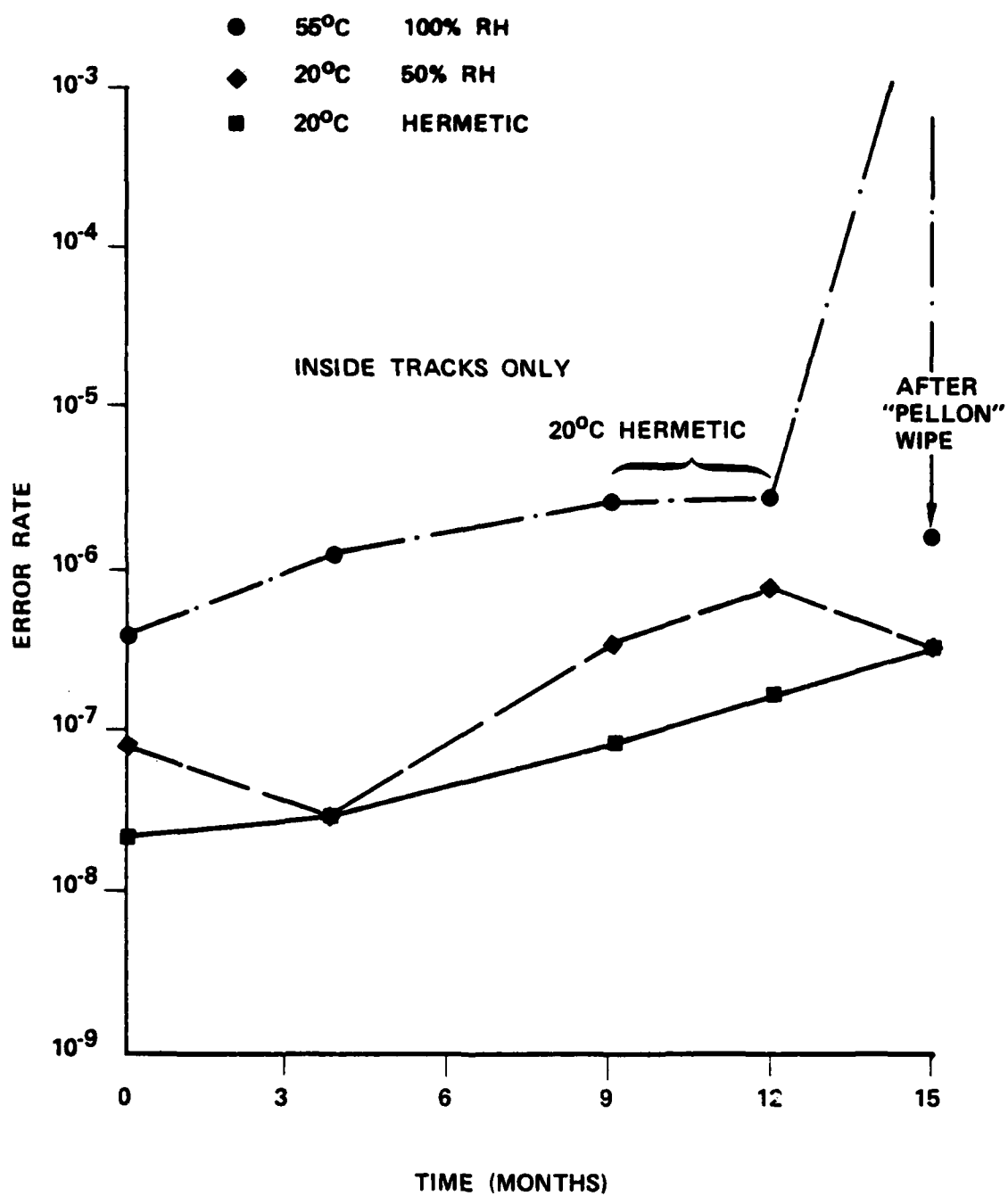


Figure 39 Error Rate vs Storage Time for Instrumentation Tape for Three Different Storage Conditions.  
Error Rate Computation Excludes Worst Track for Each Tape.

## **3.0 ARCHIVAL STORAGE RECOMMENDATIONS**

### **3.1 Qualification, Handling and Storage Procedure**

In this section the results of this study are utilized to form a set of recommendations for the acquisition and handling of magnetic tape. The recommendations are general in nature and should apply to any archival storage system utilizing magnetic recording.

Virtually all present high quality tapes utilize polyester-urethane binder systems with polyethylene terephthalate base films. The recommendations in this section apply to these systems. If tape constituents were to change significantly in the future then the recommendation presented should be reviewed accordingly. In addition, it is presumed that the recording systems utilized have high quality tape guides, tension controllers, etc., and that the recording heads are maintained in good condition. Thus, minimal tape wear should occur from tape contact with the recording system.

#### **3.1.1 Tape Qualifications**

It is the purpose of this section to give acceptability criteria by which various magnetic tape can be judged for use in an archival storage system. Such criteria must be primarily in the form of tests on as-received tapes and only to a limited extent applied to the tape constituents since such information is mostly company proprietary. It should be clear from an examination of Section 2 of this report that the archival studies performed during the course of this contract lead primarily to storage and handling criteria. In this study, state-of-the-art examples of computer, TBM, high density instrumentation tape were utilized, and it appears that they all will be good candidates for archival storage if stored properly according to the rules given in the following part of this section. The most reasonable qualification test to make is one which will disqualify extremely poor binder systems which may hydrolyze, and magnetic particles which may not be stable under long term storage.

Therefore, our qualifying specification for magnetic tape to be used in an archival system is that it meets these conditions:

- 1) Satisfy normal tape specification for system (i.e., SNR, BER).
- 2) Tape passes GSA WT 001567 test expanded to 72 hours.
- 3) The magnetic oxide is  $\gamma\text{Fe}_2\text{O}_3$  or of equivalent stability.
- 4) Tape is "new" with a "cool-dry" environment history before purchase.

Discussion of these four conditions follows. The first requirement is that the tape satisfy the system specifications such as signal to noise ratio (SNR) and Bit Error Rate (BER). It is possible, for example, that environmental extremes or contamination might increase the raw error rate when the tape is received at the recording site. Therefore, certification should be made after the tape has been allowed to equilibrate in the dry (40%RH) storage environment for several days (see Section 3.1.2) and after a two pass shuttle. If the error rate is high, a gentle cleaning might be required to remove loose surface contamination and allow a measurement of the error rate due to 'hard' or imbedded contaminants. A decision as to the precise certification technique, depends, of course, on the recording system sensitivity to raw errors. Cleaning may only be necessary, for example, for high density instrumentation systems (25 - 33 kBI) which employs no error correction.

The second test essentially qualifies the binder. This is a modified GSA test for video tape which the Ampex tape division has used for several years. Although it is not a complete test to determine archivability at our recommended storage conditions, it can be used, at least, to disqualify very poor tapes. The test is a 2-inch quad video GSA test under Section 4.5.3.13 which is designated:

#### GSA test WT 001567

The essence of the test is to store tape for 8 hours @  $120 \pm 5^\circ\text{F}$ , 80-90%RH and then stabilize for 16 hours @  $75^\circ\text{F}$ , 50%RH. An acceptable tape should exhibit less than 1 dB rf decrease, less than 1 db SNR loss, less than a doubling of the dropouts, and reasonably little shed after this test. It is very difficult to apply this test to qualifying archival tape; however, it is our feeling that an archival tape candidate, as a minimum, should pass this test modified according to Ampex experience, so that the 8 hours storage period has been expanded to 72 hours.

The third requirement concerns the magnetic oxide. As presented in Section 2.2.1, the most common oxide  $\gamma\text{Fe}_2\text{O}_3$  appears to be stable against signal loss according to the accelerated tests performed during this contract period. Thus, tapes utilizing  $\gamma\text{Fe}_2\text{O}_3$  are good archival candidates. As discussed in Section 2.2.1, relatively new oxides exist which may eventually be used in digital recording such as  $\text{CrO}_2$ , Co-doped  $\gamma\text{Fe}_2\text{O}_3\text{-Fe}$ , Co-layered  $\gamma\text{Fe}_2\text{O}_3$ . However, the first two perform poorly in accelerated tests and the last two are presently too new to yield long term assurances. Therefore, until further study on these

oxides can be performed, it is recommended that only tapes with  $\gamma\text{Fe}_2\text{O}_3$  be utilized unless a new particle candidate is given archivability assurances from the manufacturer.

The fourth qualification specifies that the tape has experienced no extreme environments from the time of manufacture to that of use. Hydrolysis may be a problem and the polyester urethane binder should not be allowed to weaken prior to use.

A final, additional, requirement is that the tape be back coated. It is perhaps a secondary requirement since most high quality magnetic tapes are back coated. Back coating provides increased interlayer friction to reduce the probability of layer to layer slippage due to tape relaxation during storage.

### **3.1.2 Tape Handling and Storage Procedure**

In this section, the results of this archival storage study as presented in Section 2 are utilized to give best estimates for the handling and archival storage of magnetic tape. The sequence will be to first discuss the various criteria and the reasons for their choice. Then, as a summary, a chart entitled "Acquisition, Handling, and Storage Sequence" will be given so that the recommended procedure can be utilized in a convenient fashion. Several aspects of tape handling which may be classified under "unusual effects" are not discussed here. Such effects, for example, include exposure to stray magnetic fields, nuclear radiation, lightning strikes, etc., and are covered in [19,20].

#### **3.1.2.1 General Storage Requirements**

Tapes should be stored in an environment which is generally dust-free. The tape reels should have aluminum flanges for long term support and should be placed in well sealed polyethylene bags and boxed for convenient stacking and stored in a vertical position on a shelf. The function of the bags is to prevent long term lubricant evaporation and perhaps act as a hermetic seal which will reduce binder degradation tendencies. The dust-free requirement applies primarily to reduce dropout accumulation when the tapes are being rewound and/or played.

It is important that reel bands be utilized not only during storage but whenever the tapes are not on the recording system since the compressibility of the flanges would permit edge damage. Current reel bands allow for easy removal after the tape has been placed on the recording system. After measurement the reel band would be replaced before the tape is removed from the system. It is also reasonable to finally wind the tapes in the same direction before storage (e.g., always "heads out").

### **3.1.2.2 Temperature-Humidity Requirement**

Based on the hydrolysis analysis of Section 2.4, limitations on the storage humidity and temperature can be placed. In Fig. 40 a replot of Fig. 37 is given. This plot gives the result of hydrolysis for two criteria when tapes are stored at a given temperature-humidity combination. The first criterion is that a tape which begins with a given state of binder degradation (near 6.7%) does not degrade further when stored at any temperature-humidity combination along this curve. This curve essentially represents a "zero" hydrolysis rate and therefore, the "zone 1" labeled "ideal" represents a safe region for tape use and storage as far as hydrolysis is concerned. The dashed curve represents storage conditions which lead to a given percent (14%) of the binder hydrolyzed. There is some experimental evidence [21], which suggests that this boundary denotes storage conditions which, if exceeded, lead to a degraded tape, thus affecting SNR and bit error rate. Thus "zone 2" which yields less hydrolysis might be considered marginal whereas "zone 3" would yield a noticeably degraded tape. Our experience discussed in Section 2.5 is, at least, in agreement with this interpretation since storage at 55°C, 100%RH yielded tapes with either shedding binder, large error rates, or both. Given the rather limited extent of knowledge of the effect of storage condition on actual tape performance, it is recommended that tapes be stored somewhat conservatively, near the zero rate curve of Fig. 40, and in addition, in an environment which is reasonable for human comfort.

Thus, our recommendation is that tapes be stored at:

$$T = 65^{\circ}\text{F}, \quad RH = 40\%$$

This condition appears safe with regard to hydrolysis and does not yield large environmental changes when the tapes are perhaps removed to another location for replay.

### **3.1.2.3 Rewind Frequency**

As tape is stored, tension induced creep causes stress relaxation which, upon replay, can lead to cinching. To avoid this difficulty, it is a common practice to rewind tapes to reset the tension. The required frequency of rewind is a function of several parameters such as: storage time, temperature level, magnitude and duration of temperature and humidity fluctuations, winding tension and speed levels and profiles, reel size, interlayer friction coefficient and acceleration levels that the reel has to withstand during rewind.

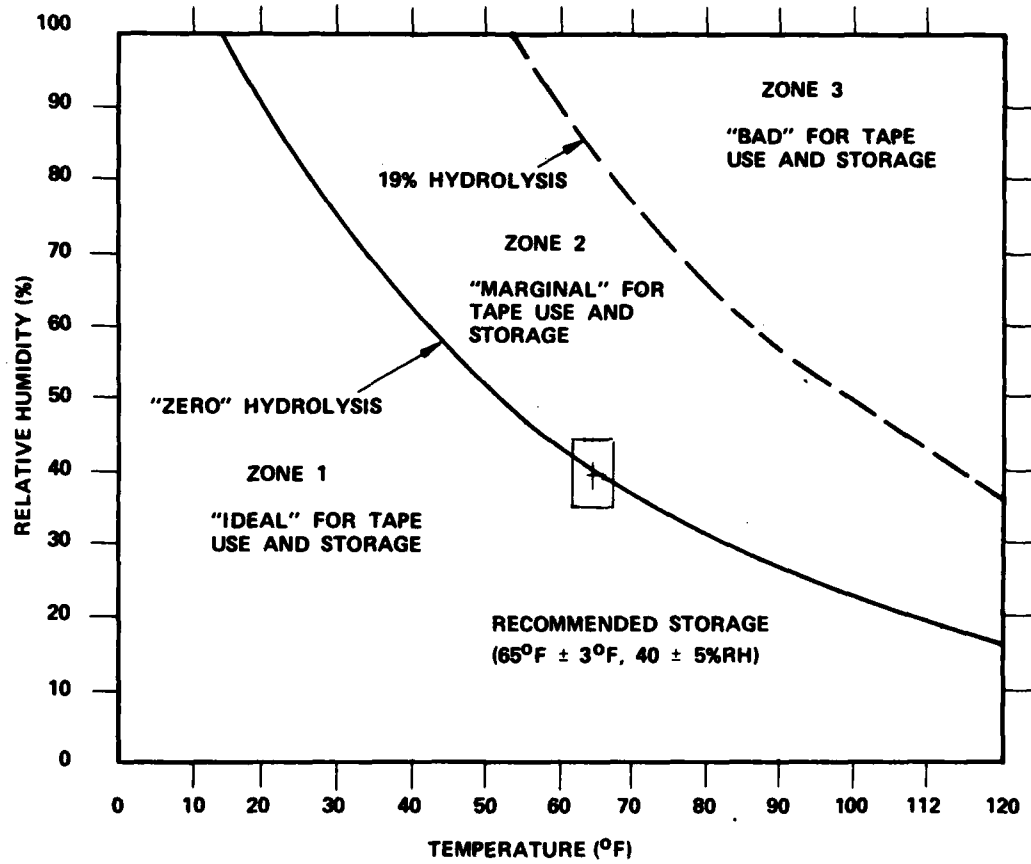


Figure 40 Tape Storage Environment Recommendation on the Basis of the Hydrolysis of the Tape Binder

Based on our experiments and data available in the literature a period between rewinds of 3.5 years is recommended for the specified storage environment of 65°F and constant relative humidity. This recommendation is in agreement with previous studies [22]. Specifically, 10-1/2" reels of Ampex 799 instrumentation tape wound at constant torque of 0.19 lb in/in and at 7-1/2 ips are predicted to withstand an angular acceleration of 400 rad/sec<sup>2</sup> (reach 1000 ips in 500 ms) if stored under the above conditions. Pointers to generalization of this prediction for other conditions are given in Sections 3.1.2.5, 3.1.2.6.

### 3.1.2.4 Temperature and Humidity Storage Fluctuation Bounds

From a mechanical point of view, it is important to impose bounds on temperature and humidity changes. Fluctuations in either of these quantities can cause tension increases or decreases in the pack which may lead to cinching and/or blocking and at the minimum will reduce the time between rewinds to restore tension. The above mentioned recommendations of an approximate rewind period of 3.5 years is based on the assumption that temperature and humidity do not change during storage. It has been estimated from the data presented in Section 2.3 that this rewind period is still applicable if the temperature fluctuations are kept within  $\pm 3^{\circ}\text{F}$  and the humidity between  $\pm 5\%\text{RH}$ . Thus our best estimate of storage environment is:

#### RECOMMENDED STORAGE ENVIRONMENT

Temperature	Humidity
$65 \pm 3^{\circ}\text{F}$	$40 \pm 5\%\text{RH}$

If advantageous for the particular facility, the winding area may be kept at  $68^{\circ} \pm 3^{\circ}\text{F}$ , i.e., at somewhat higher temperature than the storage area.

### 3.1.2.5 Recommendations for Environmental Variations

In an archival storage facility it is possible that environmental fluctuations might occur. It is conceivable that an airconditioning failure could expose a reel to a high temperature high humidity condition for perhaps a week or more. Transportations of the tape in an uncontrolled environment may have similar results. It is the purpose of this section to give procedural guidelines in order to insure maintenance of the stored data.

In Section 2.4 it was argued that tape binder rejuvenation is impractically long. In addition, precise information on the effect of various storage fluctuations on the binder system is unknown since a) binder systems vary even within the categories of polyesters-urethanes, b) the system error rate as a function of binder degradation cannot be easily

determined. Thus, a reasonable general requirement is that following an environmental adversity, a tape should be brought to equilibrium with the ideal play/storage environment ( $65^{\circ}\text{F}$ , 40%RH) prior to replay. A three day storage is a reasonable equilibration period due to hygroscopic rates [23]. The tape then should be shuttled twice before measurement to free accumulated debris. If an unacceptable error rate is measured, it is recommended that a gentle fabric (e.g., 'Pellon') wipe be used to remove the remaining debris.

For the purpose of determination of time to rewind (to restore tension) two alternative approaches are proposed. Both require a systematic indication on each reel of the date it has been last wound. It requires also a method (probably computerized) for identification of reels having been wound in a given date range.

The first approach, (see Section 2.3.5) consists of the recommendation that unrecorded test reels of the type and size used in the particular archival storage facility be stored semi-monthly with imbedded friction tabs. A semi-monthly check of the stored test reels would indicate the date range of reels requiring tension restoration. Our tests indicate that if tabs imbedded at a radius of 60 mm (2.4") of a 4000 ft Ampex 799 instrumentation tape reel can be dislodged by a force of 30N (6.8 lb) or less, it is time to rewind, if decelerations of  $400 \text{ rad/sec}^2$  are required. Similar calibration tests may be made for the specific sizes and types of reels used in a facility based on the required accelerations/deceleration of its tape transports.

As a much less reliable alternative, we propose the following approach which is based on rule of thumb crude estimates.

1 day at  $85^{\circ}\text{F}$  is equivalent to 15 days at  $65^{\circ}\text{F}$ .

1 day at  $105^{\circ}\text{F}$  is equivalent to 250 days at  $65^{\circ}$ .

These estimates assume that the winding temperature was  $65^{\circ}\text{F}$ .

It is worth mentioning that the guidelines just described are crude due to the generalizations of 1) the properties of polyester film, 2) the thermally induced stresses in the reel. It is feasible, however, to simulate with reasonable accuracy the relaxation in the reel, given the temperature and humidity in the storage area. We believe, therefore, that with further development, a real time computer simulation may virtually automate the process of determining the time to rewind in face of environmental fluctuations. A microcomputer may be used for this purpose.

Finally, it should be mentioned that the time to rewind is specified for a desired high acceleration. If a reel has been exposed to an environmental adversity beyond the accepted limits, a low acceleration wind (play mode) is recommended as a precaution.

### **3.1.2.6 Recommendation for System Variations**

#### **Acceleration/Deceleration -**

Recommendations for time to rewind given in this report assume an acceleration requirement of  $400 \text{ rad/sec}^2$  (1000 in/sec in 500 ms for 5" radius) which in our case coincides experimentally with 50% relaxation of the reel pressure. It is expected that for the same reel size, the minimum allowable reel pressure to prevent cinching is proportional to the maximum acceleration and at least inversely proportional to time to rewind. Thus if the maximum reel acceleration is only 500 in/sec in 500 ms, one may reasonably expect a need to rewind the reel in 7 years if it is kept at the specified environment.

#### **Reel Size -**

If reel pressure increases roughly in proportion to  $r_f$  (reel radius) and reel inertia is approximately proportional to  $r_f^4$ , then allowable angular acceleration is inversely proportional to  $r_f^3$  and allowable linear acceleration is inversely proportional to  $r_f^2$  (see Section 2.3.7.4). Thus if 14" reels are used instead of 10-1/2" reels and the desired time between rewinds is 5 years, then the allowable acceleration would be roughly

$$2000 \text{ in/sec}^2 \times \frac{3.5}{5} \times \left( \frac{10.5}{14} \right)^2 \approx 750 \text{ in/sec}^2$$

### **3.1.2.7 Recommendations Regarding Tape Transports**

#### **Winding Tension -**

Constant torque winding with an increased tension near the outer radius of the reel induces a preferred wound-in tension pattern. Peak winding stress level of about 1000 psi is recommended. It is believed, however, that the tension pattern is not a critical parameter and constant tension winding is reasonable except for large reel sizes.

#### **Interlayer Air -**

When fast winding is performed and prolonged reel storage is desired, it is essential to eliminate interlayer air. A packing roller assisted winding eliminates this problem. It is recommended that transports for archival storage systems will be equipped with packing rollers.

### **3.1.2.7 Acquisition Storage and Handling Sequence**

The discussion of this section is summarized in Table 9 which gives a step by step procedure for the archival storage of magnetic recording tape. The reasons for these recommendations are listed to give a convenient overview of the total archival storage philosophy.

These recommendations are guidelines based on the results of the study under this contract. It is certain that modifications may occur as practical experience is developed over long term utilization of a specific recording system.

### 3.2 Optimum System Configuration

In this section a specific optimal storage system is recommended. The guidelines are those given in the statement of work for this contract.

#### 3.2.1 Introduction

The work statement specifies the following design objectives:

Input/output rates	20 Mbps
Total capacity	$10^{14}$ bits
Bit error rate	$10^{-6}$ (raw) $10^{-10}$ (with EDAC)
Access time	< 15 seconds to a given storage unit

Unfortunately, the capacity of the "storage unit" is not defined. Consequently, in the analysis below, two different system designs will be described.

In the first, it will be assumed that the principal objective is rapid access and that the attainment of this goal will determine the capacity of the "storage unit".

In the second design, it will be assumed that a "storage unit" must contain some  $2 \times 10^{11}$  bits. Following discussions with DMA-AC, St. Louis on 4 April 1979, this figure was arrived at as follows:

A map unit, representing a  $1^{\circ}$  by  $1^{\circ}$  square of the earth's surface quantized into  $1200 \times 1200$  pixels with the elevation of each pixel given by a 16 bit number, contains about  $2 \times 10^7$  bits. Some 8000 such map units form a "data base" a "storage unit" of  $2 \times 10^{11}$  bits.

Table 9  
Acquisition Storage and Handling Sequence  
for Archival Magnetic Tape

ACTION (SEQUENTIAL)	REASON
I ORDER ARCHIVAL TAPE SPECIFYING CURRENT PRODUCTION, SATISFACTION OF MODIFIED GSA SPECIFICATIONS AS WELL AS ENVIRONMENT PRIOR TO DELIVERY	TO MINIMIZE TAPE BINDER WEAKENING PRIOR TO USE
II STORE TAPES UNSEALED FOR THREE DAYS IN STORAGE ROOM [65 ± 3°F, 40 ± 5%RH]	TO ALLOW FOR HYGROSCOPIC EQUILIBRIUM IN STORAGE ENVIRONMENT
III RECORD TAPES IF NECESSARY; PERFORM PRESTORAGE REWIND TO (E.G.) "HEADS OUT" POSITION	SET STORAGE TENSION & PRODUCE A SMOOTH WIND; USE LOW ACCELERATION PLAY MODE IF PACKING ROLLER IS UNAVAILABLE
IV USE "REEL BANDS"; PREPARE CONTROL TAPES WITH FRICTION TABS	BANDS PROHIBIT FLANGES FROM DAMAGING TAPE EDGES; FRICTION TABS MONITOR EFFECTS OF STORAGE ENVIRONMENT FLUCTUATIONS
V SEAL TAPES IN POLYETHYLENE BAGS, INSERT IN BOXES AND PLACE VERTICALLY ON SHELF	TO MINIMIZE LUBRICANT EVAPORATION, ENVIRONMENTAL FLUCTUATIONS AND SETTLING OF PACK AGAINST ONE FLANGE
VI IF STORAGE TIME REACHES 3.5 YEARS OR FRICTION TABS REACH CRITICAL FORCE, REWIND TAPE AS IN III	TO MINIMIZE CINCHING OR POSSIBLE BLOCKING DAMAGE; CHANGE REWIND FREQUENCY IF STORAGE ENVIRONMENT EXCEEDS BOUNDS OR AS SYSTEM ACCELERATIONS AND REEL SIZE VARY
VII IF STORAGE ENVIRONMENT FAILURE OCCURS; AT REWIND TIME (PERHAPS SHORTENED) PERFORM II AND REWIND SLOWLY	FOR EXAMPLE, LARGE INCREASES IN TEMPERATURE, HUMIDITY MAY YIELD SIGNIFICANTLY SHORTENED REWIND INTERVAL; TAPES SHOULD BE DRIED AND THEN REWOUND TO SET STORAGE TENSION
VIII REPLAY TAPES AS NEEDED IN CONTROLLED ENVIRONMENT; SHUTTLE TWICE SLOWLY BEFORE PLAY; IF ENVIRONMENTAL DAMAGE IS SUSPECTED, PERFORM VII AND PLAY; IF ERROR RATE APPEARS LARGE, WIPE TAPES WITH TISSUE CLEANER AND REPLAY	TO MINIMIZE TAPE DEGRADATION DURING REPLAY PERIOD AND ACHIEVE LOW ERROR RATES
IX RETURN TAPES TO STORAGE BY PERFORMING STEP V	

### 3.2.2 Summary of Limiting Parameters

This archival study program has demonstrated that the effects of time, temperature and humidity on the magnetically recorded signal is negligible even though these effects on the tape binder and base film systems may be severe.

It follows, therefore, that the tape recording format may be chosen for optimum storage density independently of the archival considerations. The basic physics of magnetic recording indicates that greater areal densities are obtainable more satisfactorily by using a larger number of narrow tracks rather than by increasing the linear density with wide tracks. This conclusion is borne out by the historical record of the evolution of all types of magnetic recording systems. For example, the trackwidths used in both computer disc files and consumer helical video tape recorders have decreased from 10-15 mils down to 1-2 mils at the present, with concomittant areal density increases exceeding an order of magnitude. Typically, disc files (Ampex 9160, IBM 3370) store  $5 \times 10^6$  bits per square inch of medium. In order to increase greatly both the total bit capacity and the data rate over disc files, Ampex has recently announced a multi-track helical digital recorder, the Super-High-Bit-Rate (S-HBR) machine.

The S-HBR, by recording a disc file like format (1 mil track widths at 10,000 bits per inch) on tape achieves a similar areal density of  $5 \times 10^6$  bits per square mil. The linear density is 10,000 bits per inch and the track density is 667 tracks per inch. (1 mil wide tracks on 1 1/2 mil centers.)

Standard, commercially available, broadcast quality video tape has been selected for use with the S-HBR system. Extensive measurements have shown that bit error rates considerably lower than  $10^{-6}$  (raw) can be achieved and it is expected that, with the addition of some 15-20% EDAC, a corrected error rate of  $10^{-10}$  will be attained.

The S-HBR employs a helical scanning principle with head-tape relative velocities in the range 1500-3000 inches per second. This corresponds to data rates of  $15-30 \times 10^6$  bits per second, which spans the desired rate of 20 Mbs. Current S-HBR designs include a multiplicity of parallel tracks but these will not be required for the present application. Since the scan length on tape is about 5 inches, it will be most natural to "block" the data into 50,000 bit word-lengths. These words may be accessed respectively (still-frame mode) or sequentially (tape-moving mode).

The tape width used in S-HBR is two inches, yielding  $10^7$  bits per inch of tape length. Previous experience has shown that fast search speeds of 500 inches per

second are suitable for video tape systems and it follows, therefore, that about  $5 \times 10^9$  bits per second can be surveyed in a fast search mode. In the table below, we show the tape lengths, the data capacities and the search times possible.

Tape Length (Ft.)	Bit Capacity	Search Time
10,000	$10^{12}$	200 secs
1,000	$10^{11}$	20 secs
100	$10^{10}$	2 secs

To these times must be added the cassette, cartridge or reel change time. For manual operations, about 30 seconds would be needed, for automatic loading, 10 seconds may be feasible. The obvious possibility of utilizing several recorders in a "ping-pong" mode is not explored here.

In the table below, we show the tape length, the number of cassettes needed to attain  $10^{14}$  bits total capacity and the sum of the loading and search times.

Tape Length (Ft.)	Number Read	Access Times (Manual)	Access Times (Auto)
10,000	100	230	210
1,000	1,000	50	30
100	10,000	32	12

### 3.2.3 Recommended Optimum System Design

#### 1) System to Meet the Access Time Specifications

Type of Recorder	Helical
Data Rate	20 Mbs
Recording Medium	Commercially available video tape
Tape Width	2 inches
Tape Length	100 feet, cassette or cartridge
Block Size	50,000 bits
Cassette Capacity	$10^{10}$ bits
Number of Cassettes	10,000
Cassette Selection	Automatic
Access Time	About 15 seconds worst case

2) System to Meet the  $2 \times 10^{11}$  Bit "Storage Unit" Criterion

Type of Recorder	Helical
Data Rate	20 Mbs
Recording Medium	Commercially available video tape
Tape Width	2 inches
Tape Length	2,000 feet
Natural Block Size	50,000 bits
Cassette Capacity	$2 \times 10^{11}$ bits
Number of Cassettes	500
Access Time	About 130 seconds worst case

## REFERENCES

1. N. Bertram, M. Stafford, D. Mills, "The Print-Through Phenomenon and its Practical Consequences", Preprint No. 1124E-1, 54th Audio Eng. Soc. Meeting, Los Angeles, CA, May 1976.
2. General Kinetics, Inc., "Magnetic Tape Study", Contract D18-119-SC42, 1959.
3. E. J. Barlow and J. N. Goodier, "Critique on the Reel Winding Analysis Made by General Kinetics", Ampex Corporation Report RB 63-28, 1963.
4. H. C. Altmann, "Formulas for Computing the Stresses in Center-Wound Rolls", Tappi 51, 1968, pp 176-179.
5. H. Tramposch, "Relaxation of Internal Forces in a Wound Reel of Magnetic Tape", Trans. ASME J. App. Mech. 1965, pp 865-873.
6. H. Tramposch, "Anisotropic Relaxation of Internal Forces in a Wound Reel of Magnetic Tape", Trans. ASME, J. App. Mech. 1967, pp 888-894.
7. C. N. Jolliffe, "Thermally Induced Stresses in Rolls of Oriented Film", Private Communication. (Author is with E. I. DuPont.)
8. S. Mukherjee, "Time Base Errors in Video Tape Packs", Trans ASME, J. Appl. Mech. 1974, pp 625-630.
9. S. Mukherjee, "Effect of Multiple Rewinds and Temperature Cycles on Time Base Errors in Video Tape Packs", Int'l J. Solids Structures, 1975, pp 887-894.
10. DuPont Mylar Polyester Film, Technical Information Manual, DuPont Film Department.
11. G. G. Dynia, ICI Americas, Inc., "Dimensional Stability of Polyester Video Tape Base", Private Communication No. 299, July 31, 1978.
12. ICI Plastics Division "Melinex Polyester Film" Industry Note MX200.
13. D. B. Bogy, N. Bugdyaci, F. E. Talke, "Experimental Determination of Creep Function for Thin Orthotropic Polymer Films", IBM J. Res. Develop. 23, 1979, pp 450-458.
14. A. Eshel and H. G. Elrod Jr., "The Theory of the Infinitely Wide Perfectly Flexible Self Acting Foil Bearing", ASME Trans. J. Bas. Eng. 87, 1965, pp 831-836.
15. J. Hawthorne, Private Communication (Author is with E. I. DuPont.)

References (Continued)

16. Anon. "Causes and Effects of Skew Error in Helical Scan Video Tape", Retentivity, 1978.
17. E. Cuddihy, "Aging of Magnetic Tape", Submitted to IEEE Trans. Mag., May 1979, (Author is with Jet Propulsion Lab, Pasadena, CA.)
18. B. F. Blumentritt, "Annealing of Poly (ethylene-terephthalate) - Film-Based Magnetic Recording Media for Improved Dimensional Stability", IBM Journ. of Res. and Dev. Vol. 23, pp 56-65, 1979.
19. O. Bessette and R. Resek, "Test and Evaluation of Airborne Digital Tape Transport", Contract Report No. AFAL-TR-76-131, Air Force Avionics Laboratory, Wright Patterson AFB, Ohio, pp 5-1 - 5-13, July 1977.
20. S. Geller, "Erasing Myths About Magnetic Media", Datamation, pp 65-70, March 1976.
21. E. Cuddihy, Private Communication.
22. W. Polard, G. Prine and T. Jones, "Archival Performance of NASA GFSC Digital Magnetic Tape", Proc. of National Computer.
23. E. Cuddihy, "Hygroscopic Properties of Magnetic Recording Tape", IEEE Trans. Mag. Vol. Mag-12, pp 126-135, March 1976.

**MISSION**  
**of**  
**Rome Air Development Center**

RADC plans and executes research, development, test and selected acquisition programs in support of Command, Control Communications and Intelligence (C<sup>3</sup>I) activities. Technical and engineering support within areas of technical competence is provided to ESD Program Offices (POs) and other ESD elements. The principal technical mission areas are communications, electromagnetic guidance and control, surveillance of ground and aerospace objects, intelligence data collection and handling, information system technology, ionospheric propagation, solid state sciences, microwave physics and electronic reliability, maintainability and compatibility.